



SKB rapport

R-97-05

March 1997

Update of the geological models of the Gideå study site

Jan Hermanson, Lars Mærsk Hansen, Sven Follin

Golder Associates AB

Svensk Kärnbränslehantering AB

Swedish Nuclear Fuel and Waste Management Co

SKB, Box 5864, S-102 40 Stockholm, Sweden

Tel 08-665 28 00 Fax 08-661 57 19

Tel +46 8 665 28 00 Fax +46 8 661 57 19

ISSN 1402-3091
Rapport R-97-05

UPDATE OF THE GEOLOGICAL MODELS OF THE GIDEÅ STUDY SITE

Jan Hermanson, Lars Mærsk Hansen, Sven Follin

Golder Associates AB

March 1997

This report concerns a study which was conducted for SKB. The conclusions and viewpoints presented in the report are those of the author(s) and do not necessarily coincide with those of the client.

**UPDATE OF THE GEOLOGICAL MODELS OF THE GIDEÅ
STUDY SITE**

by

Jan Hermanson

Lars Mærsk Hansen

Sven Follin

Golder Associates AB

MARCH 1997

Keywords: structural model, lithology, Gideå, fold, fracture zones.

ABSTRACT

During the period 1981-1983, SKB performed surface and borehole investigations at the Gideå site, as part of a site selection program of a number of study sites for the purpose of assessing their suitability for a repository of spent nuclear fuel. This study presents a review and an update of the structural and lithological models, as presented by Ahlbom et al 1983 and Ahlbom et al 1990.

In a three dimensional model of the lithology, it is demonstrated that the host rock, paragneiss (migmatite or veined gneiss), is intermingled by elongated bodies of orthogneiss (granite gneiss or granite), with a variable thickness of up to 25 m. Both gneiss types are folded, the orthogneiss bodies interpreted to be layered along the NE-SW trending, gently inclined axis of plastic folding of the rock. Lithological sequence does not change within repository depth, whereas the hydraulic conductivity of 25 m packer tests show higher magnitudes between ground level and 200 m depth than at repository depth (some 500 m). The fracture frequency of orthogneiss and paragneiss is similar.

The gneiss complex is intersected by steeply dipping dolerites trending E-W, and a few steep N-S trending post orogenic pegmatites. Subhorizontal dolerites may exist, limited in extent, however, as a steep borehole in the mid of the area does not intersect any dolerite. The dolerite dykes often show jointing forming pillars of solid rock (columnar jointing), where the joints are infilled by calcite, and are, based on geological evidence, interpreted to be less conductive than other rock types. Rock contacts between dolerites and gneisses are not extensively fractured, implying no hydraulic pathways along dolerite dykes. The pegmatites have a low fracture frequency, and are interpreted to be of minor importance in a hydraulic model.

Based on the analysis of 25 m packer tests, there is no correlation of statistical significance between $\log_{10}(K_{25m})$ and rock type. There is no obvious correlation between $\log_{10}(K_{25m})$ and the number of rock contacts, i.e. it seems that rock contacts at some locations are conductive, but impermeable at others. Some tests have been performed in 5 m sections, in order to more accurately locate hydraulic zones, but are too few to result in any conclusions.

Twelve fracture zones have been identified in the area, many of which are highly conductive. Most of the latter strike NNE to ENE (parallel with the maximum horizontal stress of the region), dipping vertical or steeply to the SE. The fracture zones intersect all rock types in the area, and do not follow rock boundaries, but may be influenced by the penetrative orientation of the foliation.

The fracture system is predominantly steep and is trending N-S and E-W and is locally influenced by the NE-SW trending zones.

SAMMANFATTNING

Under åren 1981-1983 har SKB genomfört undersökningar i Gideåområdet på och från ytan samt i borrhål som en del av programmet för platsval. Programmet har syftat till att bedöma olika platsers lämplighet för förvar av använt kärnbränsle. Denna studie presenterar en genomgång och uppdatering av de bergarts- och strukturgeologiska modeller som presenterats tidigare (Ahlbom et al. 1983, 1990).

I en tredimensionell modell av berggrunden visas att huvudbergarten sedimentgnejs (migmatit och ådergnejs) växlar med långsträckta kroppar av gnejsgranit med en tjocklek på upp till 25 meter. Bägge bergartstyperna är veckade och kropparna av gnejsgranit tolkas som liggande parallellt med veckaxeln, som är orienterad NO-SV med flack stupning. Bergartsfördelningen är den samma även vid förvarsdjup, medan den hydrauliska konduktiviteten vid 25 m testlängder med manschett visar högre värden ned till 200 meters djup än vid förvarsdjup (ca 500 meter). Sprickfrekvensen är lika i bägge gnejstyperna.

Gnejskomplexet skärs av nästan vertikala diabasgångar med öst-västlig strykning samt ett fåtal branta postorogena pegmatitgångar som stryker nord-syd. Vissa borrhål antyder att flacka diabasgångar kan finnas men de måste i så fall ha mycket begränsad utbredning, eftersom det vertikala borrhålet i områdets mitt inte skär en enda diabas. Diabaserna är ofta pelarformigt uppspruckna med sprickfyllnad av kalcit och tolkas som mindre hydrauliskt konduktiva än övriga bergarter. Kontakterna mellan diabas och gnejs är inte särskilt uppspruckna, vilket antyder att det inte finns hydrauliska läckvägar längs diabaserna. Pegmatiterna har låg sprickfrekvens och tolkas ha liten betydelse i en hydraulisk modell.

Baserad på analys av 25 meters testsektioner med dubbelmanschett, finns det inte något statistiskt säkerställt samband mellan hydraulisk konduktivitet ($\log_{10}K_{25m}$) och vare sig bergart eller antalet bergartskontakter inom testsektionerna, d.v.s. att vissa bergartskontakter är permeabla, andra inte. För vissa sektioner har även 5 meters testlängd använts för att mer exakt lokalisera vattenföringen, men antalet mätningar är för litet för att några slutsatser skall kunna dras.

Tolv sprickzoner har identifierats i området, varav flera är starkt vattenförande. De flesta av de senare stryker NNO till ONO (parallellt med största huvudspänningen i Mellersta Norrland) och stupar lodrätt eller brant åt SO. Sprickzonerna skär alla bergartstyper i området och följer inte bergartsgränser, men kan ha influerats av den genomträngande förskiffrings riktningen.

Spricksystemet är i regel brantstupande med sprickorientering nord-syd och öst-väst liksom pegmatit- respektive diabasgångar och är lokalt influerat av de NO-SV strykande zonerna.

TABLE OF CONTENTS

ABSTRACT	i
SAMMANFATTNING	ii
1 INTRODUCTION	1
1.1 SITE LOCATION	1
1.2 GEOLOGICAL MODELS PRIOR TO UPDATE	1
1.3 EXTENT OF UPDATE	1
1.4 GEOLOGICAL PARAMETERS USED AND TREATED IN THE STRUCTURAL MODEL UPDATE	2
1.5 CO-ORDINATE SYSTEM CONVENTIONS	5
2 OVERVIEW OF REGIONAL GEOLOGY	7
2.1 VEINED GNEISS AND MIGMATITE	8
2.2 INTRUSIVE GRANITE AND PEGMATITE	8
2.3 DOLERITES	8
2.4 ROCK STRESSES AND TECTONIC ZONES	9
3 SURFACE INVESTIGATIONS, SITE SCALE	13
3.1 GEOLOGICAL MAPPING	13
3.2 FRACTURE MAPPING	13
3.3 GEOPHYSICAL SURVEY	13
4 SUBSURFACE INVESTIGATIONS	19
4.1 INVESTIGATIONS IN CORED DRILL HOLES	19
4.2 INVESTIGATION RESULTS	21
5 ANALYSIS OF INVESTIGATION RESULTS	25
5.1 LITHOLOGICAL DATA	25
5.2 ZONE DATA	26
5.2.1 Zones I and II. Interpretation Alternative 1	26
5.2.2 Zones I and II. Interpretation alternative 2	27
5.2.3 Zone III	28
5.2.4 Subhorizontal zones	31
5.3 RESULTS OF CROSSHOLE SEISMIC INVESTIGATIONS	31
5.4 CORRELATION OF LITHOLOGICAL UNITS AND HYDRAULIC CONDUCTIVITY	40
6 RESULTS OF UPDATE	47
6.1 LITHOLOGY	47
6.1.1 Lithological units	47
6.1.2 Lithological model	48
6.2 FRACTURE ZONES	51
6.2.1 Zone model	51
6.3 HYDRAULIC PROPERTIES OF LITHOLOGICAL UNITS	54
7 CONCLUSIONS	61
8 REFERENCES	63

LIST OF APPENDICES

Appendix 1 Reliability criteria for dolerite dykes

Appendix 2 Reliability criteria for zones (Bäckblom. SKB 25-89-007)

Appendix 3 Co-ordinates of zones and lithological units

LIST OF TABLES

Table 1-1 Geological parameters used in the structural model update.	3
Table 2-1 Main geological events, rocks and age relationships of the region	7
Table 4-1 Summary of percussion drillings	19
Table 5-1 Dolerite dykes at the Gideå Study Site	29
Table 5-2 Reliability levels of fracture zones at Gideå	30
Table 5-3 Occurrence of migmatite, pegmatite, granite and dolerite according to the lithological logs of boreholes KG01-KGI08 and KGI11 at Gideå. The statistics of cored lengths refer to the straddle intervals of the 25 m packer tests conducted in these boreholes. The total number of intervals is 204 (corresponding to 5,100 m of core length). By occurrence we mean here that the considered rock type is present, either alone or together with the other rock types.	42
Table 6-1 Lithological units of the Gideå Site	47
Table 6-2 Characteristics of fracture zones	52
Table 6-3 Statistics of $\log_{10}(K_{25m})$ of the 25 packer tests at Gideå. Data are gathered according to the lithological logs of boreholes KG01-KGI08 and KGI11 at Gideå. By occurrence it is meant here that the considered rock type is present, either alone or as one of 2-4 possible rock types.	54

LIST OF FIGURES

Figure 1-1 Location of the Gideå study site (Ahlbom et al. 1991)	5
Figure 1-2 Lithological and tectonic models prior to update.	6
Figure 2-1 Map of regional lithology	10
Figure 2-2 Orientations of maximum horizontal stresses in Scandinavia	11
Figure 2-3 Map of regional structures	12
Figure 3-1 Rock outcrop map of the Gideå Study Site (Albino et al 1983). With foliations (Ericsson & Ronge 1986) and with interpreted folds.	14
Figure 3-2 Fracture orientation map (Eriksson & Ronge, 1986)	15
Figure 3-3 Magnetic anomalies with interpreted dolerite dykes (Albino et al 1983)	16
Figure 3-4 Map of seismic velocity anomalies and resistivity with interpretation (Albino et al 1983)	17
Figure 4-1 Drill hole locations	20
Figure 4-2 Profile with results from percussion drillings HGI 14, 15 & 16 and Core drilling KGI 05.	22
Figure 4-3 Profile with results from percussion drillings HGI 01, 02, 05, 23, & 24 and Core drilling KGI 02.	23
Figure 4-4 Profiles with results from percussion drillings over Zone I (a), Zone II (b) and Zone III (c, d).	24

Figure 5-1 Profiles AA' and BB' showing the folded nature of the migmatite in the Gideå study area with bodies of orthogneiss along the foliation. Dark cylinders represent orthogneiss in drill cores situated in the vicinity to the profiles.	32
Figure 5-2 Conceptual cartoon of the occurrence of orthogneiss along profile B-B'	33
Figure 5-3 Profile athwart D1	33
Figure 5-4 Map of interpreted fracture zones in the Gideå Study Area	34
Figure 5-5 Profile of HGI 14-16 and KGI 05 with Interpretation Alternative 1	35
Figure 5-6 Profile of HGI 01, 02, 23 & 24 and KGI 02 with Interpretation Alternative 1	36
Figure 5-7 Profile of HGI 14-16 and KGI 05 with Interpretation Alternative 2	37
Figure 5-8 Profile of HGI 01, 02, 23 & 24 and KGI 02 with Interpretation Alternative 2	38
Figure 5-9 Profile with results from percussion drilling HGI 11 and Core drilling KGI 06.	39
Figure 5-10 Hydraulic conductivity versus depth	40
Figure 5-11 Overview of packer test conductivities at Gideå. The screening straddle interval is 25 m. The other intervals are less frequent and used for special purposes.	43
Figure 5-12 K_{25m} plotted as function of depth of interval center. Data comes from boreholes KGI01-08 and KGI11.	44
Figure 5-13 K_{5m} plotted as function of depth of interval center. Data comes from boreholes KGI01-08 and KGI11.	45
Figure 5-14 K_{25m} plotted as function of depth of interval center. The boreholes are given different colors.	46
Figure 6-1 Three-dimensional model of dolerite bodies	49
Figure 6-2 Three-dimensional model of foliation, fold structures and orthogneiss bodies	50
Figure 6-3 Three -dimensional model of fracture zones	53
Figure 6-4 K of 25 m long packer test intervals which contain 0-25 m of Migmatite	55
Figure 6-5 K of 25 m long packer test intervals which contain 0-13 m of Pegmatite	56
Figure 6-6 K of 25 m long packer test intervals which contain 0-25 m of Orthogneiss.	57
Figure 6-7 K of 25 m long packer test intervals which contain 0-17.5 m of Dolerite.	58
Figure 6-8 K plotted as a function of the number of rock contacts.	59

1 INTRODUCTION

1.1 SITE LOCATION

The Gideå study site is located near the town Örnsköldsvik, Västernorrland County, Sweden, some 600 km to the North of Stockholm (Figure 1-1). The site is characterised by a low relief, at an altitude varying between 100 and 130 m a.s.l. Typical characteristics of the area are well exposed rock, with flat or nearly flat top surfaces eroded by glaciation and with some steep edges, swamps and moraine deposits with coniferous wood.

1.2 GEOLOGICAL MODELS PRIOR TO UPDATE

Existing geological models are presented by Ahlbom et al. (1983) and Albino et al (1983) and later compiled and evaluated by Ahlbom et al. (1991). The models are outlined in Figure 1-2. The major lithological elements of the conceptual model are migmatites intermingled with thin layers of bodies of granodioritic orthogneiss (hereinafter called orthogneiss or granite) of unknown extent and a set of dolerites crossing the study area in an East-West orientation. 10 fracture zones have been defined. The main hydraulic units in the rock mass are the comparatively low conductive migmatite and the more conductive orthogneiss layers and the major hydraulic pathways, the fracture zones.

A review of the conceptualisation of the performed investigations show that several issues remain to be interpreted. A number of open questions are presented regarding the lack of three dimensionality in the geological model, uncertainties in the extension at depth of lithological units and fracture zones, relation between lithology and hydraulically active zones as well as a need for re-evaluation of hydraulic parameters for the rock mass units (Ahlbom et al. 1991). A new three dimensional geological model is requested while both two- and three-dimensional models exist for fracture zones. Furthermore, the review shows the need of clarifying some of the investigation results, in particular, the drillings around Zones I and II and, to some extent, also Zone III.

1.3 EXTENT OF UPDATE

The update comprises an upgrade of the existing two-dimensional model of the lithology to include the spatial variability of lithological units in three dimensions, and a review of the existing three-dimensional model of tectonic zones. The work has also comprised a site visit and examination of selected cores. Core log data (SICADA 1996) have been used for input in computerised three-dimensional models and for analysis of vertical sections of percussion and core drillings sites. The outcome of the update presents a model of the lithology as well as a refined structural

hydraulic model. The association between lithological units and brittle highly conductive zones have been re-evaluated. Also the correlation of lithological units and measured conductivity have been evaluated. Geometric and hydraulic parameters for zones and lithological units are presented in tables. Co-ordinates for lithological units and fracture zones is presented in Appendix 3 and is also available in SICADA (SKB's site characterisation database). A further output are conceptual models of the foliated host rock with orthogneiss, dolerites and fracture zones, in digital form. These models are supplied at request from SKB and can be run with a supplied freeware on Win95/NT platforms and are possible to rotate and zoom in on model specific details in real time.

1.4 GEOLOGICAL PARAMETERS USED AND TREATED IN THE STRUCTURAL MODEL UPDATE

When describing the rock of a site it is of importance to be consistent between different subject areas. The purpose of this geological description is two-fold; one which is to deliver quantified parameters for performance assessment calculations and another which is to conceptualise the obtained geological information to establish a visual picture of the rock mass and its structures. With a trustworthy and understandable geological model, performance assessment calculations based on geological data increases in credibility. Andersson et al (1997), presents lists of parameters that is of importance to geological, rock mechanical, chemical and hydraulic model descriptions in site investigations of nuclear waste repositories. To provide a condense summary of utilised geological information in the updating process, the table concerning geological parameters in Andersson et al (1997) have been used in this report. Table 1-1 summarises both used background data in the updating of the structural model and, when further interpretations have been performed, its mode of application. References are given where to find the output parameters in the report.

Table 1-1 Geological parameters used in the structural model update.

Influence, meaning SUBJECT AREA	Input data to the structural model update		Output from the structural model update		
	Type	Source	Treatment	Output	Reference
GEOLOGY					
Topography					
Topography					
Lithology					
Rock mass lithology					
Rock distribution	Core logs	SICADA 1996	Compilation	3D lithological and structural model	Table 6-1
Xenolites Veins and dikes	Core logs	SICADA 1996	Compilation	3D lithological model	Table 5-1
Rock contacts	Core logs	SICADA 1996	Compilation	3D lithological model	Table 5-1
Age Ore potential industrial mineralizations					
Rock type description					
Mineralogy Grain size Mineral orientation Micro fracturing Density Porosity Susceptibility/gamma radiation etc	Susceptibility/gamma radiation	SKB AR 83-19	Compilation	3D lithological and structural model	Table 5-1, 5-2
Alteration and weathering	Core logs	SICADA 1996	Compilation	3D lithological and structural model	Table 5-2
SUBJECT					
Structural geology					
Ductile structures					
Folds	Magnetic, radiometric, seismic and resistivity data, surface obs, core log		Reinterpretation	3D lithological model	Figure 5-1, 5-2, 6-2
Foliation	Surface obs.	SKB TR 86-19, SGU Bedrock map Ba 31	Reinterpretation	3D lithological model	Figure 5-1, 5-2, 6-2
Shistosity	Surface obs.	SKB TR 86-19, SGU Bedrock map Ba 31	Reinterpretation	3D lithological model	Figure 5-1, 5-2, 6-2
Mylonites Banding	Core logs Core logs	SICADA 1996 SKB TR 86-19, SGU Bedrock map Ba 31		3D lithological model	Figure 6-2
Rods Age					

Table 1-1 Geological parameters used in the structural model update (continued).

Influence, meaning SUBJECT AREA	Input data to the structural model update		Output from the structural model update		
	Type	Source	Treatment	Output	Reference
Regional and local discontinuities					
Location	Previous structural model, magnetic, radiometric, seismic and resistivity data, surface obs, core log	Albino et al 1983 Ahlbom et al 1991	Reinterpretation	3D structural model	Table 5-2
Orientation	Previous structural model, magnetic, radiometric, seismic and resistivity data, surface obs, core log	Albino et al 1983 Ahlbom et al 1991	Reinterpretation	3D structural model	Table 5-2
Length	Previous structural model, magnetic, radiometric, seismic and resistivity data, surface obs, core log		Reinterpretation		
Width	Previous structural model, magnetic, radiometric, seismic and resistivity data, surface obs. core log	Albino et al 1983 Ahlbom et al 1991	Reinterpretation	3D structural model	Table 5-2, 6-2
Movement (amount, direction, age) Genetic type	Previous structural model	Albino et al 1983 Ahlbom et al 1991			
Characteristics <i>no. fracture groups</i> <i>spacing</i> <i>block size</i> <i>fracture roughness</i> <i>mineral filling</i> <i>alteration</i>	Core logs	SKB AR 85-03			
Local smaller discontinuities					
(data for stochastic and deterministic description) Location Orientation Length Width Movement (amount, direction, age) Genetic type Characteristics <i>no. fracture groups</i> <i>spacing</i> <i>block size</i> <i>fracture roughness</i> <i>mineral filling</i> <i>alteration</i>					
Single fractures					
(stochastic description) Frequency (different groups) Orientation Length Termination Fracture width Roughness Mineral filling Alteration and weathering	Surface obs.	Eriksson & Ronge 1986	Compilation		Figure 3-2

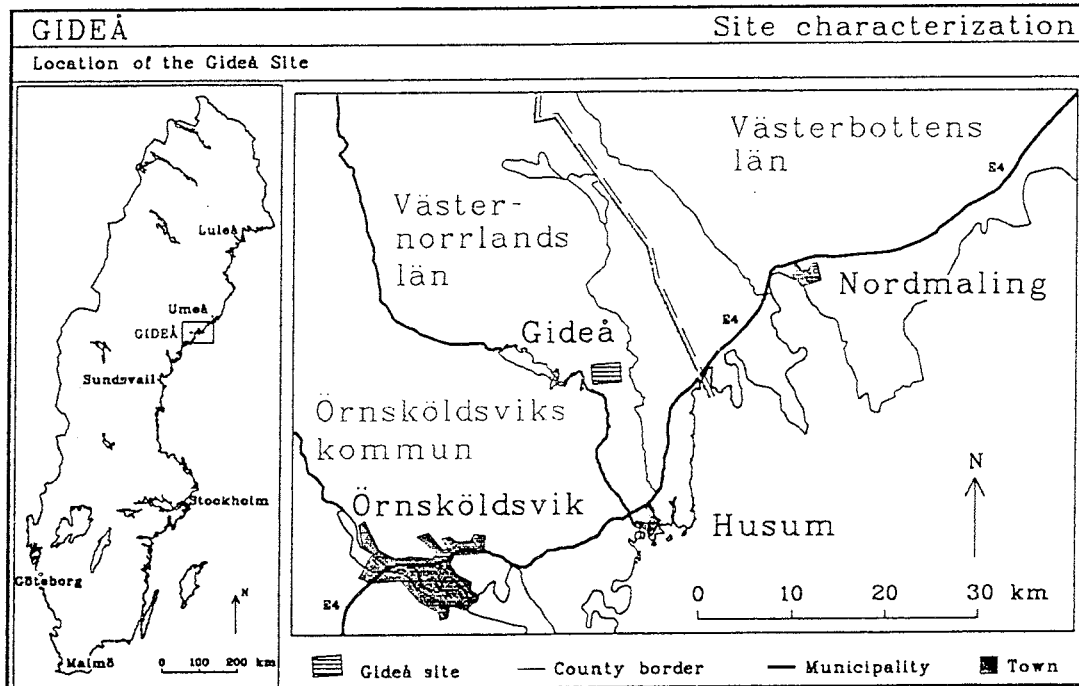


Figure 1-1 Location of the Gideå study site (Ahlbom et al. 1991)

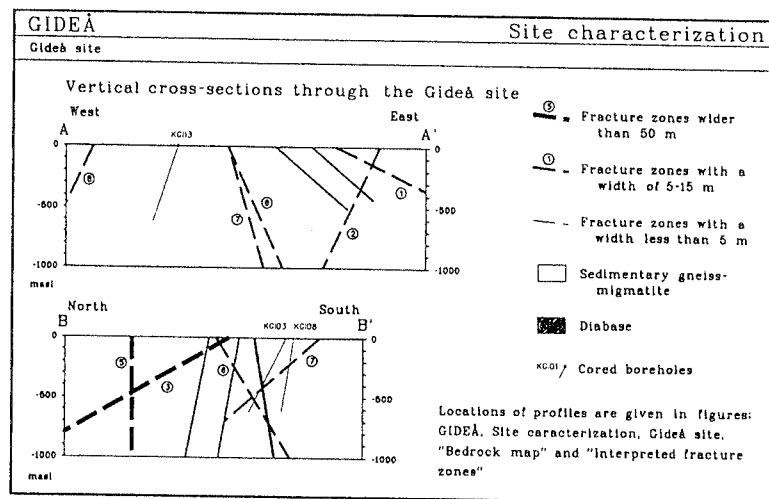
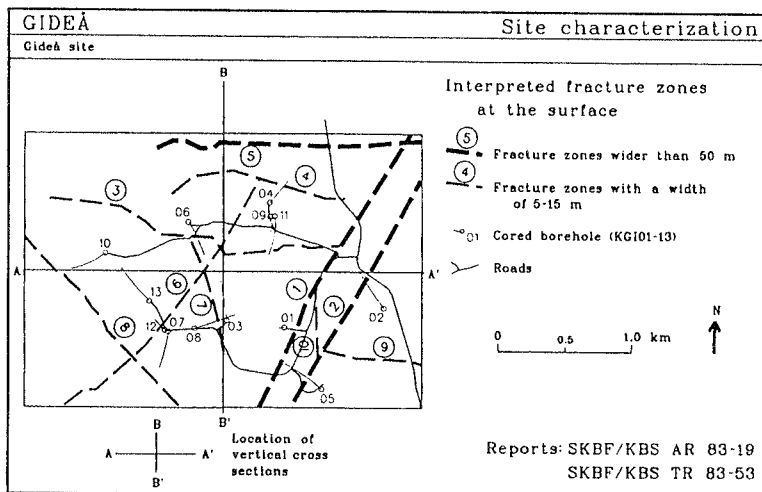
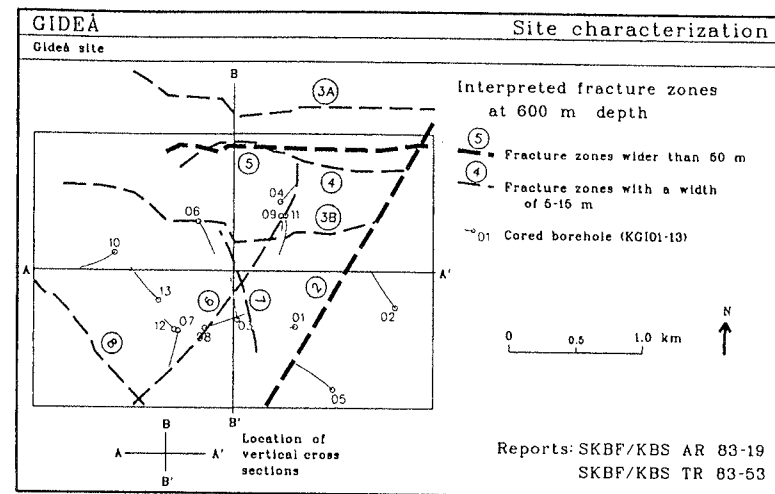
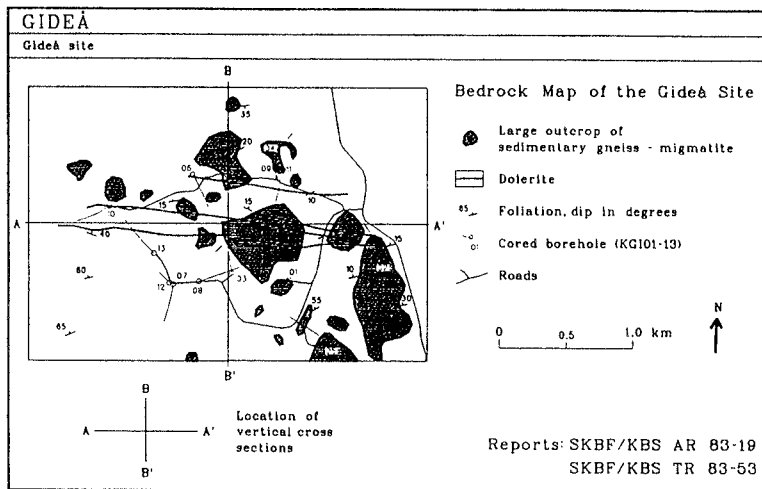
1.5 CO-ORDINATE SYSTEM CONVENTIONS

A local co-ordinate system for the Gideå site have been used in all *site* scale maps, figures and models throughout the report. This local system was implemented at the time of the previous investigation and deviates from the co-ordinate system fixed by the National Land Survey of Sweden (RT38) by 3 degrees W. The origin of this local system in RT38 co-ordinates is RT_X= 7044290 and RT_Y= 1662790.

The *regional* geological maps presented in this report originates from SGU and are all based on the RT38 co-ordinate system.

Output co-ordinates from the structural model given in Appendix 3 are in the RT38 system.

Figure 1-2 Lithological and tectonic models prior to update (after Ahlborn et al 1983). The co-ordinate system used in figures of *site* scale models and maps throughout the report is a local system with a 3 degree deviation W of the national co-ordinate system RT38.



2 OVERVIEW OF REGIONAL GEOLOGY

The regional geology has been described in a publication from the Geological Survey of Sweden (Lundqvist et al. 1990). The rocks in the Gideå region are all of Precambrian age and comprise migmatized veined gneiss, mainly of sedimentary origin, intrusive prim-orogenic granodiorite and granite (orthogneiss), pegmatite, and dykes and sills of dolerite. Figure 2-1 shows the distribution of rock types in the surrounding area and Figure 2-3 shows the structural elements, such as dolerite dykes, foliation, fold axes and lineaments. The age and structural relationships of the different rock types and geological events are outlined in Table 2-1.

Table 2-1 Main geological events, rocks and age relationships of the region

Age, million years	Volcanic and sedimentary rocks	Plutonic rocks	Veins, dykes and sills	Geological events
400	Ordovician graywacke, limestone, shale		Possible dolerite	Caledonian thrusting. Possible marine intrusions
500	Cambrian sandstone and shale			Sedimentation in the Caledonian and in the Bothnian Sea
600		Alnö Massif	Carbonatitic dykes	Intrusion and volcanic activity at Alnön. Fracturing
	Tillite, quartzite, varved slate (Vendian)			Glaciation
800	Sandstone (Rifeikan)			Sedimentation
1200	Sandstone, shale, conglomerate (Jotnian)		Postjotnian dolerites	Intrusion of large volumes of dolerite dykes and sills
		Anorogenic intr: Granitoids, Anorthosite, Gabbro	Porphyrite, Porphyry, granite veins	Fracturing. Sedimentation
1600				Formation of massifs, dykes and veins, thermal metamorphism
1700		Postorogenic granitoids	Turingen Dolerite	Postorogenic intrusions. Thermal metamorphism. Fracturing
1800		Serorogenic granite and pegmatite	Dolerite	Serorogenic intrusion, Fracturing
1850		Bothnian superficial rocks	Amphibolites	Regional metamorphism, migmatization and folding
	Sandstones, Rhyolite	Primorogenic Granitoids, Diorite and Gabbro	Amphibolite and Greenstone dykes	Primorogenic intrusions
1900				Sedimentation and volcanism

2.1 VEINED GNEISS AND MIGMATITE

The Study site is located in the dominating rock unit in the region, which is a formation of mainly greywacke with subordinate schist, phyllite and slate in different stages of metamorphic alteration. Some of the rocks show well preserved sedimentary structures, such as graded bedding, turbidity currents, erosion surfaces. Thermal metamorphism, due to granite intrusion can also be observed in the area.

Due to regional tectonic processes, a large amount of the sedimentary rocks have been altered into paragneiss of different stages of metamorphism, from a common gneissic foliation, to veined gneiss and migmatite. The veined gneiss has formed when the quartz and feldspar constituents of the sedimentary rock has molten and thus been able to intrude in fractures in the rock, while the migmatite consists of bodies of greywacke-gneiss in a matrix of intrusive granitoid rock, derived from partial melting of the gneiss. Most of the study area lies in rocks of latter two types. The transition between these rock types may be abrupt or more or less gradual.

Adjacent to the intrusions, thermal metamorphism can be traced in the shape of metamorphic minerals, in particular in the schists. The gneissic and schistose nature of the rock is due to a regional folding process. It is worthwhile to note that the penetrative foliation in the rock is of orogenic nature and is not bedding related. In the region, the fold axis is horizontal or gently dipping, oriented more or less East-West.

2.2 INTRUSIVE GRANITE AND PEGMATITE

Granitic and granodioritic dykes intruded during the Svecokarelian orogeny (1800 Ma). Some granite intrusions in the study area, reported by Lundquist (1990) are of prim-orogenic age and therefore interpreted to follow the induced foliation in the migmatized sediments. Other granite dykes are of ser- or post-orogenic age. To the South of the study area there is a large body of prim-orogenic orthogneiss of granitic and granodioritic composition, and to the West, there is a large body of post-orogenic intrusive porphyric granite. In all these rocks, there are pegmatite veins of different ages, which are often difficult to determine (Lundquist, 1990).

2.3 DOLERITES

A main characteristic of the region is the presence of post-Jotnian dolerite, which has intruded in the other rocks, either as flat lying sheets with a thickness of up to several hundred metres or as vertical dykes, with a thickness of up to fifteen metres. Post-Jotnian dolerites intrude 500 Ma years after granite intrusions and folding of the rock complex. It is likely that the larger South East dipping subhorizontal sill south east of Gideå may have extended over the study area, but have been eroded. Its presence possibly induced thermal metamorphism in the contact zone, close to the present day ground level. As no subhorizontal dolerite sheets appear north west of Gideå it is considered that there are no sills with a similar dip and thickness that intersect the study area at a depth relevant to the repository. However, there are a number of

thinner flat lying sheets of dolerite in the region, some of which are situated near the study area.

2.4 ROCK STRESSES AND TECTONIC ZONES

Regional rock stresses in the area have been calculated from focal mechanism and measured by means of hydraulic fracturing at a number of locations from Gideå in the Southeast to the Norwegian coast in the Northwest of the region. The maximal regional horizontal stresses are shown in Figure 2-2 and strike NNE to ENE (Müller et al. 1992) which is consistent with stress measurements on site (Ahlbom et al. 1991), and from the newly established rock stress database in Luleå (pers. comm. Ljunggren, 1996). A few of the lineaments in the region strike in this direction, which thus may form the present tensile fracture set corresponding to the stress field.

The predominant lineament directions, however, strike Northwest-Southeast and East-West, the latter being parallel with most of the dolerite dykes (Figure 2-3). This indicates an East-West trending post-Jotnian palaeo stress. North-South striking post-Jotnian normal faults exist, both before and after the intrusion of the dolerite. Northwest-Southeast striking lineaments are common from the Protogine zone to the Skellefteå field. For example at Äspö outside Oskarshamn, the Northwest set, parallel with the major component of horizontal stress, dominates the site scale hydraulic connectivity. Zones in Gideå, parallel to the major stress field, may also show a similar behaviour. As a matter of fact, a number of the most water-bearing fracture zones in the study area strike in this direction.

Earthquakes are known to have occurred in the 1920's (Sahlström 1930) and 1983 (Kulhánek & Wahlström 1985) with the last of a magnitude of 4.1 on the M_L (UPP) scale, indicating that the area is still tectonically active to a minor extent. The epicenter was located at 40 km of depth and no evidence of earth surface faults have been found.

Regional zones are shown on Figure 2-3. Regional and local zones which may be used for hydraulic model boundaries are shown as dashed black lines. It is worthwhile to notice that three larger lineaments surround Gideå with River Lögdeälven, to the Northeast of the map area as the largest regional structure in the vicinity to the study area.

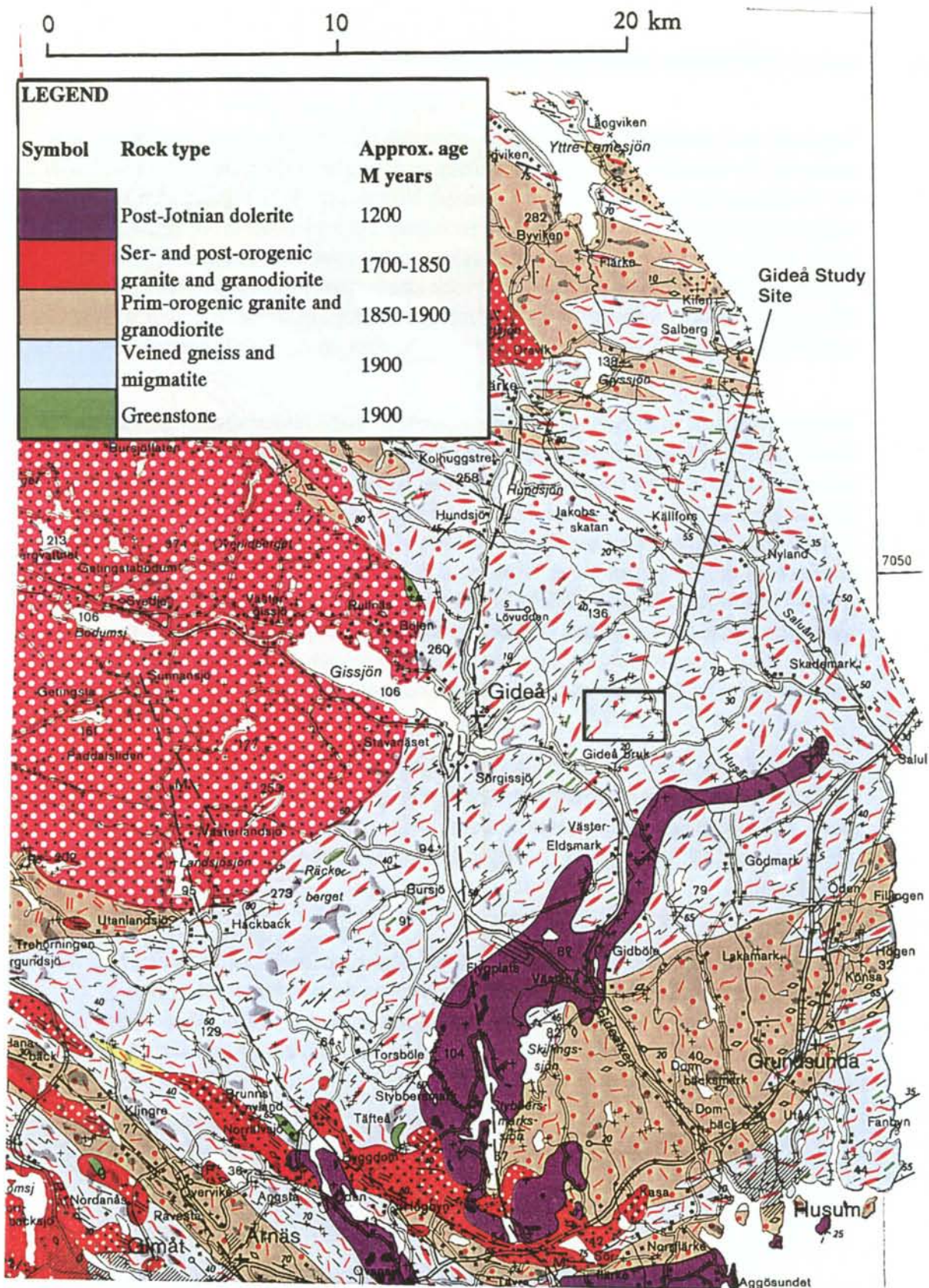


Figure 2-1 Map of regional lithology (Lundquist et al SGU Ba 31, 1990). The coordinate system in SGU maps throughout the report is fixed by the National Land Survey of Sweden to system RT38.

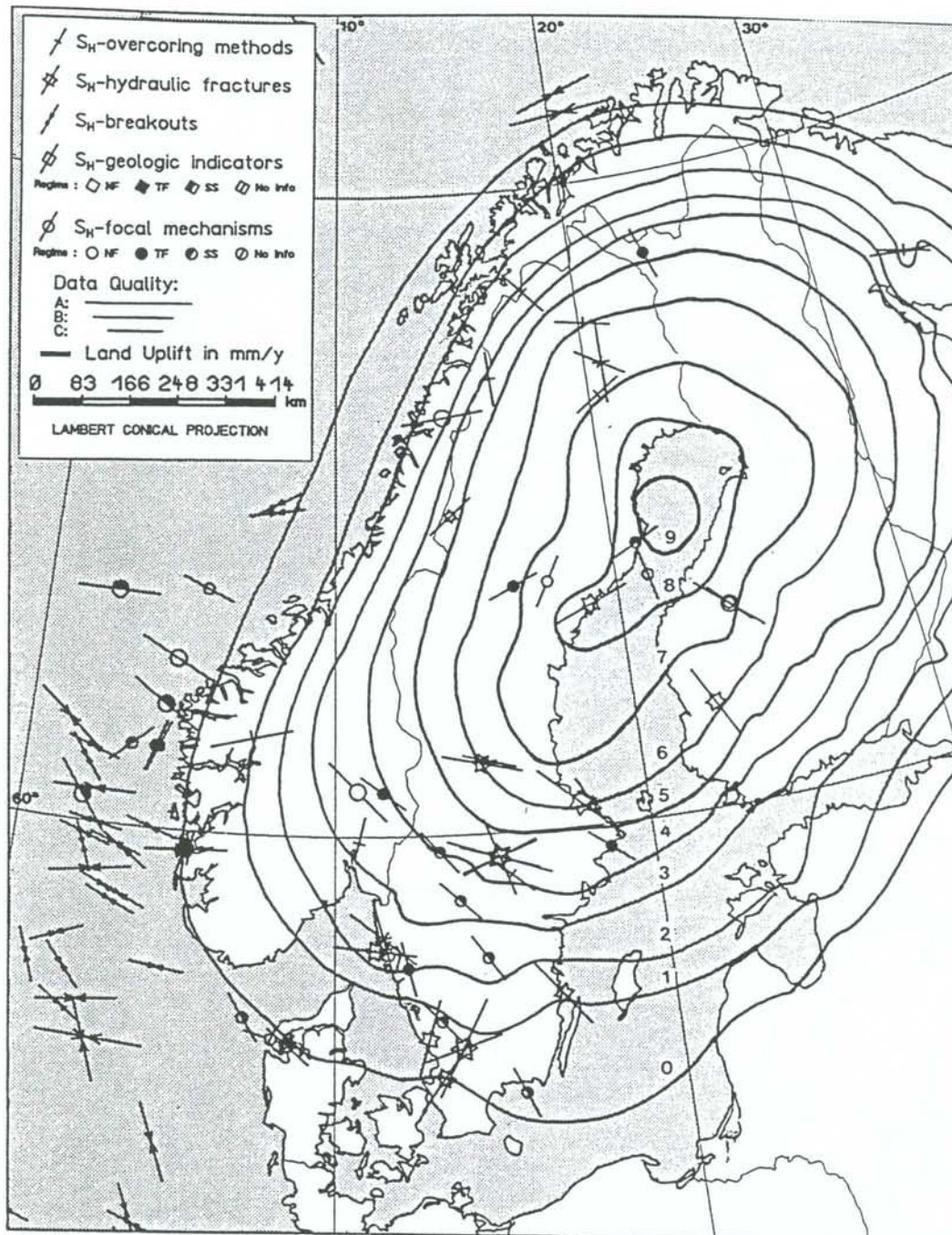


Figure 2-2 Orientations of maximum horizontal stresses in Scandinavia (Muller et al 1992)

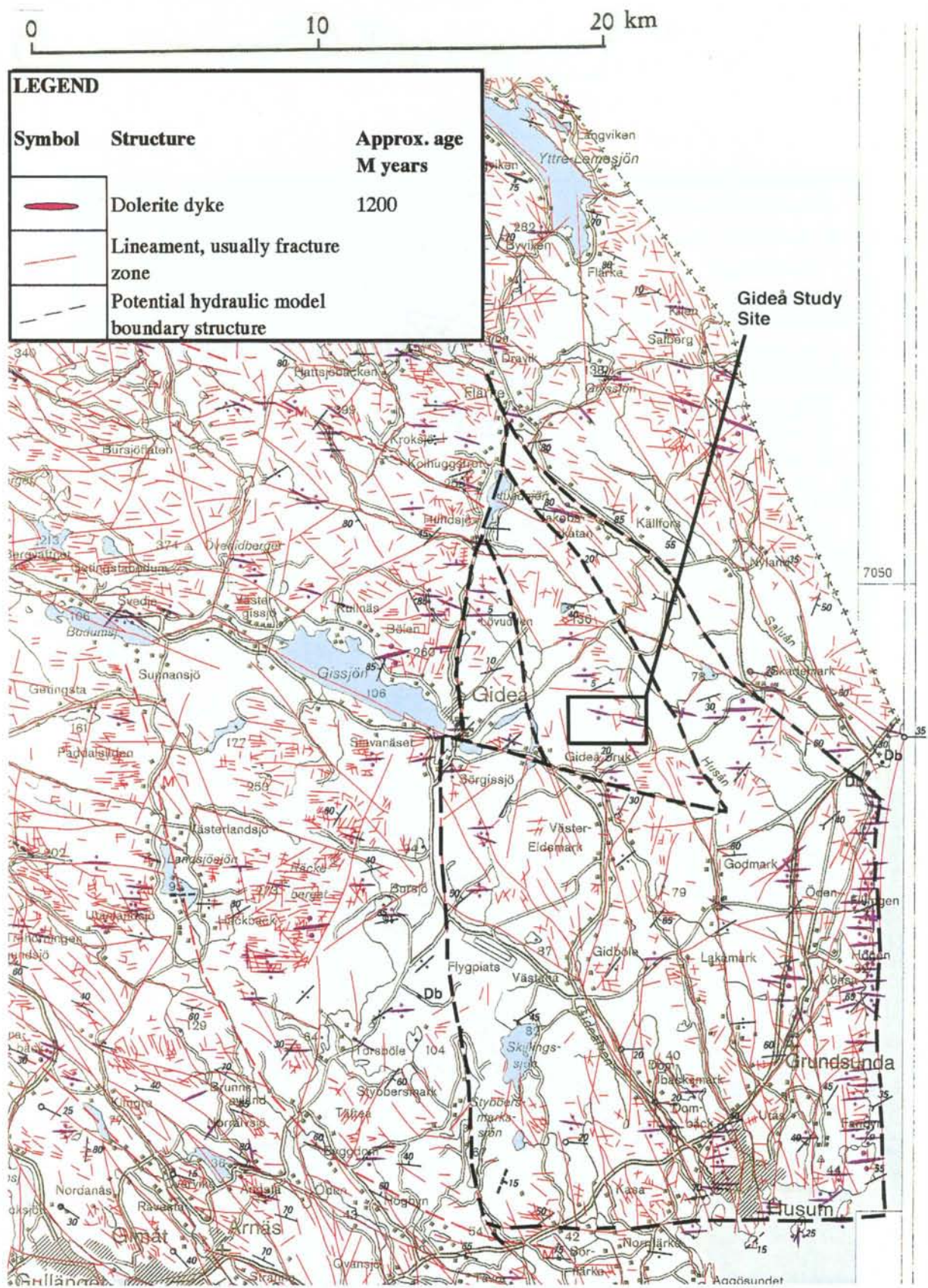


Figure 2-3 Map of regional structures (Lundquist et al, SGU Ba 31, 1990).

3 SURFACE INVESTIGATIONS, SITE SCALE

3.1 GEOLOGICAL MAPPING

The result of the geological mapping investigation (Albino et al 1983) is shown in Figure 3-1 as an outcrop map. The performed reviewing of the mapping show that some of the large outcrops do not feature bare, well defined outcrops, but are, at places, covered by soil, i.e. the area of rock exposures is less than what is indicated in the maps. The soil covered outcrop parts may, in some cases, be fracture zones or dolerite dykes. The noted rocktypes on the map are paragneiss-migmatite, dolerite and pegmatite. Unfortunately there has been no identification of the orthogneiss, an intrusive rock that may play an important role in hydraulic permeability. The same is the case for any ser- or post-orogenic granite dykes. Also outcrops mapped as gneiss may be intersected by dolerites of limited extent. Mapped foliations (Ericsson & Ronge 1986) have been added, as well as an interpretation of fold axes (antiforms and synforms). The host rock foliation varies over the study area, indicating folding or faulting. In the southeast quadrant foliations appear as both subhorizontal, dipping NW, and dipping SE and is interpreted as a fold axis with a gently dipping fold axis trending NE. There are a few more indications of fold axes in the south central part of the area, as shown in the figure.

3.2 FRACTURE MAPPING

Fracture mapping has been carried out and reported (Ericsson & Ronge 1986). Figure 3-2 shows fracture orientation diagrams for the study area and its surroundings. In the mid of the area, N-S and E-W striking joints appear to be predominant, while E-W and NE-SW striking joints dominate the SW corner of the study area, which may be explained by the location of Northeast trending zones I and II in this corner. East-West trending Zone III and IV may explain the more East-Westerly jointing found in the central region.

3.3 GEOPHYSICAL SURVEY

The geophysical survey has comprised a number of investigations, including magnetic, electric, electro-magnetic and seismic methods. Figure 3-3 shows results and interpretation of magnetic total intensity measurements. The map shows a number of E-W striking anomalies interpreted as dolerite dykes, some of which also appear in rock exposures. Figure 3-4 shows seismic velocity anomalies, results from resistivity measurements electro-magnetic investigations. Here, the interpreted lineaments possibly represent fracture zones in the rock mass. Seismic velocity anomalies more or less coincide with the electric and electro-magnetic anomalies.

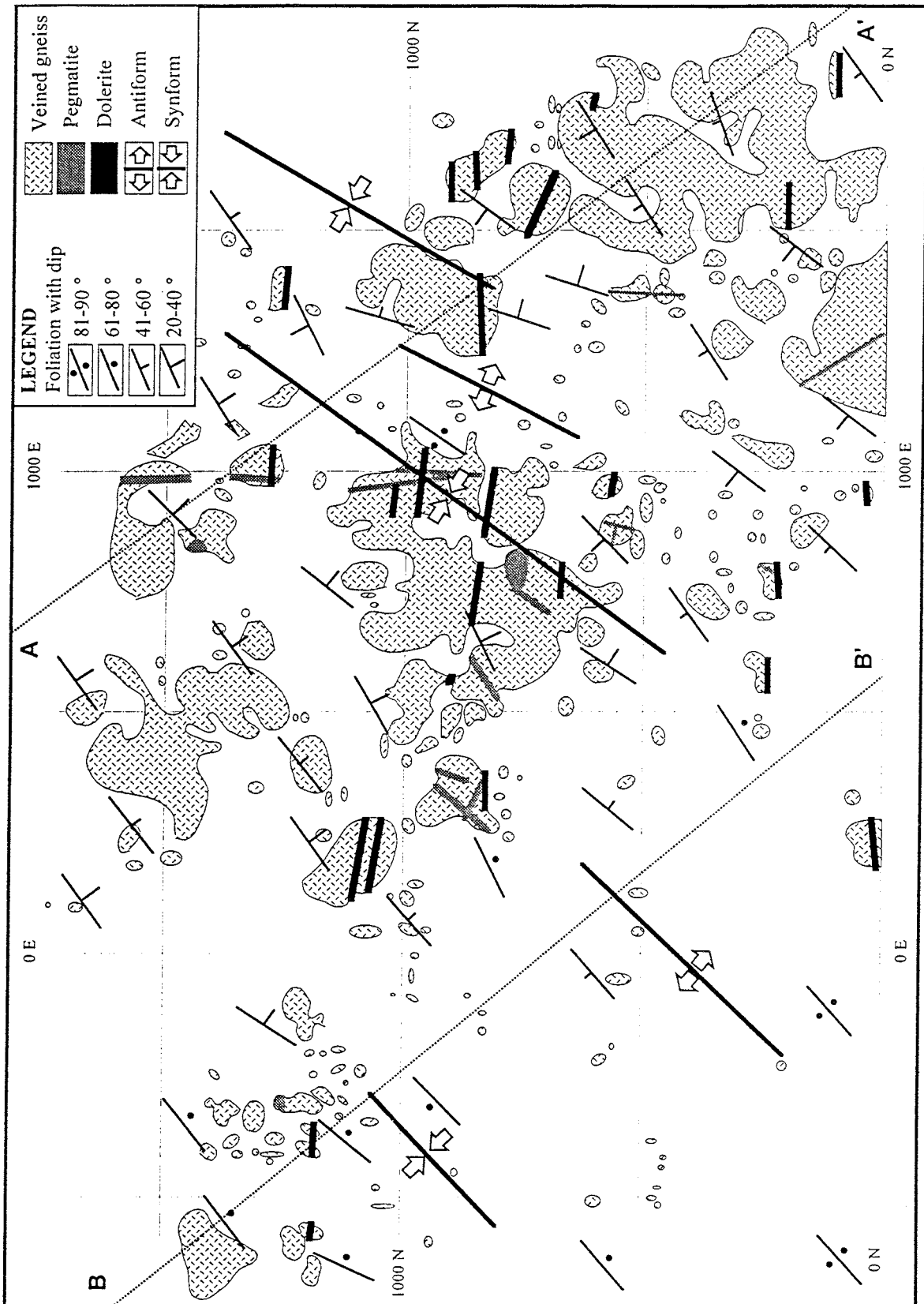
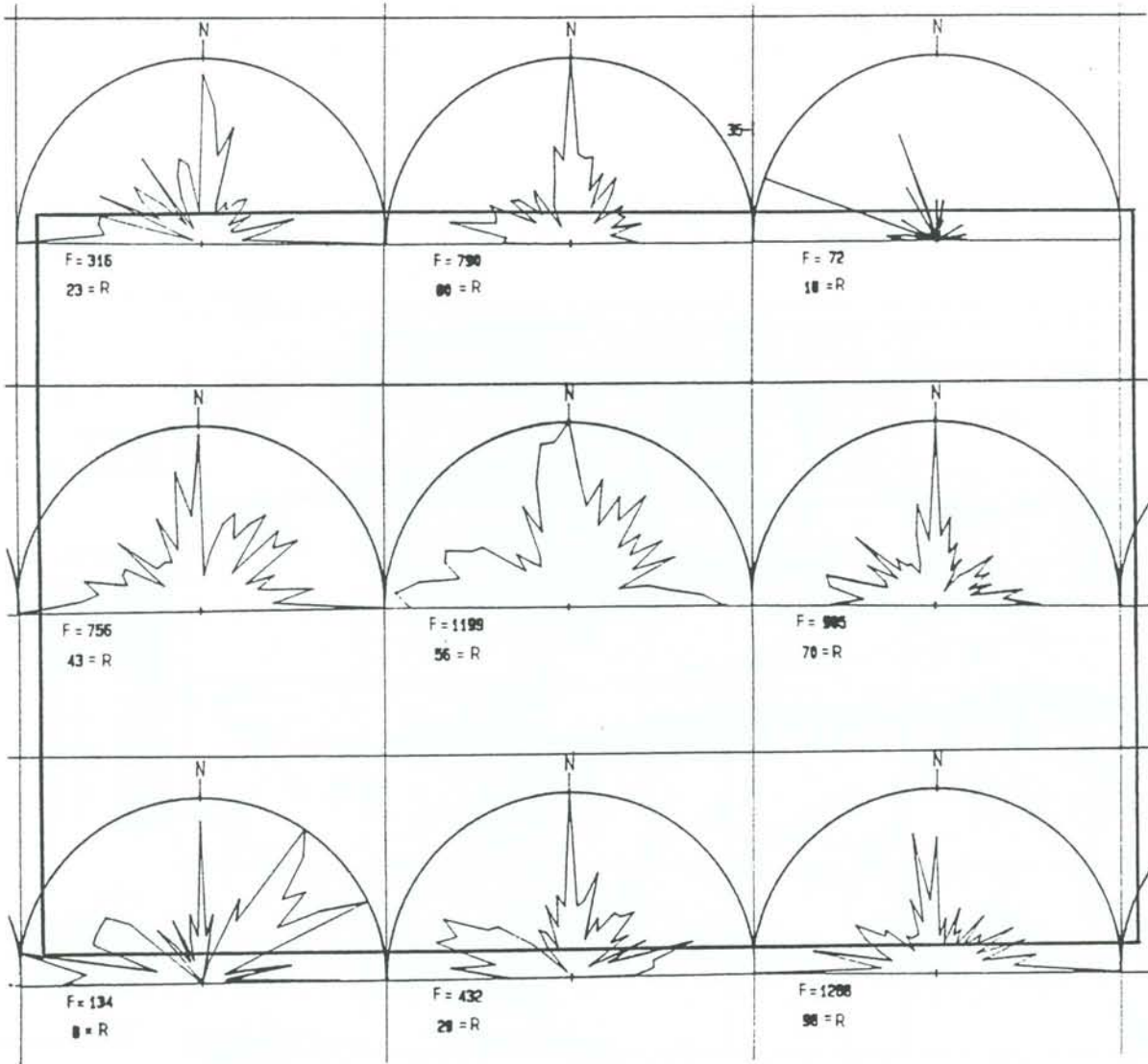


Figure 3-1 Rock outcrop map of the Gideå Study Site (Albino et al 1983). With foliations (Ericsson & Ronge 1986) and with interpreted folds.



LEGEND

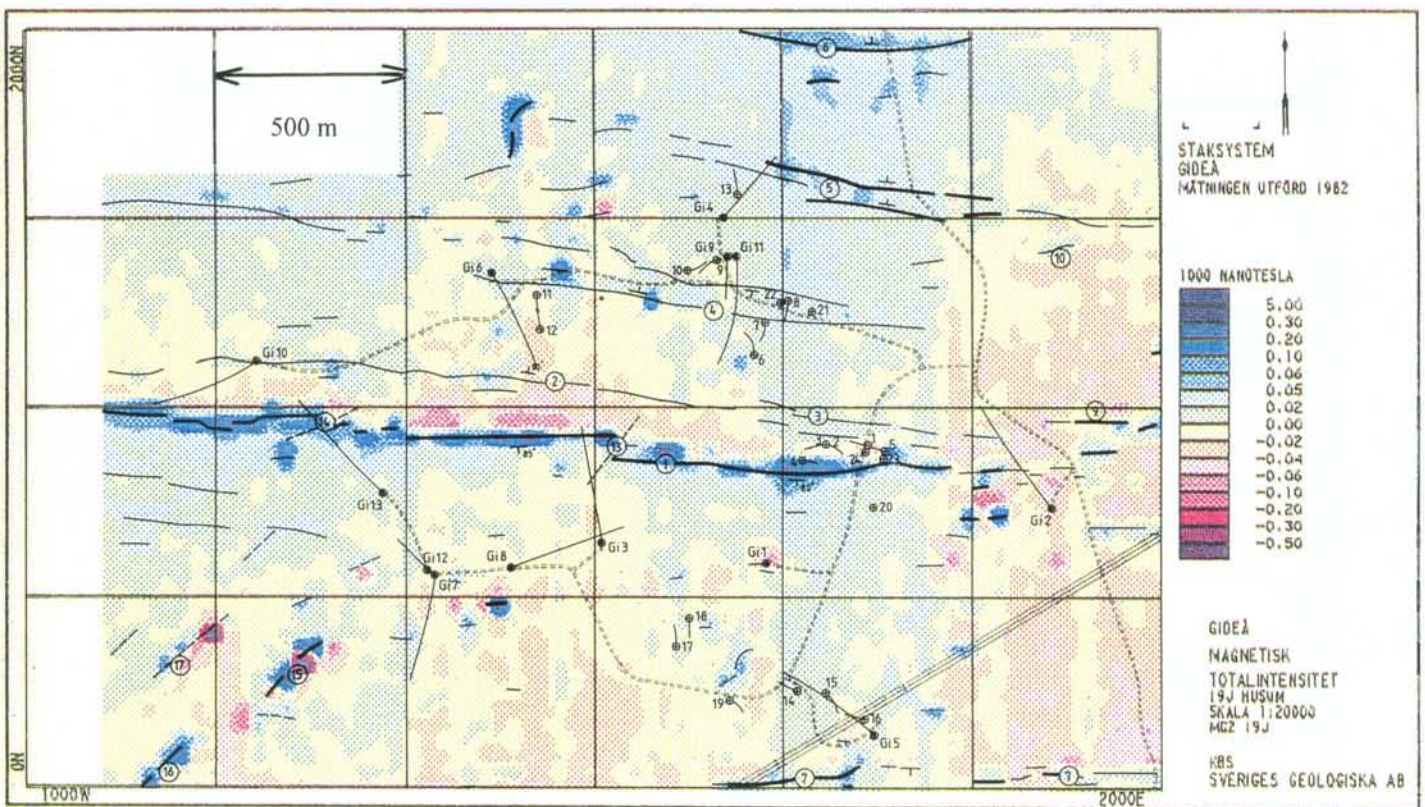
F=72 72 measured fractures in investigated area

56=R Radius correspond to 56 fractures



= Gideå study area

Figure 3-2 Fracture orientation map (Eriksson & Ronge, 1986)



LEGEND	
Magnetic lineaments	--- Fault
— Distinct	Weak
Gi 11 ● Core drilling	○ Percussion drilling

Figure 3-3 Magnetic anomalies with interpreted dolerite dykes (Albino et al 1983).

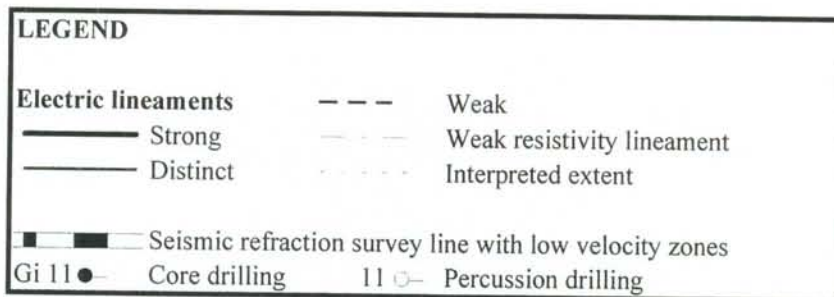
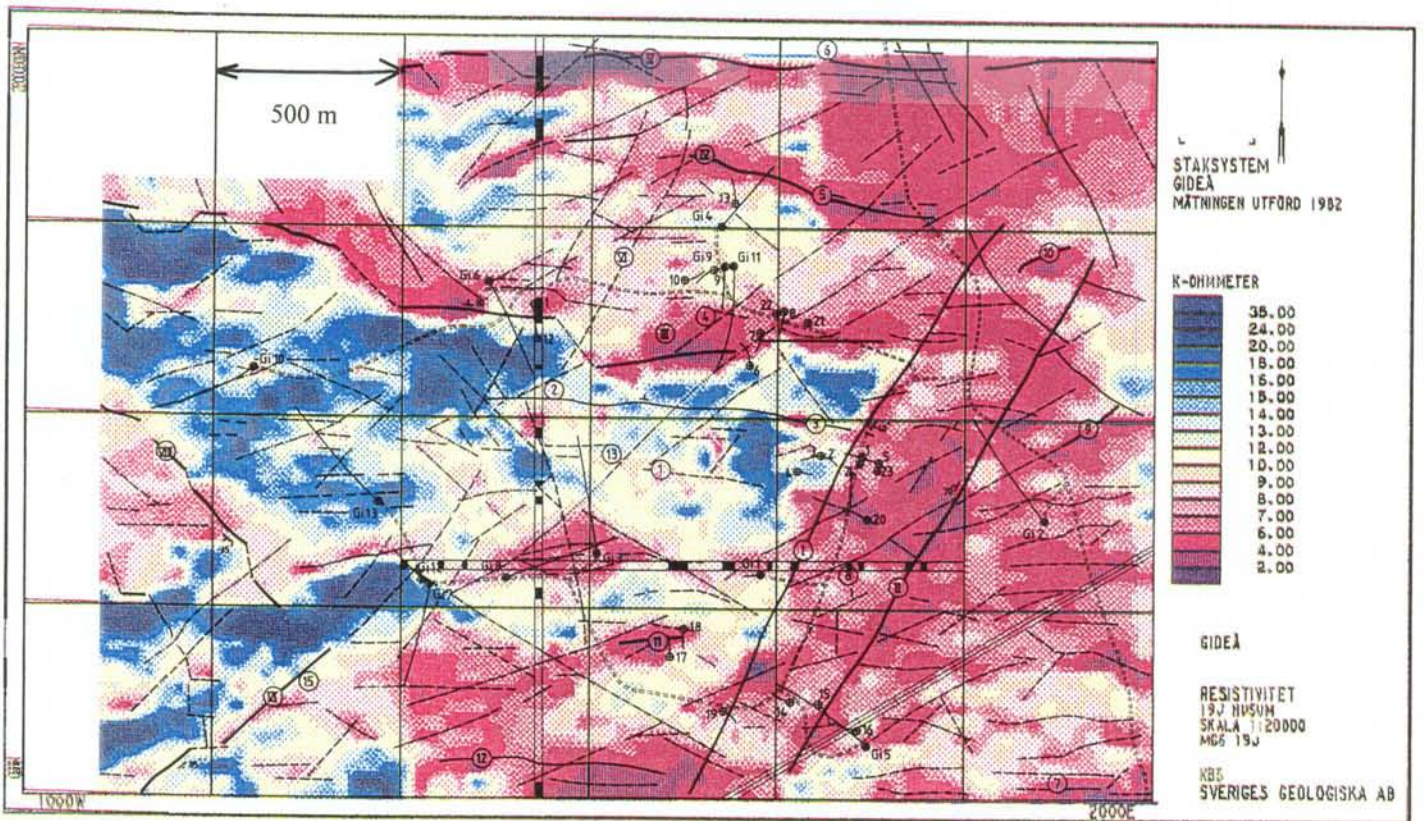


Figure 3-4 Map of seismic velocity anomalies and resistivity with interpretation (Albino et al 1983).

4 SUBSURFACE INVESTIGATIONS

Subsurface investigations include core drilling, percussion drilling and geophysical measurements in drill holes. Figure 4-1 shows the locations of the drill holes. The percussion drilling program has been designed in order to investigate dip directions and water occurrence in the fracture zones, while purpose of the core drillings has been to investigate rock mass properties, such as rock type, joint frequency, joint filling minerals, and hydraulic conductivity. In the percussion drilling program only a few parameters have been recorded, such as penetration rate, yield and inflow level. A compilation of percussion drilling from SICADA (1996) is shown in Table 4-1.

Table 4-1 Summary of percussion drillings

HGI No	Bearing	Plunge	Length	Depth	Yield, l/h	Inflow level, m
01	290	55	153	143	4000	28
02	90	55	141	130	0	-
03	250	55	125	113	0	-
04	90	55	100	92	0	-
05	290	55	115	105	4000	48
06	0	55	150	135	600	4
07	180	55	150	139	2000	28,32
08	180	55	130	118	6000	44
09	240	55	150	137	240	46
10	60	55	150	142	480	-
11	180	55	132	127	0	-
12	0	55	125	106	0	-
13	355	55	150	136	0	-
14	300	55	55	107	480	-
15	120	55	120	103	9000	116
16	300	55	132	117	6000	124
17	0	55	120	107	0	-
18	180	55	100	84	0	-
19	115	55	100	87	0	-
20	-	90	100	99	9000	95
21	-	90	90	90	0	-
22	-	90	60	60	0	-
23	-	90	90	90	0	-
24	-	90	40	40	3000	2,10,14,22

4.1 INVESTIGATIONS IN CORED DRILL HOLES

The investigations in the cored drill holes have been summarised by Ahlbom et al. (1991) from Albino et al (1982) and includes a statement of the availability of each hole (pp 71-89), and comprise core logging, sampling and analyses, petrophysics, geophysical logging, rock mechanical testing and hydraulic tests. For a comprehensive compilation of these parameters, the reader is referred to Ahlbom et al (1991) Appendix B p. 90-94.

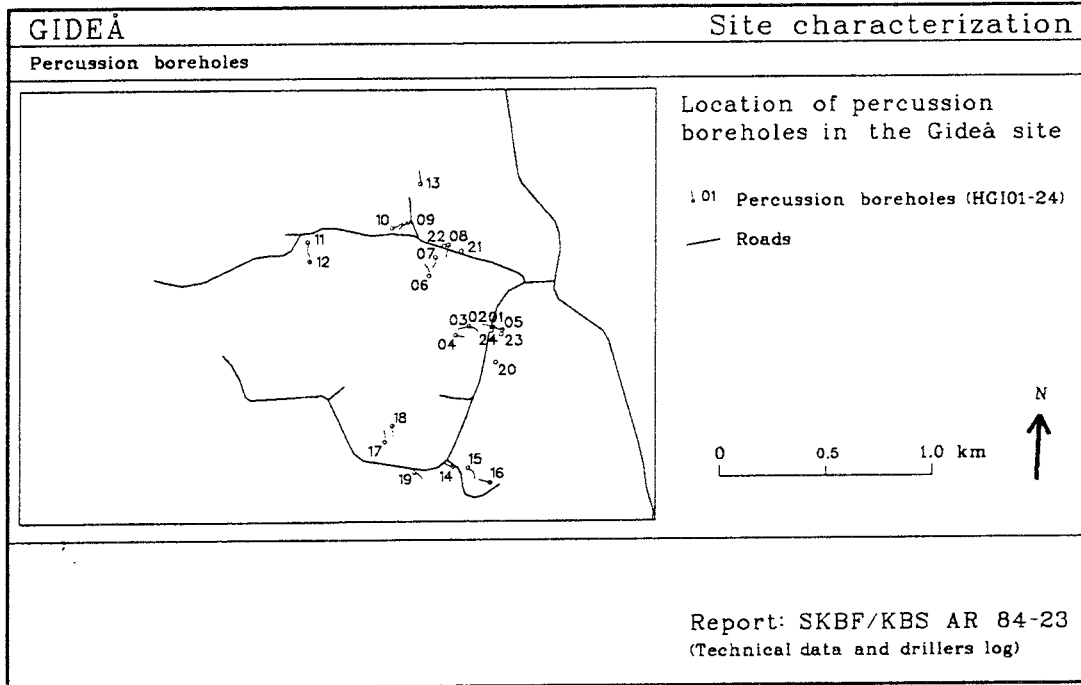
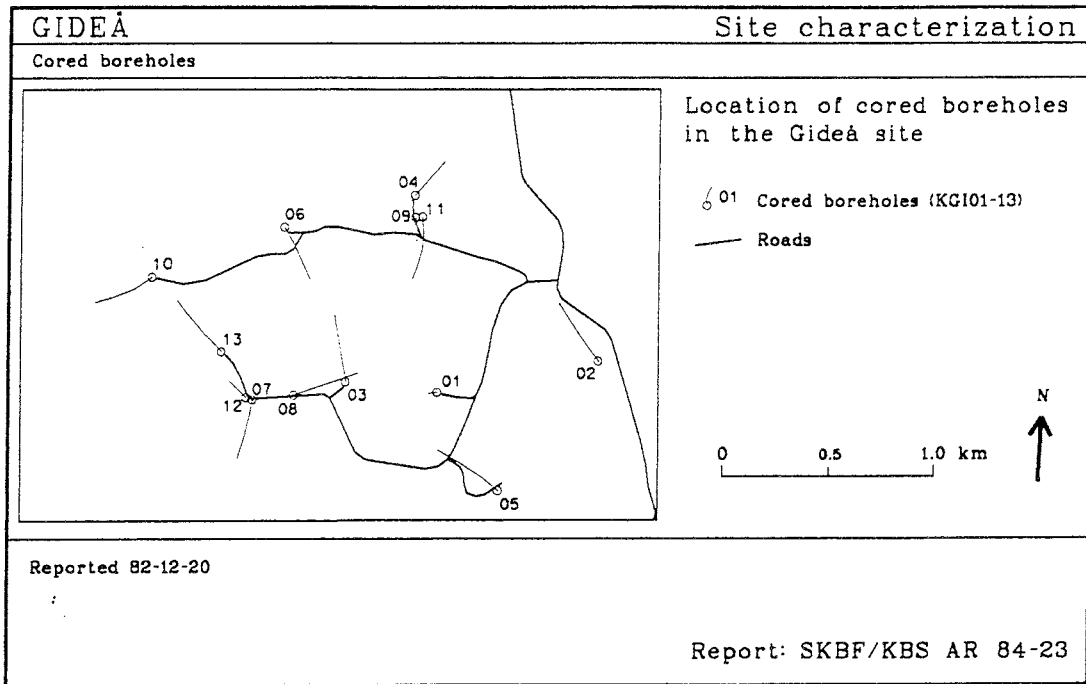


Figure 4-1 Drill hole locations (Ahlbom et al 1983).

4.2 INVESTIGATION RESULTS

The general results from the subsurface investigation can be summarised as follows;

- paragneiss-migmatites dominate
- orthogneiss occur frequently and in variable thickness throughout the site
- a number of steeply dipping dolerites can be correlated with surface investigations
- existing core logging does not distinguish well between granitic migmatite, orthogneiss and granitic dykes
- ten zones can be distinguished with variable degree of reliability
- difficulties to distinguish zones from surrounding bedrock due to little difference in fracture frequency
- conservative interpretation exclude subhorizontal zones

A number of possible models of interpretation exist for both lithology and zones. It is pointed out by Ahlbom (1991) that the correlation of a three-dimensional lithological model with the tectonic structures and highly conductive borehole sections in the area is largely missing. Also, looking at details of the presented interpretation reveals a few inconsistencies exist regarding interpreted zones.

Figure 4-2 shows a compilation of the results from core drilling KGI 05 and adjacent percussion drillings with indication of geophysical anomalies for Zones I and II and position of seismic anomalies transposed along the zones. The high yield in HGI 16 is in good accordance with the increased hydraulic conductivity in KGI 05 at about 150 m, and the high yield in HGI 15 may fit with the increased hydraulic conductivity in KGI 05 at about 200-250 m. The MaM (*mise a la masse*) measurement (Magnusson 1985) in KGI 05 indicate a connection between 547 m of depth and the surface at the position of the geophysical anomaly of zone I, and no connection with the anomaly of Zone II. Figure 4-3 shows a compilation of the results from core drilling KGI 02 and adjacent percussion drillings with indication of geophysical anomalies for Zones I and II. Figure 4-4 shows a compilation of the results from percussion drillings over zones I, II and III. It may be noticed that HGI 14 has a low yield and HGI 11, 22 and 23 are all dry, in spite of being interpreted to intercept major water-bearing zones.

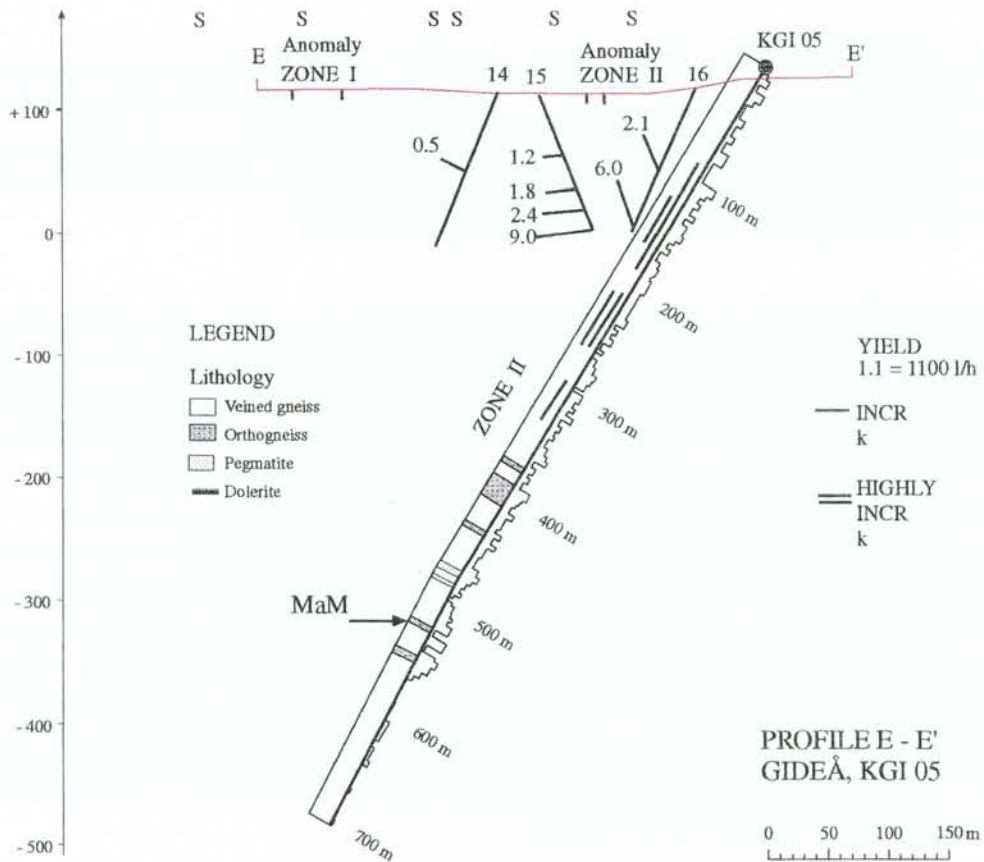
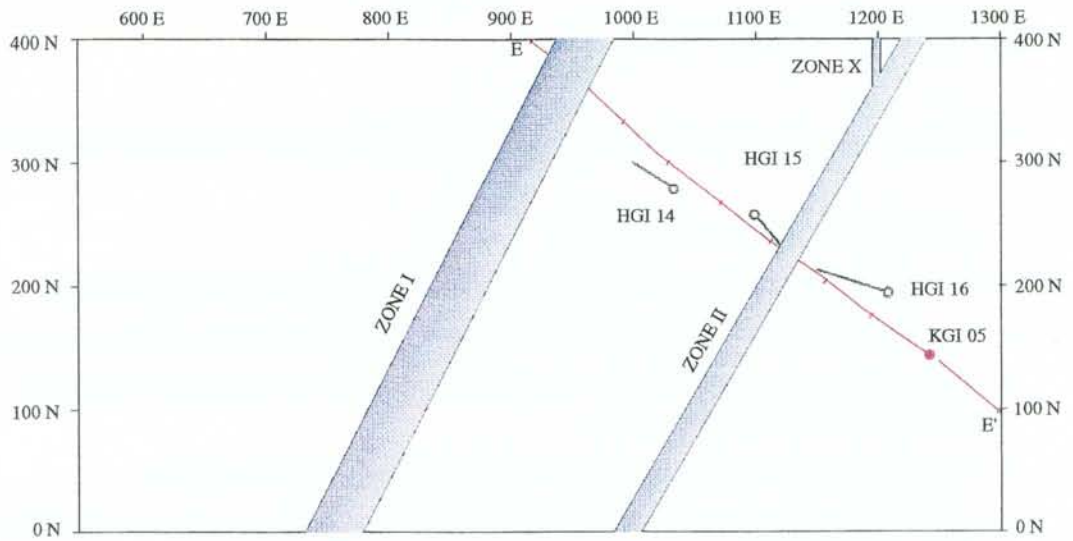


Figure 4-2 Profile with results from percussion drillings HGI 14, 15 & 16 and Core drilling KGI 05.

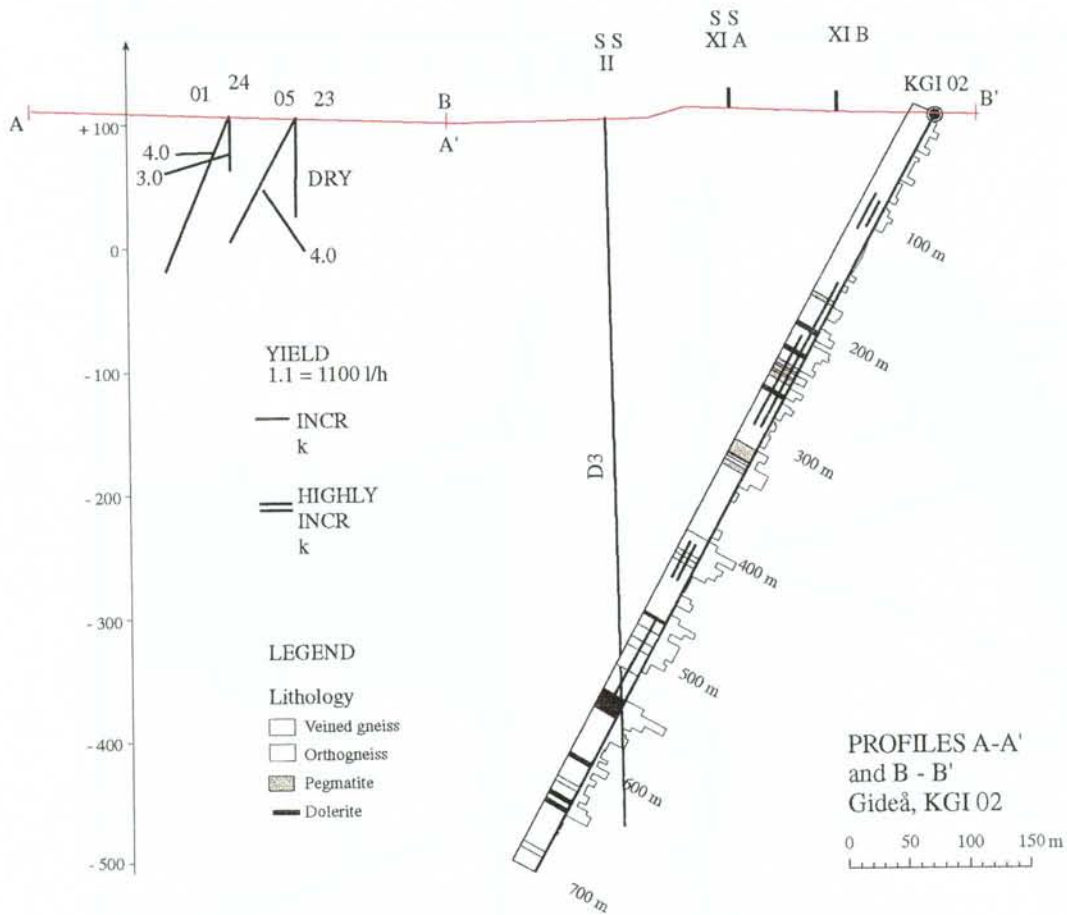
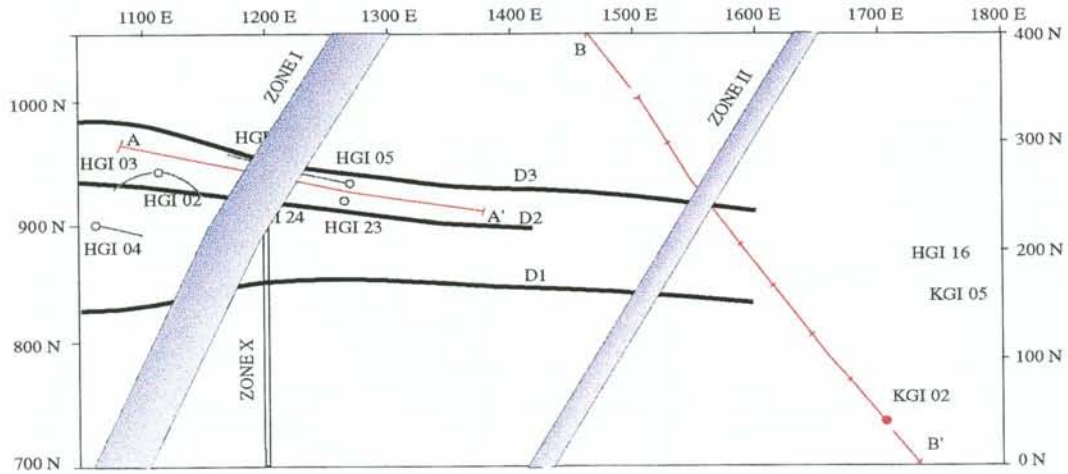


Figure 4-3 Profile with results from percussion drillings HGI 01, 02, 05, 23, & 24 and Core drilling KGI 02.

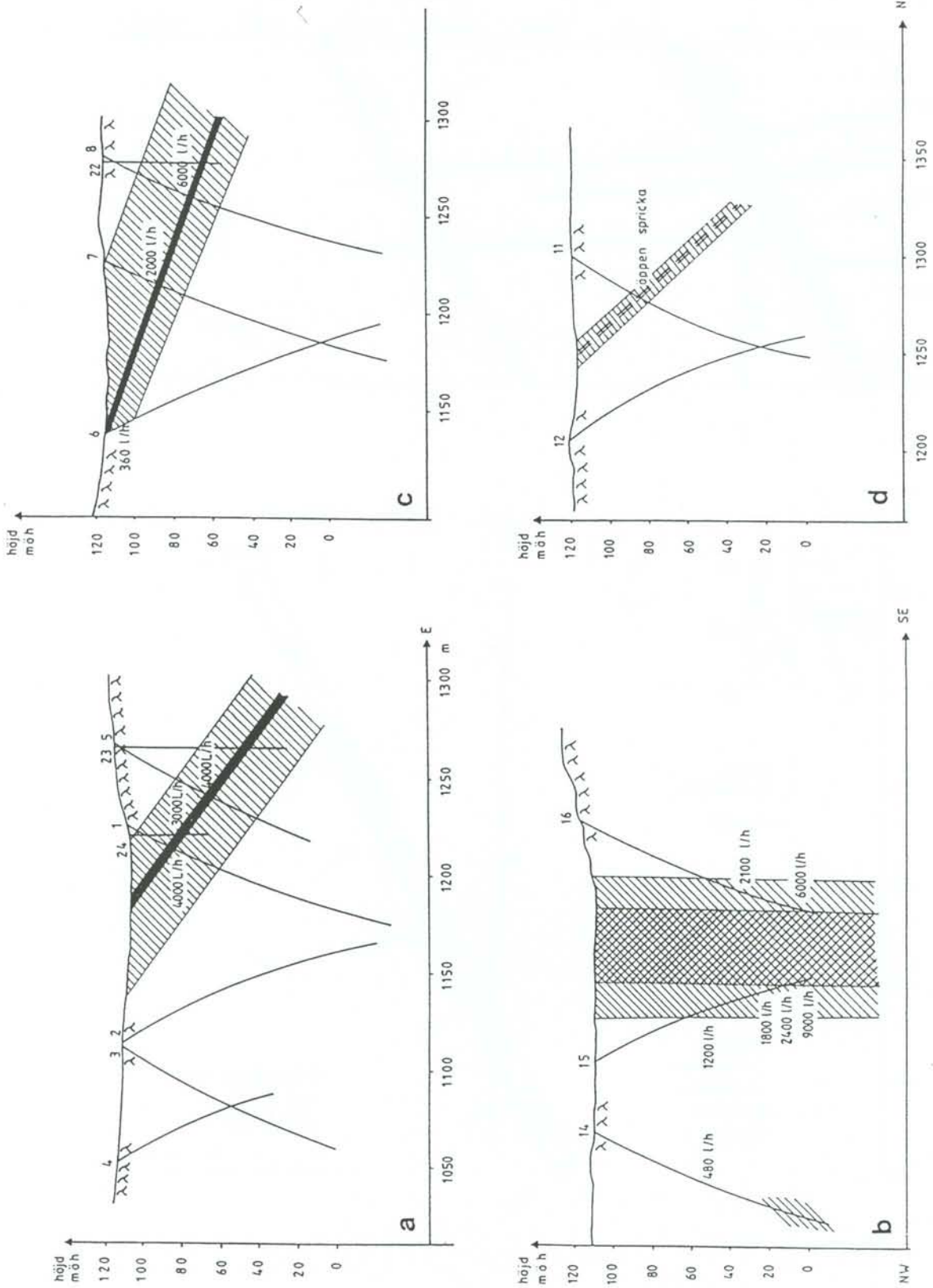


Figure 4-4 Profiles with results from percussion drillings over Zone I (a), Zone II (b) and Zone III (c, d) (after Ahlbom et al 1983).

5 ANALYSIS OF INVESTIGATION RESULTS

5.1 LITHOLOGICAL DATA

Based on variations in the orientation of foliation, measured by Eriksson & Ronge (1986), and on the regional geology (Lundqvist 1990), the migmatized greywackes in Gideå have been reinterpreted to be folded with gently dipping fold axes trending NE. The foliation in the Gideå area is interpreted to be mainly related to the deformation and does not constitute remainders of a primary bedding. The orthogneiss found in the cores as dm to m wide sections are interpreted to be of prim- orogenic age and thus deformed by the same forces which have deformed the paragneiss (Lundqvist 1990, Ahlbom et. al. 1991). The folding as shown in Figure 5-1 thus comprise the orthogneiss as well as the paragneiss, but appear not to influence the intrusion of later magmatic bodies of dolerite.

By studying the foliation measured by Eriksson & Ronge (1986) folding is more gentle in the Northeastern part of the area, as shown in profile A-A' with one anticline and two synclines with gently dipping fold legs. In the Southwestern part foliation is steeper (profile B-B') which can be interpreted as steep fold legs in two synclines and a minor anticline in the center. Studying the occurrence of orthogneiss in the cores situated close to the profiles, show that orthogneiss, folded with the sedimentary migmatites, occurs predominatly in fold legs and can be interpreted to occur in folded layers of variable extent. In profiles A-A', B -B' orthogneiss along cores are shown as dark cylinders and lines represent the folded horizon which the orthogneiss once intruded. Figure 5-2 visualizes a conceptual picture of how orthogneisses may occur throughout the site, with larger bodies in the fold legs. Fracturing seem little influenced by change in orientation of foliation (cf Figure 3-2).

By means of data from magnetic anomalies, rock exposures and core drillings (extracted from SICADA 1996), a number of dolerite dykes have been identified. Table 5-1 shows a compilation of the results and an analysis of the reliability levels for each dyke. For reliability criteria, see Appendix 1.

Some of the core drillings have been designed in order to intercept the dolerite dykes, while others intercept by incident. Figure 5-3 shows a profile athwart Dolerite dykes Nos. D1, D4a, D4b and D8 with intercepting holes. It should be borne in mind that the holes are transposed on the profile. Dolerite D1 is also exposed in several rock outcrops. KGI 13 features two interpreted intercepts with D1, fitting with the faulting of this dyke (cf Figure 3-3). The D8 dolerite in KGI 07 corresponds to a minor magnetic anomaly, but there are no outcrops in that area. D2 is also exposed in a number of outcrops. However, it is not interpreted as just one consistent dyke, but as a number of dykes in and around the D2 plane. The same is assessed to be the case for D3.

One of the purposes for an update of the lithological model to three dimensions was to analyse the possibility for the existence of subhorizontal dolerite bodies in the rock mass. Such dolerite sills exist in the adjacent area (Lundqvist et al. 1990). Based on the intersection angle with the borehole axis, an interpretation of dolerites being steep or gently dipping is possible. Core drilling KGI 01 is the only vertical hole, and thus the only hole where it should be possible to identify horizontal dolerites which should have a contact with the side rock almost perpendicular to the core axis. According to the files, four dolerites are intercepted by the drilling. During the core inspection, no dolerite could be traced at the four positions or in the adjacent core boxes, while dolerite was encountered at the logged positions in all the other cored boreholes. In holes KGI08, 10, 12 and KGI13 there are a few dolerite encounters, the core axis angle of which do not fit with vertical dolerites striking East-West, but well with horizontal dykes.

Through 3-dimensional geometric modelling it is obvious that if these dolerites are subhorizontal their extent seem very limited, which is very much different from the subhorizontal dolerites reported by Lundquist (1990) south of Gideå. Also, with the results from KGI 01 in mind, horizontal dolerites appear to be small and limited in extent, if present, at least in the southern part of the study area.

5.2 ZONE DATA

Based on the original investigation material (extracted from SICADA 1996), the conceptual model by Albino (1983) and the proposed weaknesses by Ahlbom (1993), a new updated structural model is presented. However, as the update is based on a number of indications that supports a simpler and more conservative explanation than presented by Albino (1983), the previous model is not considered to be wrong but rather to be an alternative more complex interpretation.

Figure 5-4 shows interpreted lineaments with locations of drill holes. The difference from the first model (Albino et al. 1983) is the addition of Zones XI and XII and some resistivity anomalies important for the analysis. For zones I and II, two interpretation dip alternatives exist:

Alternative 1 (Albino et al. 1983)	Zone I dips 30-40 degrees to the Southeast Zone II dips steeply to the Northwest
Alternative 2 (this report)	Zones I and II both dip steeply to the Southeast

5.2.1 Zones I and II. Interpretation Alternative 1

Figure 5-5 and Figure 5-6 show compilations of investigation data at KGI 05 and KGI 02, respectively, (Albino et al. 1983), with Zone I dipping gently to the Southeast and Zone 2 dipping steeply to the West. This is the interpretation presented

in the conceptual model (Albino et al. 1983 and Ahlbom et al. 1991), here called Alternative 1. Although Ahlbom et al. (1991) presented data from *mise a la masse* measurements indicating a steeper dip of Zone I, the final interpretation did not include this, although the reliability level was set to **probable** due to the doubt concerning the dip. For this reason, the investigation data have been reviewed in the present work. A look at the figures results in the following list of weaknesses in Interpretation 1:

- The low yield in HGI 14 does not fit with a highly conductive zone as indicated by the extremely high yields in HGI 15 (Figure 5-5).
- The interpretation does not give any explanation to the very high yield in HGI 16 and the high conductivity in KGI 05, 150 m.
- The interpretation features a very narrow Zone II, while the results from HGI 15 and 16 show a wide zone (cf Figure 4-4b).
- The interpretation does not satisfy the result from the *mise a la masse* measurements, which indicates a connection between level 547 m in KGI 05 and the surface at Zone I, but not with Zone II.
- The interpretation does not satisfy the results from hole HGI 23 which is completely dry, while the nearby holes HGI 01, 05 and 24 all have high yields (Figure 5-6).
- The interpretation does not give any explanation to the high conductivity in KGI 02, 100 and 200-300 m.

5.2.2 Zones I and II. Interpretation alternative 2

Within this study a new interpretation is made of the fracture zone model. Based on re-evaluated *mise a la masse* tests and logistics in borehole intercepts of fracture zones, Zones I and Zone II are updated. Also two new fracture zones have been added to the model (cf Figure 5-4). Figure 5-7 and

Figure 5-8 show Interpretation Alternative 2 with Zones I and II both dipping steeply towards the Southeast and with Zone II divided into two zones: II a and II b, the latter dipping less steeply. At KGI 02, two geophysical anomalies XI a and XI b (Figure 5-4) are interpreted to cross KGI 02 at 100 (XI b) and 200-300 m (XI a). Interpretation Alternative 2 feature the following advantages:

- Satisfies the *mise a la masse* test
- Satisfies the low yield in HGI 14 (Figure 5-7) and the dry hole HGI 23 (Figure 5-8).
- Satisfies the two zones with high conductivity in KGI 05, 150 and 200-250 m and connects them with corresponding high yields in HGI 15 and 16 (Figure 5-7)
- Satisfies the two seismic anomalies at Zone II (cf Figure 3-4)
- Fits with the high conductivity zones in KGI 02, 200-300 m and 400 m (Figure 5-8).
- Explains the high conductivities at 100 m and 200-300 m in KGI 02
- Explains the wide high conductivity zone in KGI 02 at 200-300 m as a crossing

- Satisfies the two seismic anomalies at Zone X (one of them fits with Zone XI a)

5.2.3 Zone III

Figure 5-9 shows a compilation of the results from core drilling KGI 06, the adjacent percussion drilling HGI 11 with indication of geophysical anomaly for Zone III and the interpretation. At this location, the conditions are much more complex. Hole KGI 06 penetrate a shear zone, interpreted to be Zone III a, the same as penetrated by KGI 04, 09 and 11 and HGI 07, 08 and 11. The following questions remain:

- Holes HGI 11 and 22 are completely dry while holes HGI 07 and 08 yield a lot of water, and hole KGI 06 feature high hydraulic conductivity at the passage, but not considerably higher in the zone than in the side rock.
- Hole KGI 11 feature the same low hydraulic conductivity at the Zone III passage as for the side rock, but lower than average for the site (Figure 5-10).

The results fit well with the concept of a shear zone which can feature different yields along its extension. However, there is also a geophysical anomaly Zone XII which can explain the high yields in HGI 07 and 08. It is parallel with the regional maximum horizontal stress and with the highly conductive Zone XI. It should be mentioned that the water bearing holes HGI 07 and 08 are inclined while the dry holes HGI 21 and 22 are vertical. Zone XII would fit these data better than Zone III a. Figure 5-4 shows the alignments of the fracture zones and

Table 5-2 shows the data and the reliability of the zones according to the criteria in Appendix 2.

Table 5-1. Dolerite dykes at the Gideå study site

Dolerite No	Magn anom	Magn dip	El/EM interp	Slingr anom	VLF anom	Seism anom	Resis anom	Surface observ	Surf dip observ	Core No	Appr depth	Maximal thickness	Reliability (App 1)
D1	M1 strong	80 S	weak	weak	none	weak	weak	5 exposures	80 S	KGI 02	200	2.4	certain
										KGI 03	460	4.1	
										KGI 13	244&299	4.8	
D2	M2 weak	80N	distinct	distinct	no data	no data	none	3 exposures, 1 depression	steep	KGI 02	259	0.3	certain
										KGI 06	570	12.8	
										KGI 10	130	4.8	
D3	M3 weak	no data	distinct	distinct	no data	no data	weak	2 exposures, 1 depression	steep	KGI 11	683	2.6	certain
										KGI 02	550	12.8	
										KGI 11	665	1.8	
D4a	M4a weak	N	weak	weak	no data	no data	weak	no exposures	no data	KGI 06	40	25.8	certain
										KGI 09	190	1.9	
D4b	M4b weak	steep S	none	none	no data	no data	none	1 exposure	steep	KGI 11	190	1.0	certain
										KGI 09	144	2.4	
D5a	M5a weak	N	none	none	no data	no data	none	no exposures	no data	no core observations		no data	probable
D5b	M5b strong	N	strong	strong	no data	no data	strong	no exposures	no data	no core observations		no data	probable
D6	M6 strong	N	strong	strong	no data	no data	strong	no exposures	no data	no core observations		no data	probable
D7	M7 strong	steep S	weak	none	no data	no data	weak	1 exposure	no data	no core observations		no data	certain
D8	weak	steep S	no data	no data	no data	no data	no data	no exposures	no data	KGI 08	570	1.4	probable

Table 5-2. Reliability levels of fracture zones at the Gideå Study Site

Zone No	Zone No	interpr anomaly dip	Slingr anom	Resis. anom	VLf anom	Seism ref width, velocity	Surface observ	Core drilling No	Approx depth	Percus. drilling No	Yield (l/h), Appr depth (m)	Remarks (MaM = mise a la masse test)	Strike	dip	Reliability (App 2)
1	I	E	strong	strong	E dip	10, 3300	200 m wide depression	KGI 02	prob beyond hole end (possibly 650)	HGI 1 HGI 5 HGI 23 HGI 24	4000, 24 4000, 48 dry 3000, 21	MaM: pos result with electrode at 547 in KGI5	NNE	steep East	certain
2	II	steep W uncert	strong	strong	steep	10, 3500 (A) 10, 4000 (B)	depression, steep outcrop edges	KGI 02 KGI 05	520-567 210-290 (B) 400-420 (A) high k 120-160 (B) 220-260 (A) high k	HGI 15 HGI 16	9000, 116 6000, 124	MaM: no result with electrode at 547 in KGI5	NNE	80 East (A) 60 East (B)	certain
3A	III A	N	strong	strong	N	50, 3700	E-W striking depression	KGI 04 KGI 06 KGI 09 KGI 11	230, crushed rock 60, shear indication 130, shear, clay 130, shear ind	HGI 11	dry, fracture at 40 prob w clay	Clay, shear, low hydr cond in cored holes	E-W	30 N	certain
3B	III B	N	strong	strong	N	50, 3700	E-W striking depression	KGI 06 KGI 11	220 340	none		Low hydr cond in cored holes	E-W	steep N	probable
4	IV	N	strong	strong	N	50, 4500	depression	KGI 04	630, low k	none			E-W	Steep N	possible
5	V	steep S	none	none	N	100, 4500 20, 3600	depression	no holes		none			E-W	Steep N	possible
6	VI	E	distinct	none	no data	10, 4000	depression	KGI 03 KGI 04 KGI 07 KGI 12	625 680 380 60	none		MaM: pos result at 293 and 372 in KGI7	NNE	70 SE	probable
7	VII		weak	weak	no data	no anomaly	weak depression	KGI 03 KGI 06	335 450	none			NNW	75 E	possible
8	VIII		strong	strong	no data	no data	depression	none		none			NW	steep SW	possible
9	IX		weak	weak	no data	no data	depression	none		none			E-W	N	possible
10	X		weak	weak	no data	5, 3500	depression	none		none			N-S	vertical	possible
11	XI		weak	strong	no data	5, 3500	depression	KGI 2	90-110 (XI B) 200-300 (XI A)	none			ENE	75 SE	probable
12	XII		weak	distinct	no data	no data	depression	KGI 11	possibly 650	HGI 7 HGI 8	2000, 28 6000, 44		ENE	75 SE	probable

5.2.4 Subhorizontal zones

No subhorizontal zones were included in the Albino (1983) model for conservative reasons since generic modelling showed that subhorizontal conductive zones above the repository depth would substantially reduce the ground water flow. In other words, there were little efforts to investigate any occurrence of subhorizontal zones in Gideå.

An analysis of possible indications of subhorizontal zones in Gideå show that there are a few possible conductive structures intersecting HGI 20 and KGI 02. HGI 20 features a high artesian yield (Timje 1983) which would fit more or less with a more gentle dip of zone I, as in Alternative 1 (Albino 1983), but in that case problems described in Section 5.2.1 would remain. However, there are also other nearby geophysical anomalies (Figure 5-4) which could explain the water occurrence. HGI 20 lies on or very close to a WNW striking anomaly with connections (Zones X, II, XI c, XI a and XI b) to the rocky hills NNE and ESE of the hole at an altitude of some 25 metres higher up, high enough to explain the artesian water in HGI 20 as well as in KGI 02. Further, horizontal fractures have been mapped in the hills between HGI 20 and KGI 02. However, in HGI 20 no water has been encountered until at a depth of 95 metres, where it could well intersect a subvertical offspring to zone II. The results from the other percussion holes generally show no water, unless the hole is inclined towards a zone. These results indicate that, at the Gideå site, the water bearing fracture zones are more or less steep, and that horizontal or gently dipping water bearing fractures are absent or rare, or limited to stress relief subhorizontal joints in the hills.

5.3 RESULTS OF CROSSHOLE SEISMIC INVESTIGATIONS

Crosshole seismics have been carried out in a number of holes by Pihl et al (1987) and has resulted in three interpreted low velocity layers;

1. Located in the northern part of the study area dipping gently to the North. This zone fits well with Zone IIIa.
2. Also located in the northern part of the study area, but dipping gently to the South. It does not fit with any of the zones, but fits with the Southeast dipping foliation in the surrounding area and may be interpreted as a mica rich part of the migmatite.
3. Located in the southern part of the study area dipping gently to the North. It does not fit with any of the zones, but fits with the northwest dipping foliation in the surrounding area. It may also be interpreted as a mica rich part of the migmatite, possibly the same layer as layer No 2.

The crosshole seismics are in accordance with observations in the field, such as foliation records (Ericsson & Ronge 1986), geophysical anomalies and with borehole results.

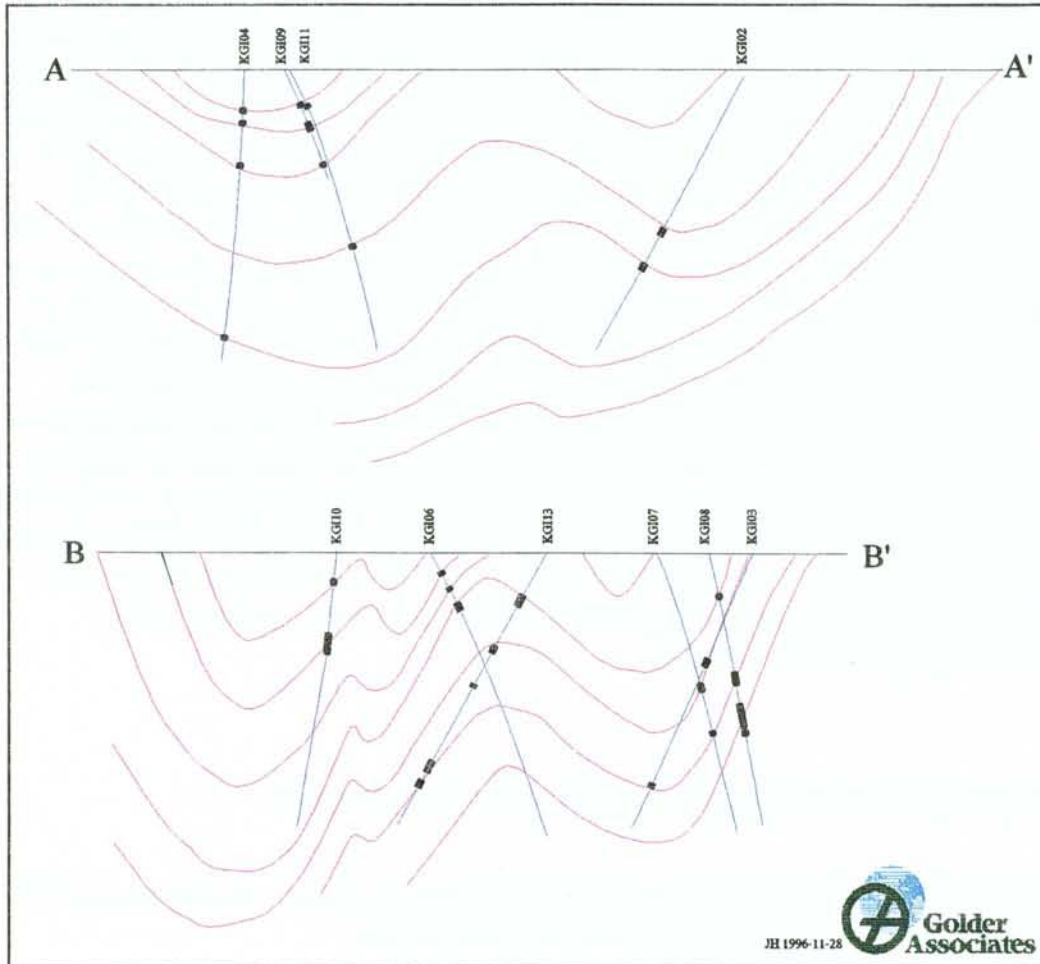


Figure 5-1 Profiles AA' and BB' showing the folded nature of the migmatite in the Gideå study area with bodies of orthogneiss along the foliation. Dark cylinders represent orthogneiss in drill cores situated in the vicinity to the profiles.

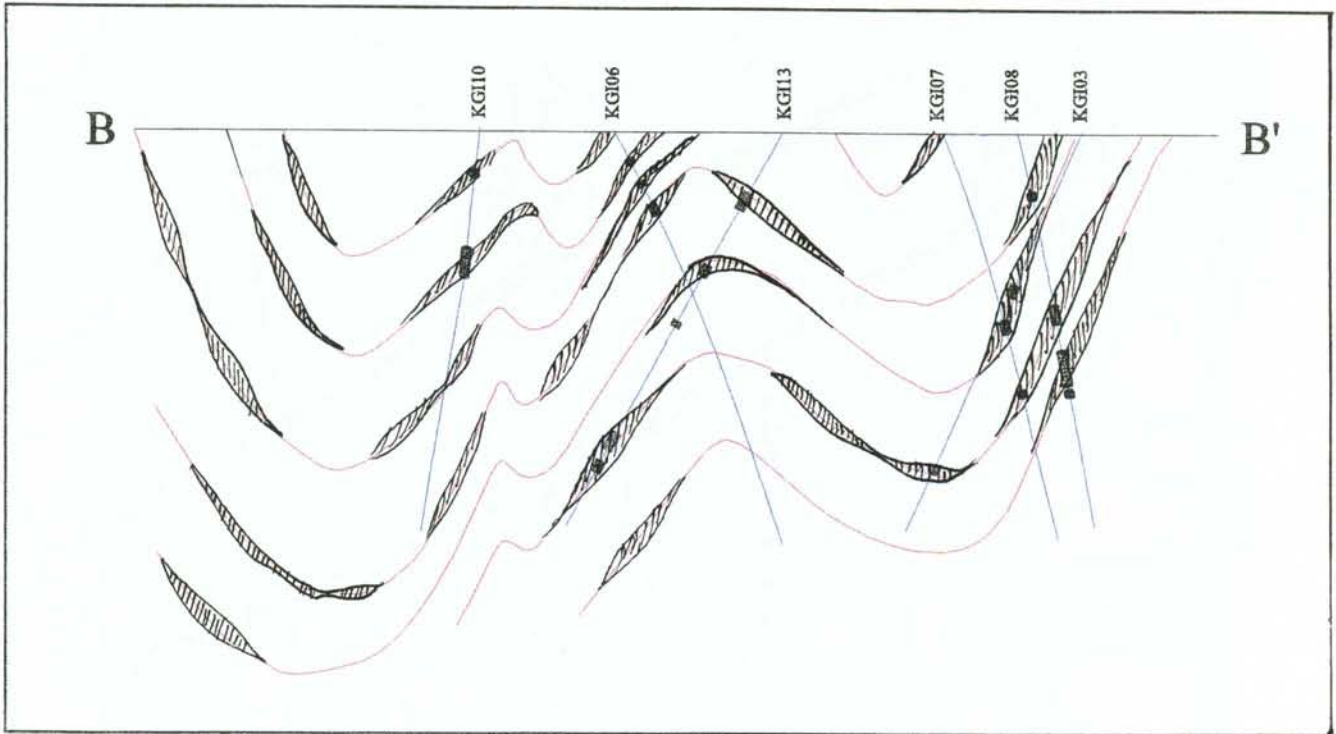


Figure 5-2 Conceptual cartoon of the occurrence of orthogneiss along profile B-B'

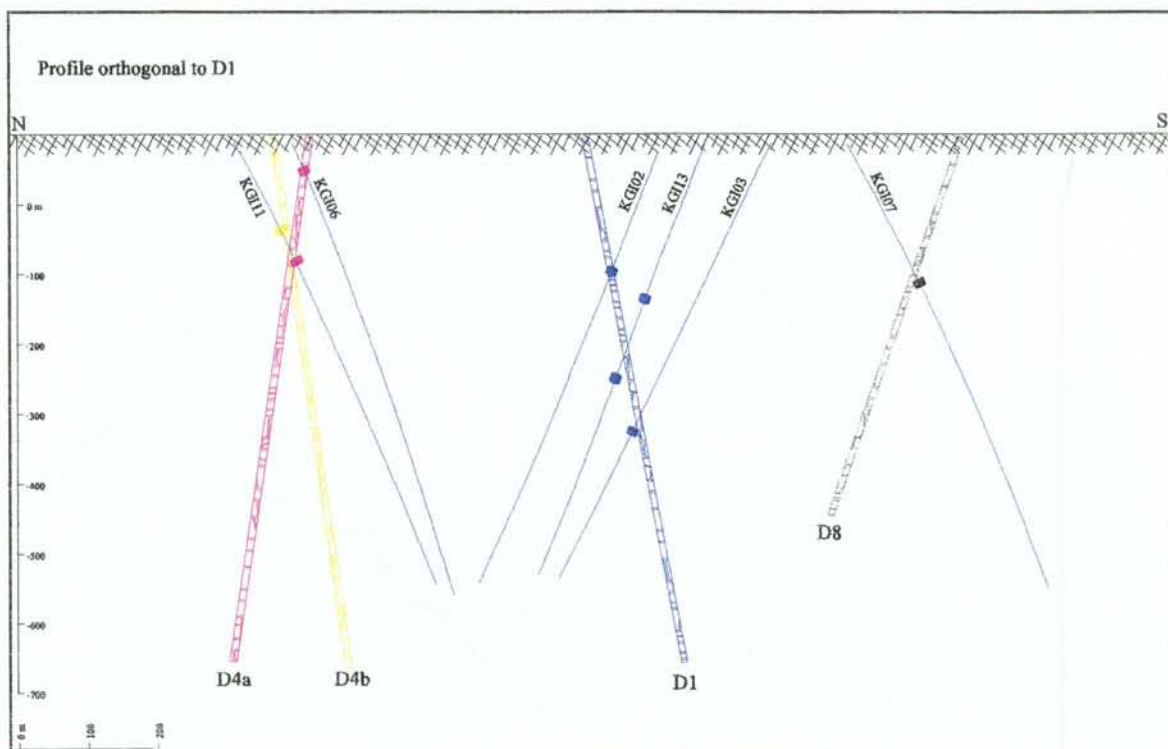


Figure 5-3 Profile athwart D1

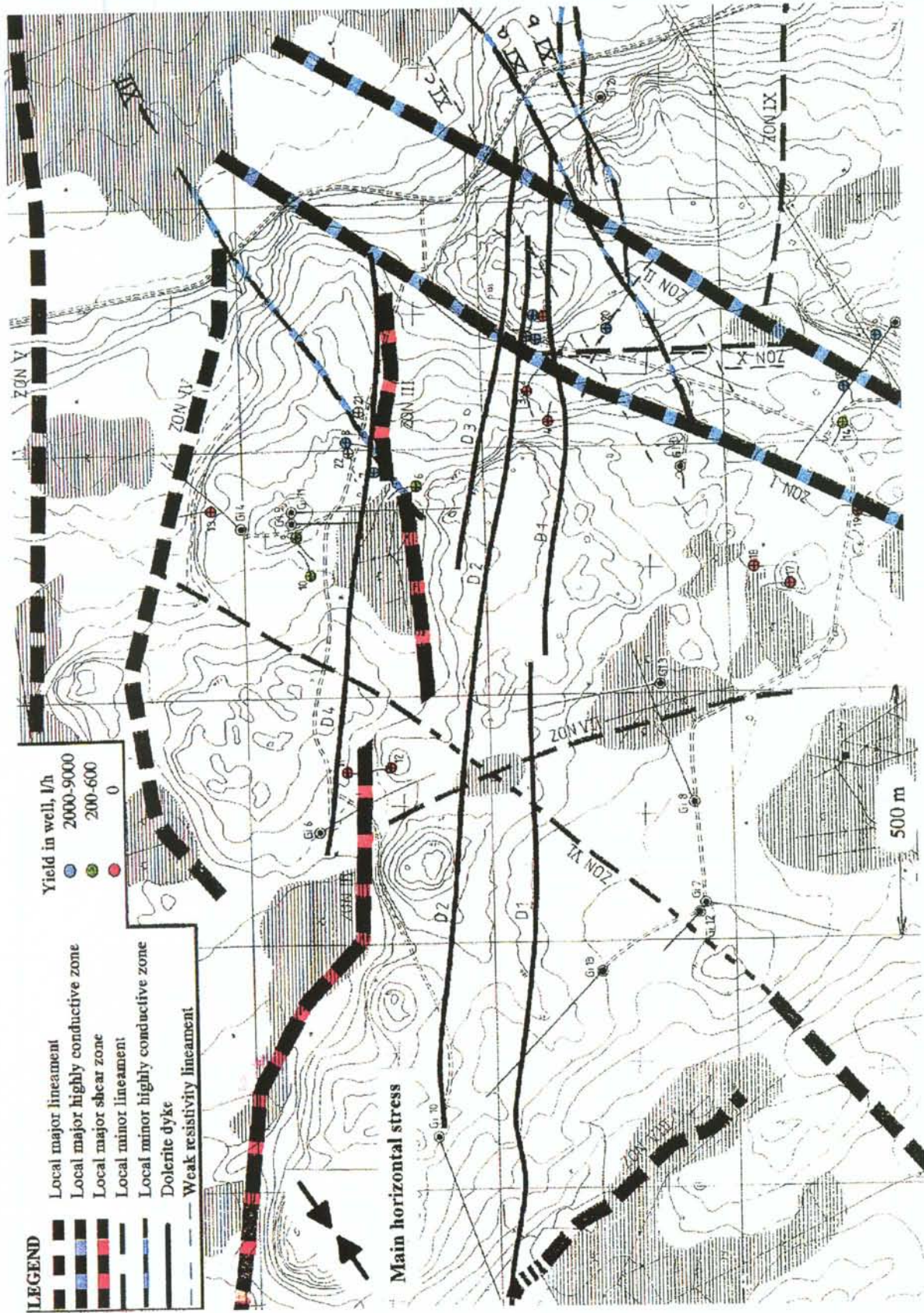


Figure 5-4 Map of interpreted fracture zones in the Gideå Study Area

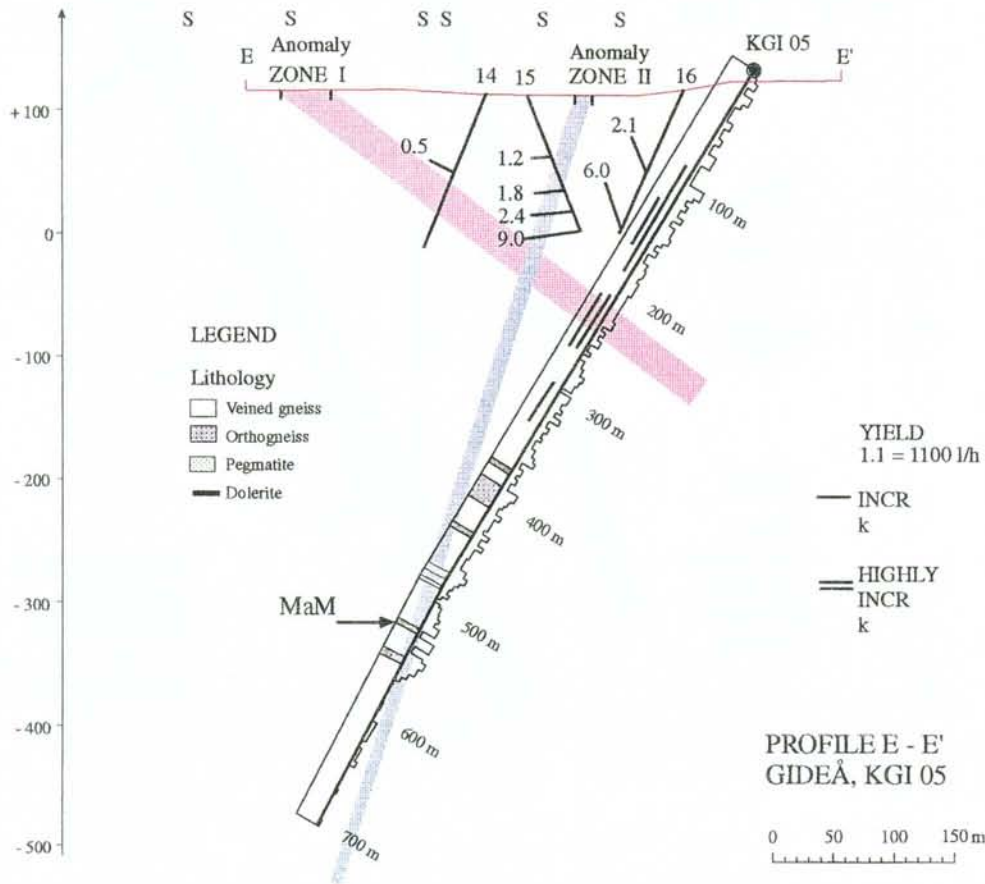
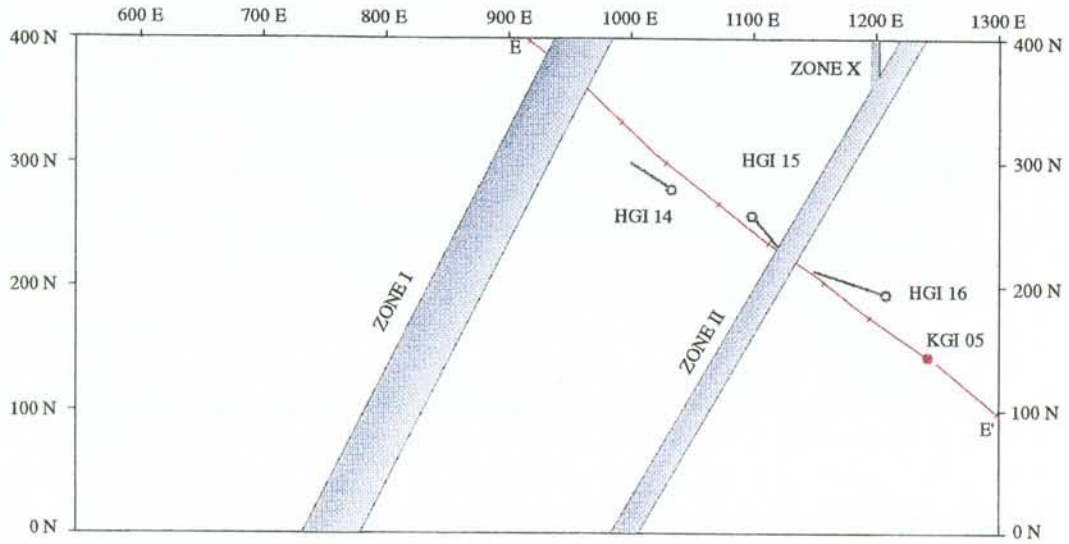


Figure 5-5 Profile of HGI 14-16 and KGI 05 with Interpretation Alternative 1

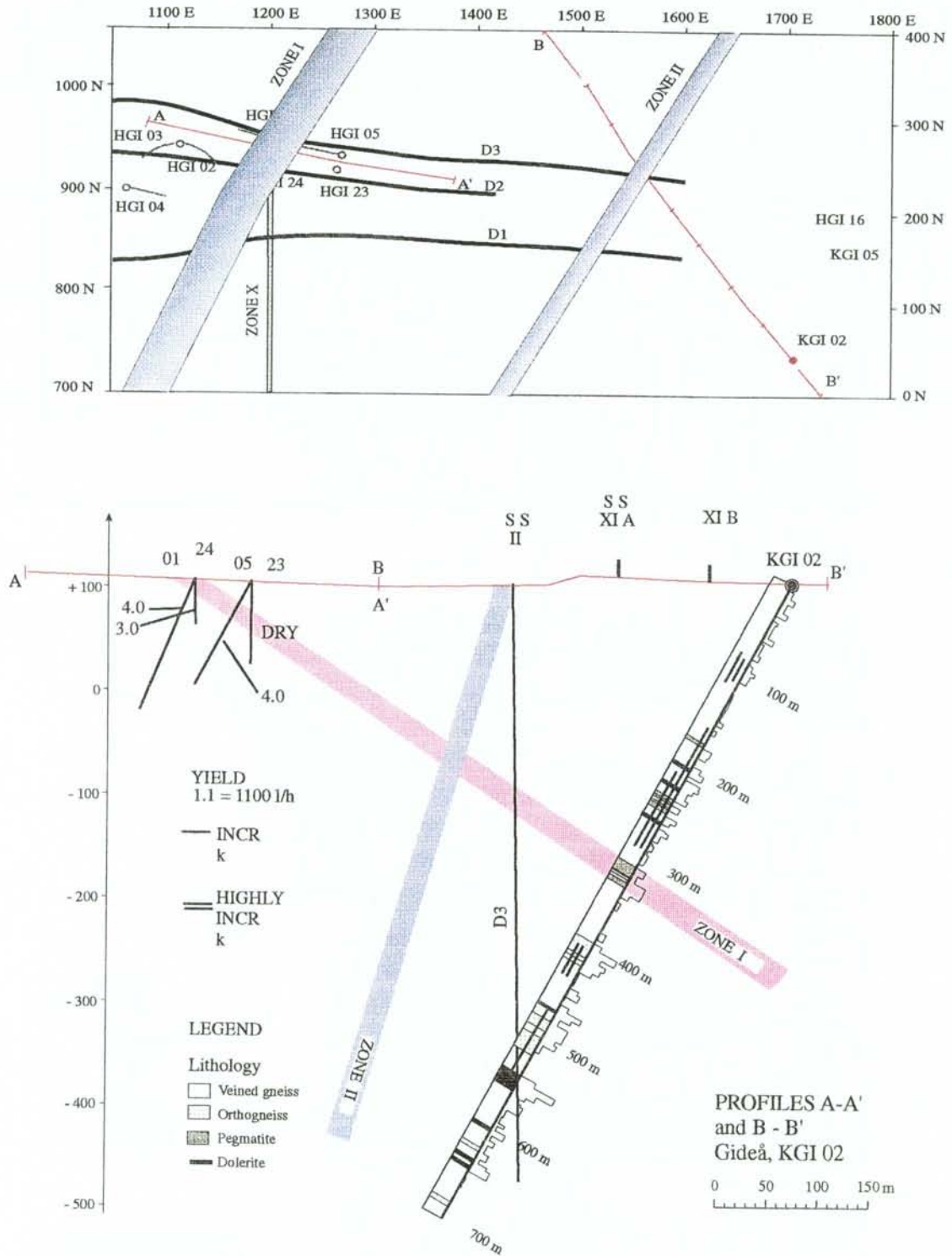


Figure 5-6 Profile of HGI 01, 02, 23 & 24 and KGI 02 with Interpretation Alternative 1

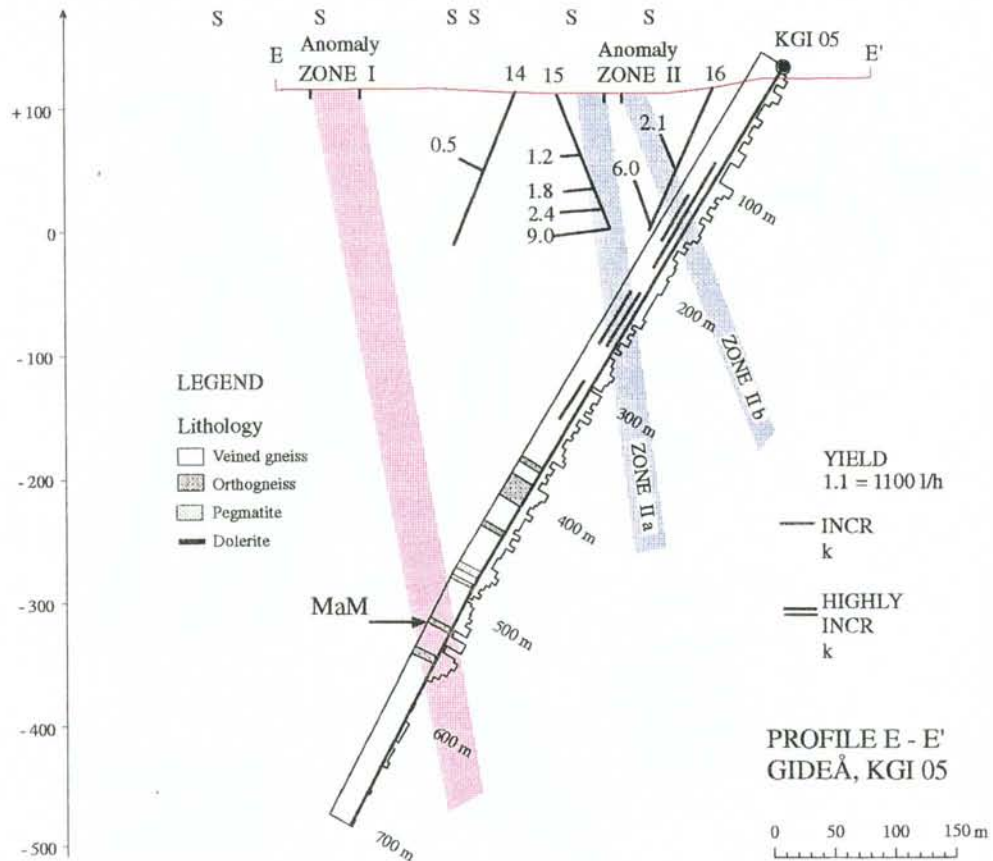
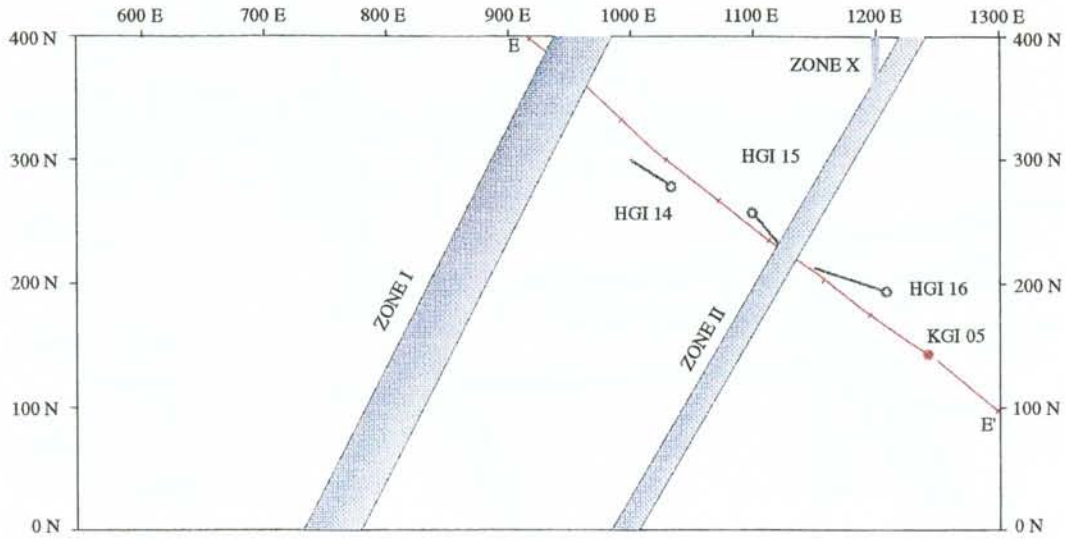


Figure 5-7 Profile of HGI 14-16 and KGI 05 with Interpretation Alternative 2

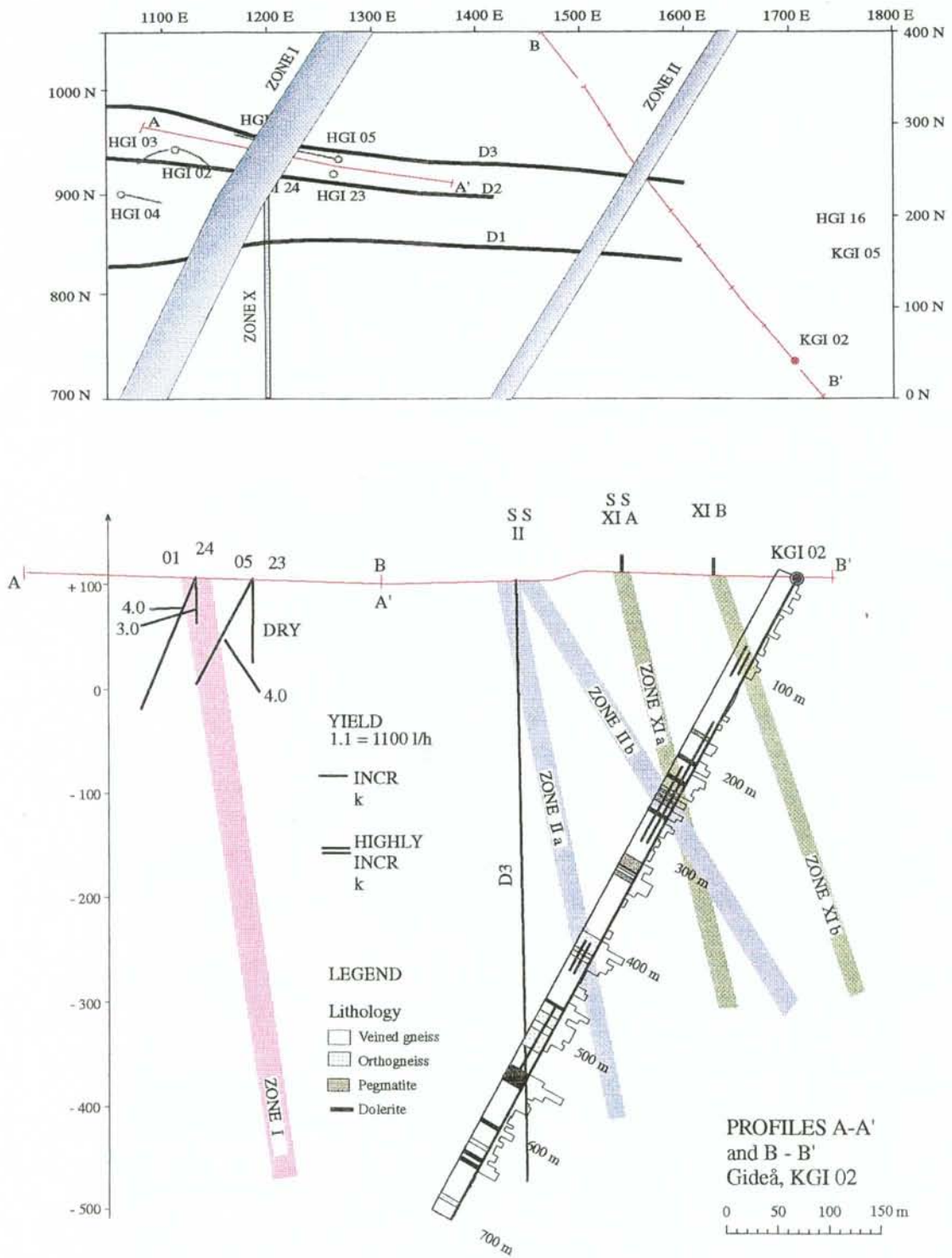


Figure 5-8 Profile of HGI 01, 02, 23 & 24 and KGI 02 with Interpretation Alternative 2

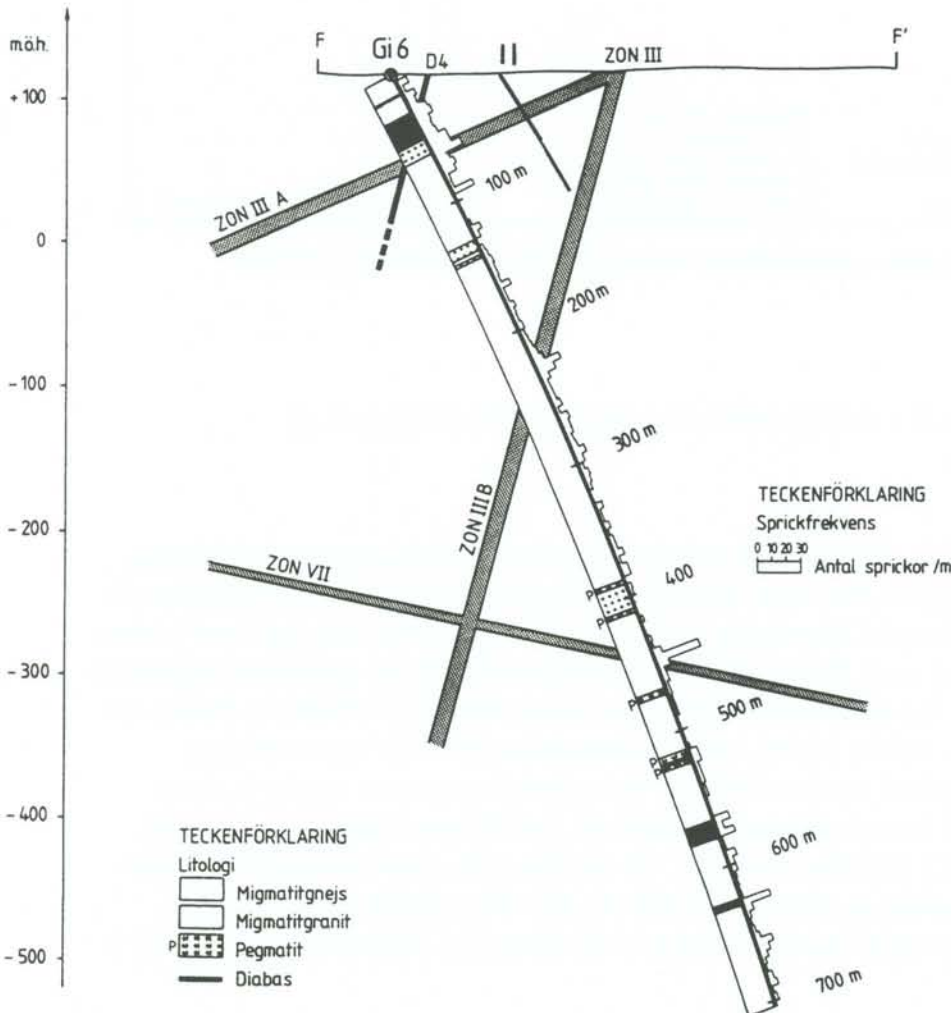
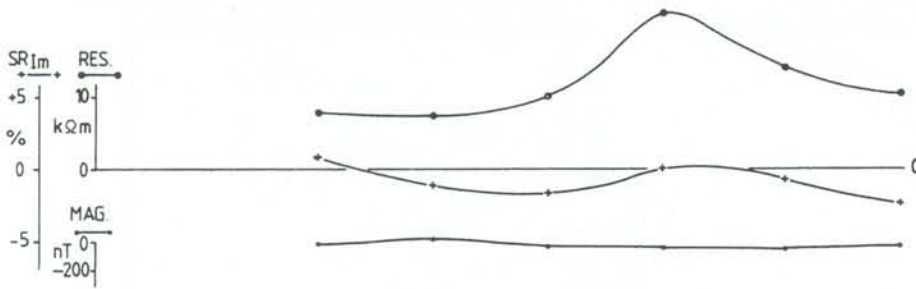
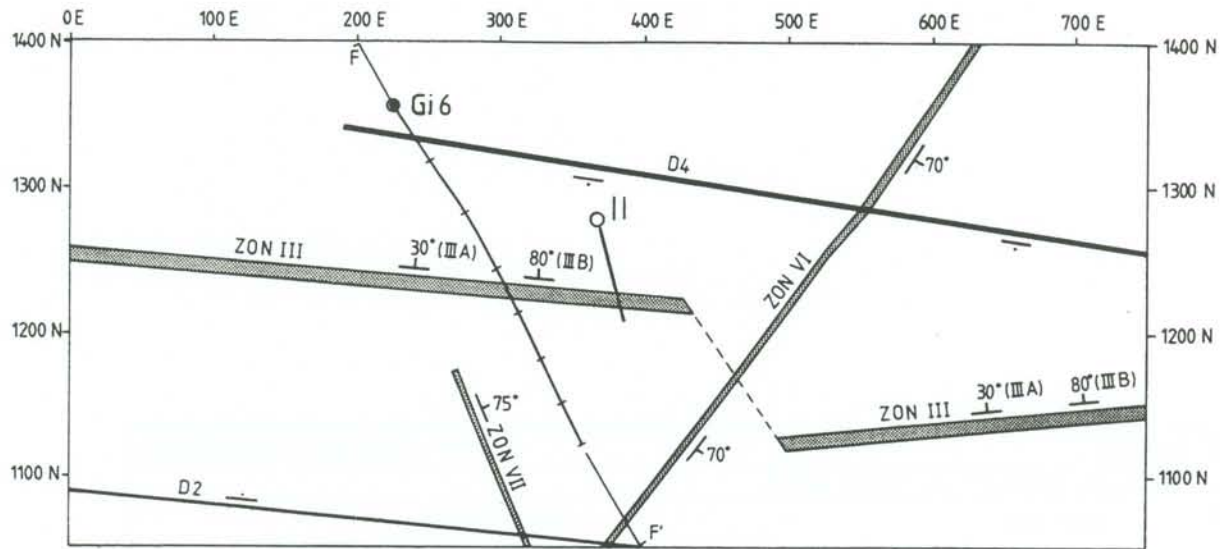


Figure 5-9 Profile with results from percussion drilling HGI 11 and Core drilling KGI 06.

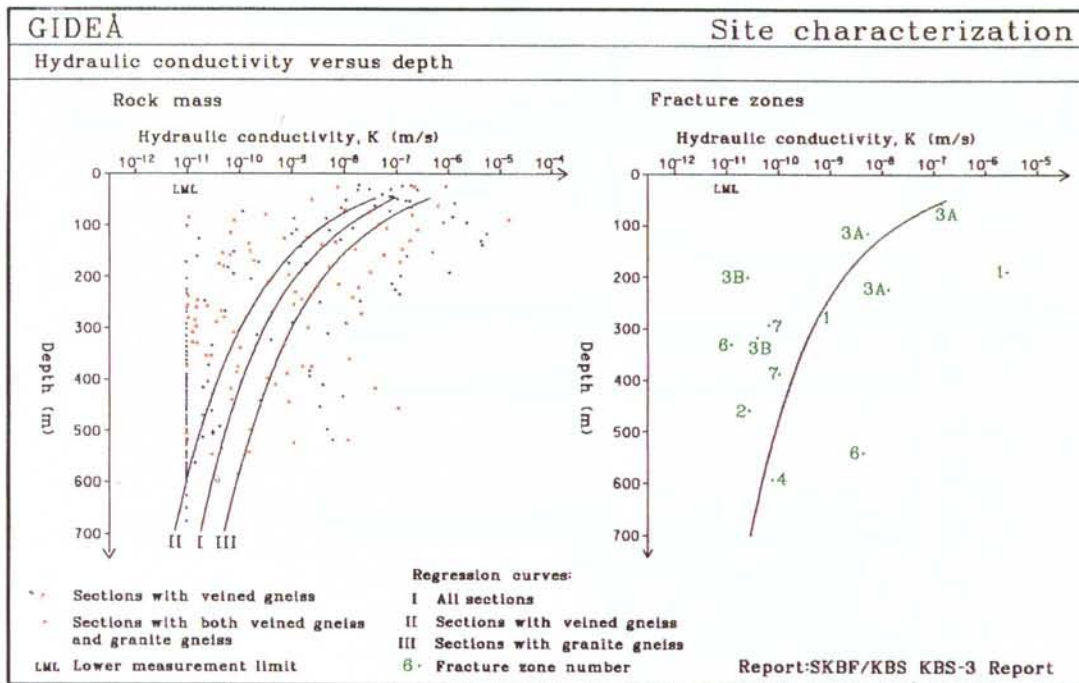


Figure 5-10 Hydraulic conductivity versus depth (Ahlbom et al 1991)

5.4 CORRELATION OF LITHOLOGICAL UNITS AND HYDRAULIC CONDUCTIVITY

Ahlbom et al. (1991) concluded by means of regression analyses that the hydraulic conductivity at Gideå is rock type dependent; the granite was said to be significantly more conductive than the migmatite and even more conductive than the local fracture zones in the studied area. However, a perspicuous review of the performed regression analyses indicates that the used methodology behind Figure 5-10 leads to biased and ambiguous results. Above all, the a priori assumption that only two rock types (granite and migmatite) are considered in the regression analysis appear to be an invalid and strongly biased approach. In addition, the different regression analyses were made for all 25 m packer tests, i.e. values above the lower measurement limit were mixed with values at this limit. However, the effect of this mixing on the outcome of the regression analyses was not considered by Ahlbom et al. (1991). It is

noted here that the values below or at the lower measurement limit constitute more than 1/3 (35%) of all 25 m packer tests.

For the purpose of the present study, hydraulic conductivity's from the 25 m packer tests (K_{25m}) have been reinvestigated for rock type (SICADA 1996). The range of variation in K for all packer tests conducted in the core boreholes KGI01-KGI08 and KGI11 at Gideå is compiled in Figure 5-11. The 25 m straddle interval was used for screening purposes; the total number of 25 m packer tests at Gideå is 204. The other straddle intervals were used for special purposes. In particular, the 5 m straddle interval was frequently used for investigating conductive 25 m packer tests below 200 m depth. Figure 5-12 and Figure 5-13 show the vertical distribution of the 25 m and 5 m packer tests, respectively.

In Figure 5-14, the 25 m packer tests are colored in respect to borehole ID. Figure 5-14 indicates an important feature for a statistical treatment of measured hydraulic conductivities at Gideå, namely that the spatial variability of K_{25m} is not homogeneous. Several boreholes show values which suggest a presence of fracture zones, whereas other boreholes have almost all their values at or below the lower measurement limit thus suggesting rock without fracture zones. Furthermore, the rock between ground level and 200 m depth appears to be more conductive than the rock below 200 m depth. Although, the vertical distribution of K_{25m} is not very attractive from a mathematical point of view, Ahlbom et al. (1991) consider the outcome of their regression analyses ($K = a b^{-z}$) as indicative of significant differences in K_{25m} . The following degrees of determination (r^2) were reported by Ahlbom et al. (1991): migmatite 0.52; granite 0.28; rock mass 0.46; and local fracture zones 0.32.

Be as it may with a depth dependence in K_{25m} , there is no depth dependence in the lithology at Gideå. For this reason, the approach used here for the reinvestigation of K_{25m} for rock type assumes that a significant correlation between these two entities must be independent of depth in order to be useful. The handling of data (lithology and hydraulic conductivity) was carried out as follows:

1. The lithology at Gideå was classified according to four rock types; migmatite, pegmatite, granite and dolerite. The occurrence of these four rock types in the deep core boreholes differs significantly; the most frequent rock type being migmatite and dolerite the least, see Table 5-4.
2. For each 25 packer test interval the total cored length of each rock type between the packers was calculated. Table 5-4 shows some statistics deduced from the lithology logs and the actual straddle intervals of the 25 m packer tests.
3. For each packer test K_{25m} was plotted as a function of the core length for each rock type, the latter ranging from 0 to 25 m. The conductivity of an interval where the considered rock type was absent was plotted versus 0 m of core length and the

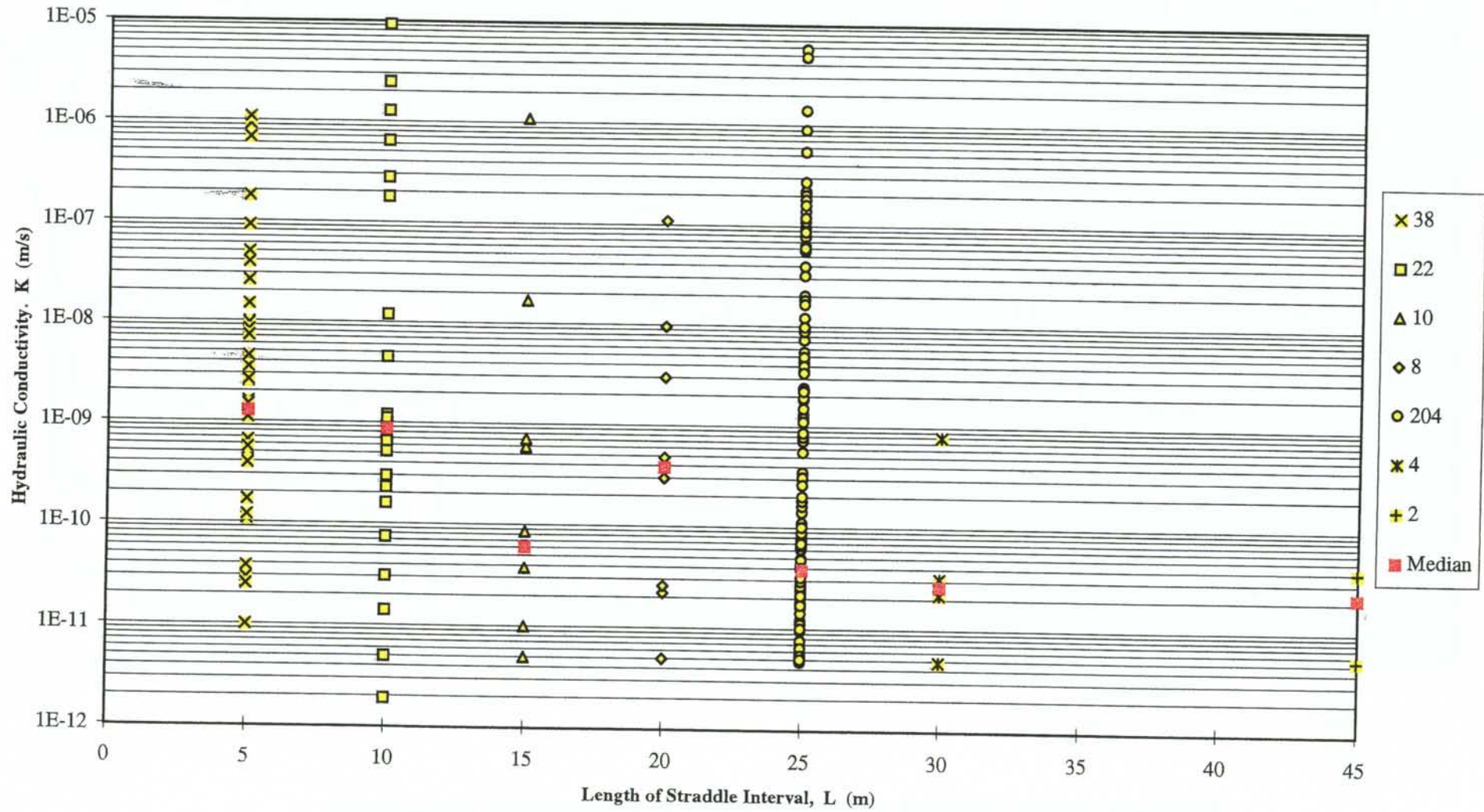
conductivity of an interval where the considered rock type was the only one present was plotted versus 25 m of core length.

4. Finally, the statistics for $\log_{10}(K_{25m})$ was calculated and compiled in accordance to Table 5-4. The calculations were made for all data as well as for all data above the lower measurement limit.

Table 5-3 Occurrence of migmatite, pegmatite, granite and dolerite according to the lithological logs of boreholes KG01-KGI08 and KGI11 at Gideå. The statistics of cored lengths refer to the straddle intervals of the 25 m packer tests conducted in these boreholes. The total number of intervals is 204 (corresponding to 5,100 m of core length). By occurrence we mean here that the considered rock type is present, either alone or together with the other rock types.

	<i>Migmatite</i>	<i>Pegmatite</i>	<i>Granite</i>	<i>Dolerite</i>
<i>Number of intervals</i>	200	109	61	37
<i>Average length, m</i>	21.95	2.26	6.04	2.58
<i>Median length, m</i>	23.75	1.25	3.00	1.15
<i>STD, m</i>	4.39	2.84	7.02	3.84

HYDRAULIC CONDUCTIVITY OF DOUBLE PACKER TESTS AT GIDEÅ



Figur 5-11 Overview of packer test conductivities at Gideå. The screening straddle interval is 25 m. The other intervals are less frequent and used for special purposes.

HYDRAULIC CONDUCTIVITY OF 25 m DOUBLE PACKER TESTS AT GIDEÅ

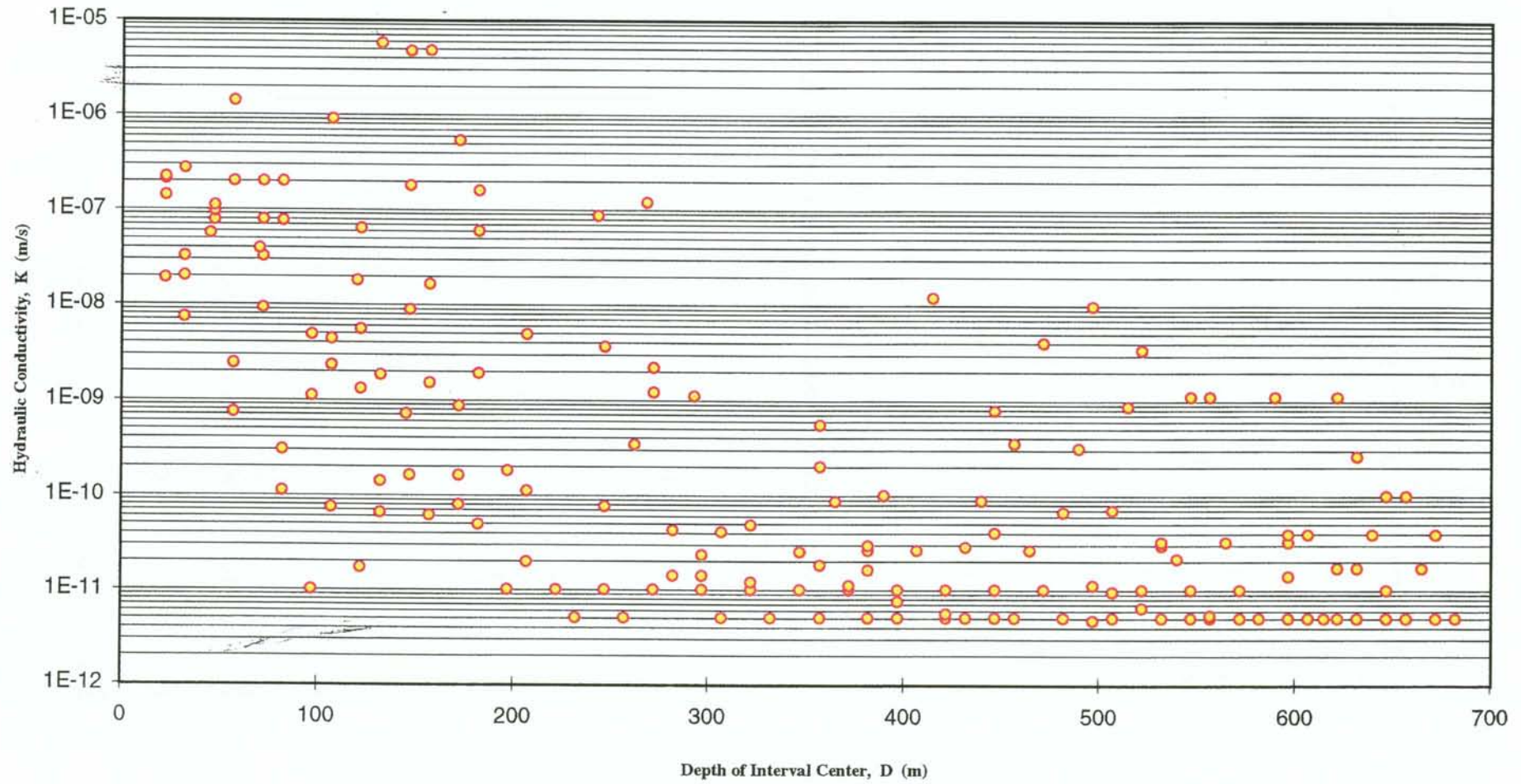
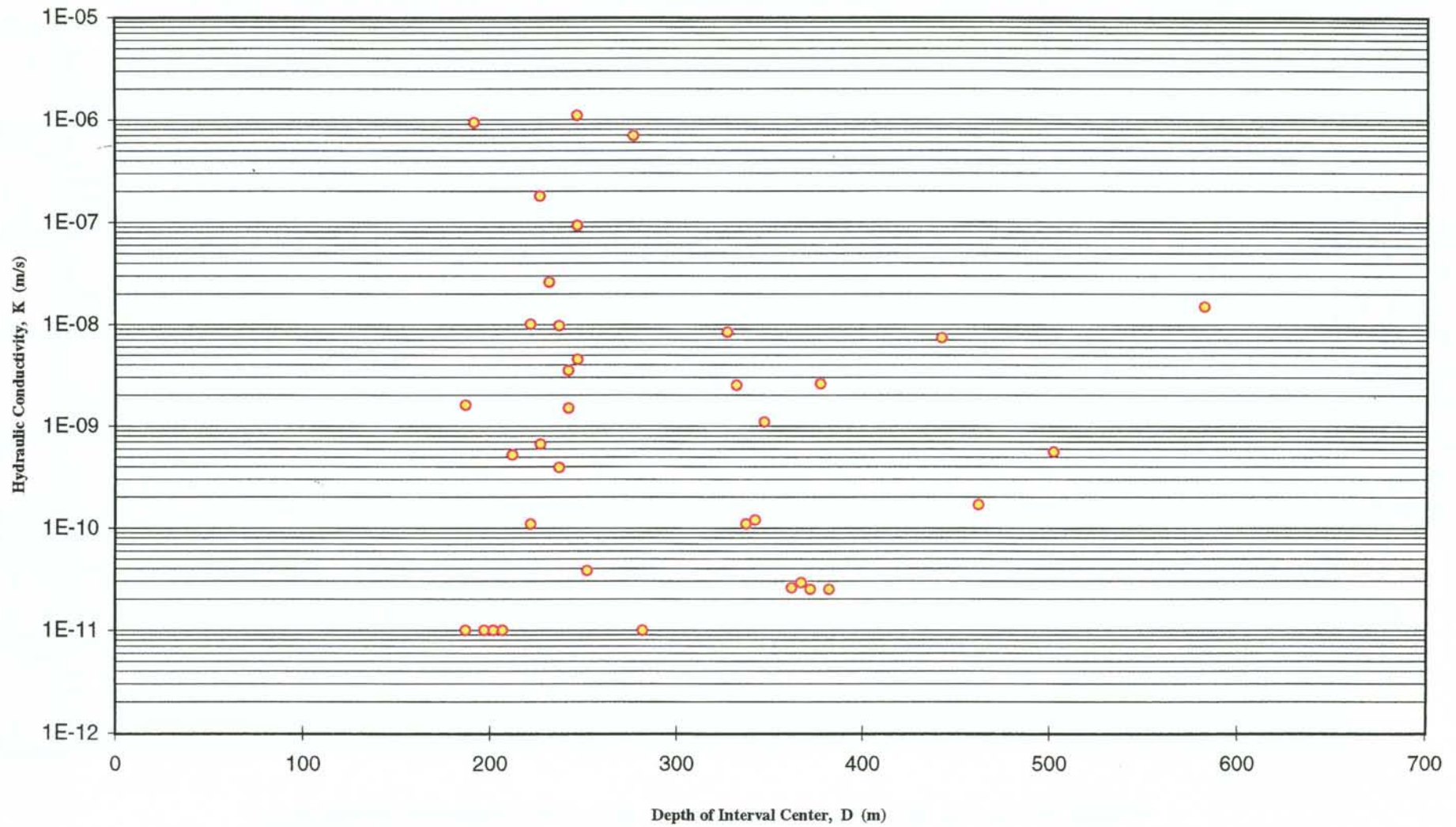


Figure 5-12 K_{25m} plotted as a function of depth of interval center. Data comes from boreholes KGI01-08 and KGI11.

HYDRAULIC CONDUCTIVITY OF 5 m DOUBLE PACKER TESTS AT GIDEÅ



Figur 5-13 K_{5m} plotted as a function of depth of interval center. Data comes from boreholes KGI01-08 and KGI11.

HYDRAULIC CONDUCTIVITY OF 25 m DOUBLE PACKER TESTS AT GIDEÅ

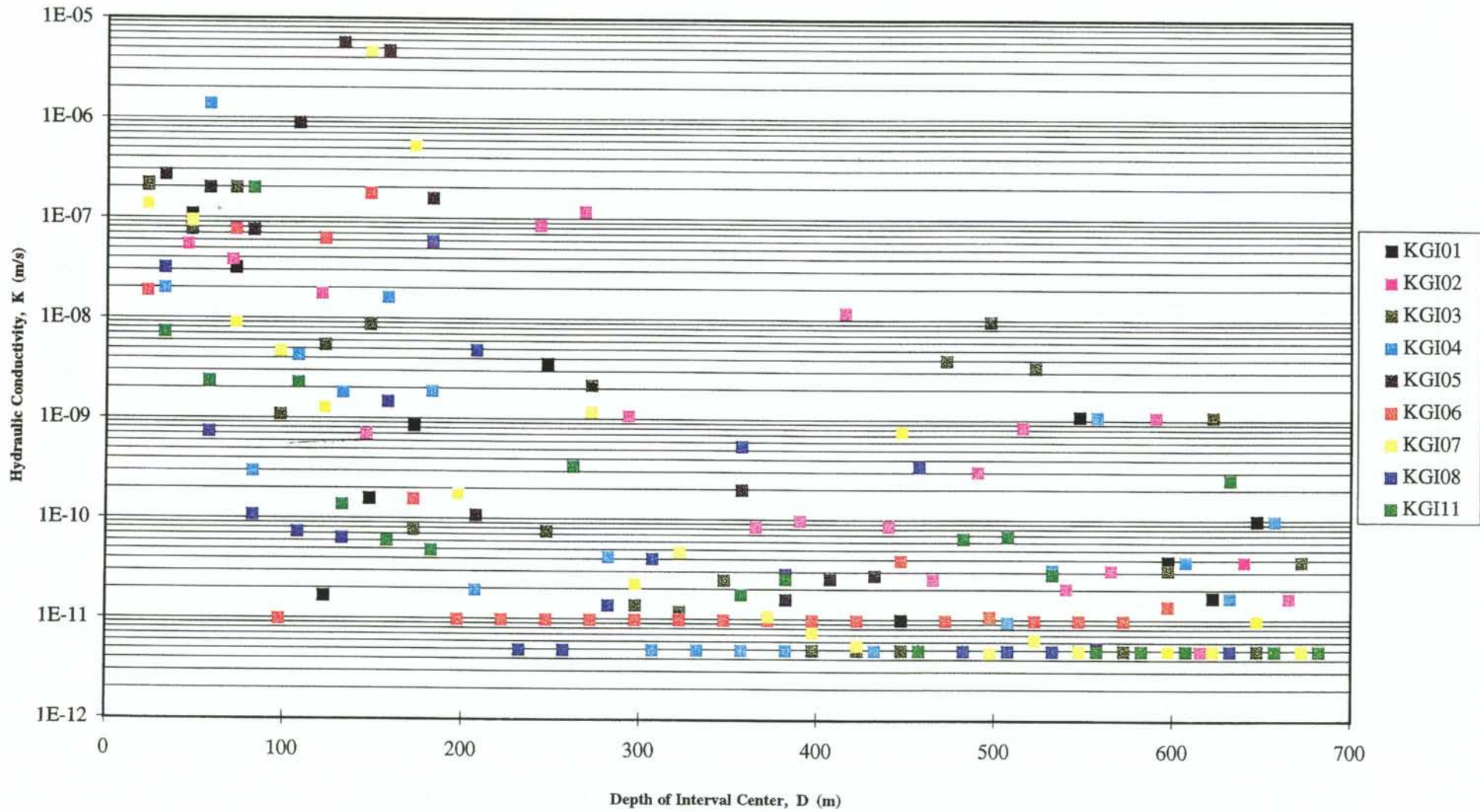


Figure 5-14 K_{25m} plotted as a function of depth of interval center. The boreholes are given different colors.

6 RESULTS OF UPDATE

6.1 LITHOLOGY

6.1.1 Lithological units

Six main rock types exist in the area, as outlined in Table 6-1. The three first are paragneisses which all have the same origin and are summarised in the corelogs under the label migmatite. The foliation of the migmatite is of secondary nature with no remainders of the original bedding.

The orthogneiss is of prim-orogenic age and form bodies along the folded foliation. It cannot easily be traced between the drill holes, due to the folding in the area (cf Figure 3-1) and the wide spacing of the holes. The extent of the orthogneiss is interpreted to be limited and variable in width which is quite reasonable with concern of its metamorphic origin.

One larger pegmatite dyke is intersecting the study area. The pegmatite is steeply dipping and trends N-S. A few more is visible on the outcrops but are too minor (<50 m length) to be included in the model. The pegmatite is competent in relation to the migmatite and is usually easy to see on outcrops. It is not extensively fractured and is not believed to be a hydraulic pathway, in general. The width is irregular so it is not considered to act as an impermeable hydraulic boundary.

Table 6-1 Lithological units of the Gideå Site

Rock type	Characteristics	% of core material	Formation and age, million years
Gneissose metasediments	Layered graywacke gneiss with no veins	90	Sedimentation and volcanism, 1900
Veined gneiss	Fine to medium grained layers of graywacke gneiss varved with veins of granitic material		Folding, metamorphism and migmatitisation, 1850
Migmatite	Graywacke or veined gneiss in an irregular mixture with granitic material		
Granite veins	Gneissose granodiorite as layers along with the regional foliation	6	Primorogenic intrusion, 1850
Pegmatite	Small massifs and vertical narrow dykes	4	Serorogenic intrusion, 1800
Dolerite	Vertical dykes with lengths of up to 2 km and with a thickness of up to several metres	2	Postjotnian intrusion of dykes and sills, 1200

The dolerites are essentially the same as defined in the first model. The main addition is the three-dimensional model describing the possible extent at depth of these bodies. Based on borehole intercepts the dolerites seem generally planar in trend, with a variable width with some intercepts in the order of 25 m thick decrease to only

a few meters thick intercept 50 m away with other boreholes. No sub-horizontal dolerites have been identified with certainty, but some of the intercepts in the drill holes, in particular KGI 08, appear to be horizontal. The subhorizontal dykes must be limited in areal extent as no obvious subhorizontal dolerite can be extrapolated through more than two boreholes. Further, KGI01, mapped to intersect subhorizontal dolerites, proved as not intersecting any dolerites at the mapped borehole depths.

The dolerites often feature columnar jointing, oriented athwart each dyke. The joints are mostly filled with calcite. In intersections with drill cores, the difference in competence between the migmatite and the dolerite often results in intense fracturing of the dolerite. The dolerites are not believed to be any major hydraulic pathways, nor do they seem to be correlated to the fracture zones. The dolerite dykes are likely to act as impermeable hydraulic boundaries against transport in the orthogneiss, but not against transport in the fracture zones.

6.1.2 Lithological model

Figure 6-1 shows an overview of the dolerite model and Figure 6-2 shows a model of foliations and folds in the migmatite, including bodies of orthogneiss. The input to the models is mapped rock exposures (cf Figure 3-1) magnetic anomaly interpretations (cf Figure 3-3) and core drilling intercepts. The lithological bodies included in the dolerite model are defined by at a least a magnetic anomaly (reliability level: probable) and surface observation and/or borehole intercepts (reliability level certain). Although there are many more dolerites of lesser width, they have not been included in the 3-dimensional model as no interpolation over any larger (>50 m) distance have been possible to perform. The only larger sized pegmatite is also included in the model as a near vertical plane trending N-S (reliability level: Certain).

The input for the model of foliations, folds and orthogneiss (Figure 6-2) is borehole intercepts combined with recorded foliations and the assumption that the orthogneiss bodies follow the foliation (reliability level is set to probable). The orthogneiss is interpreted to lie as elongated lenticular bodies with the long axis along the fold axis. Due to the absence of records of orthogneiss in the outcrops, the reliability level of this model is lower than for the dolerite model.

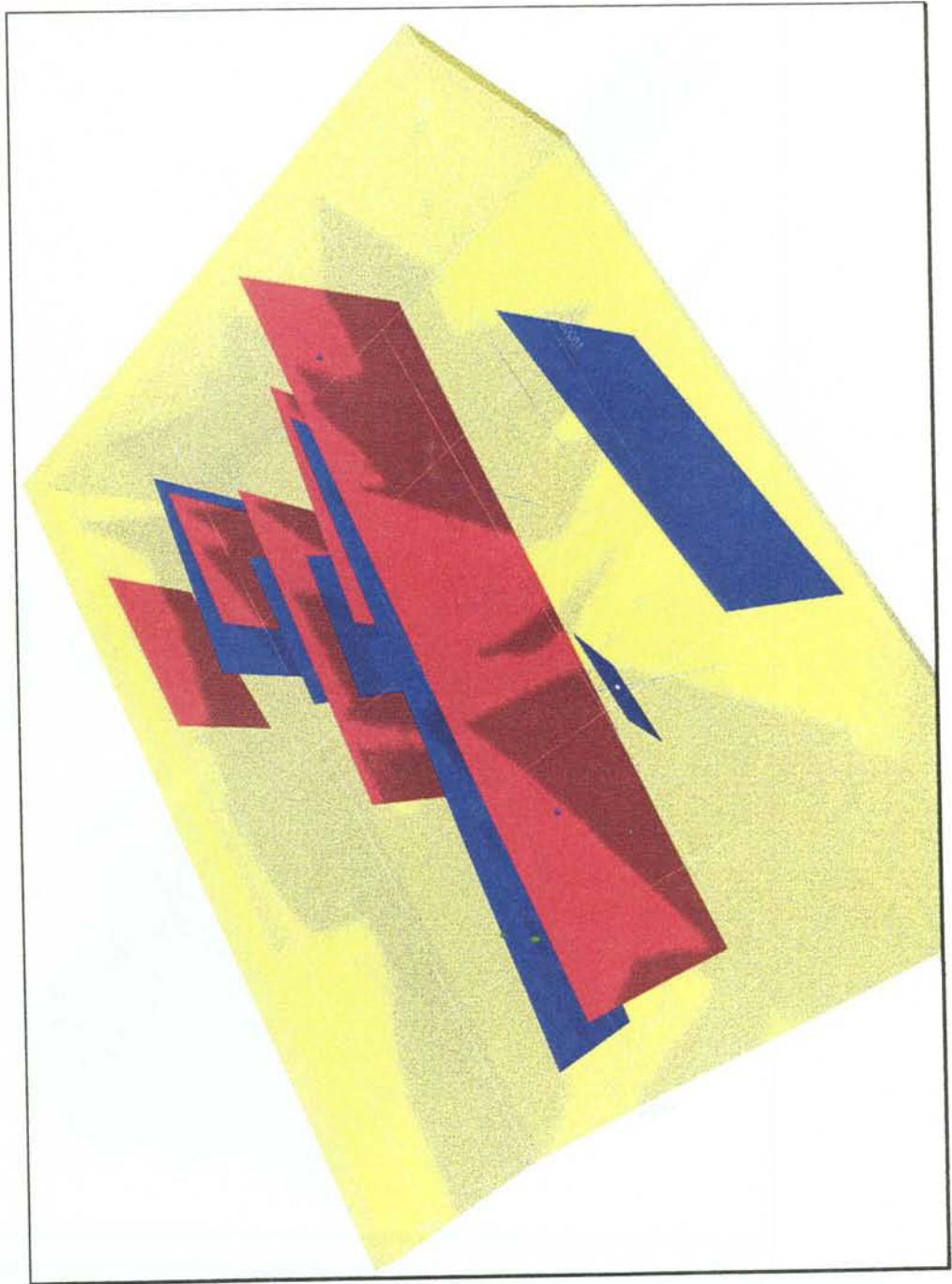


Figure 6-1 Three-dimensional model of dolerite bodies

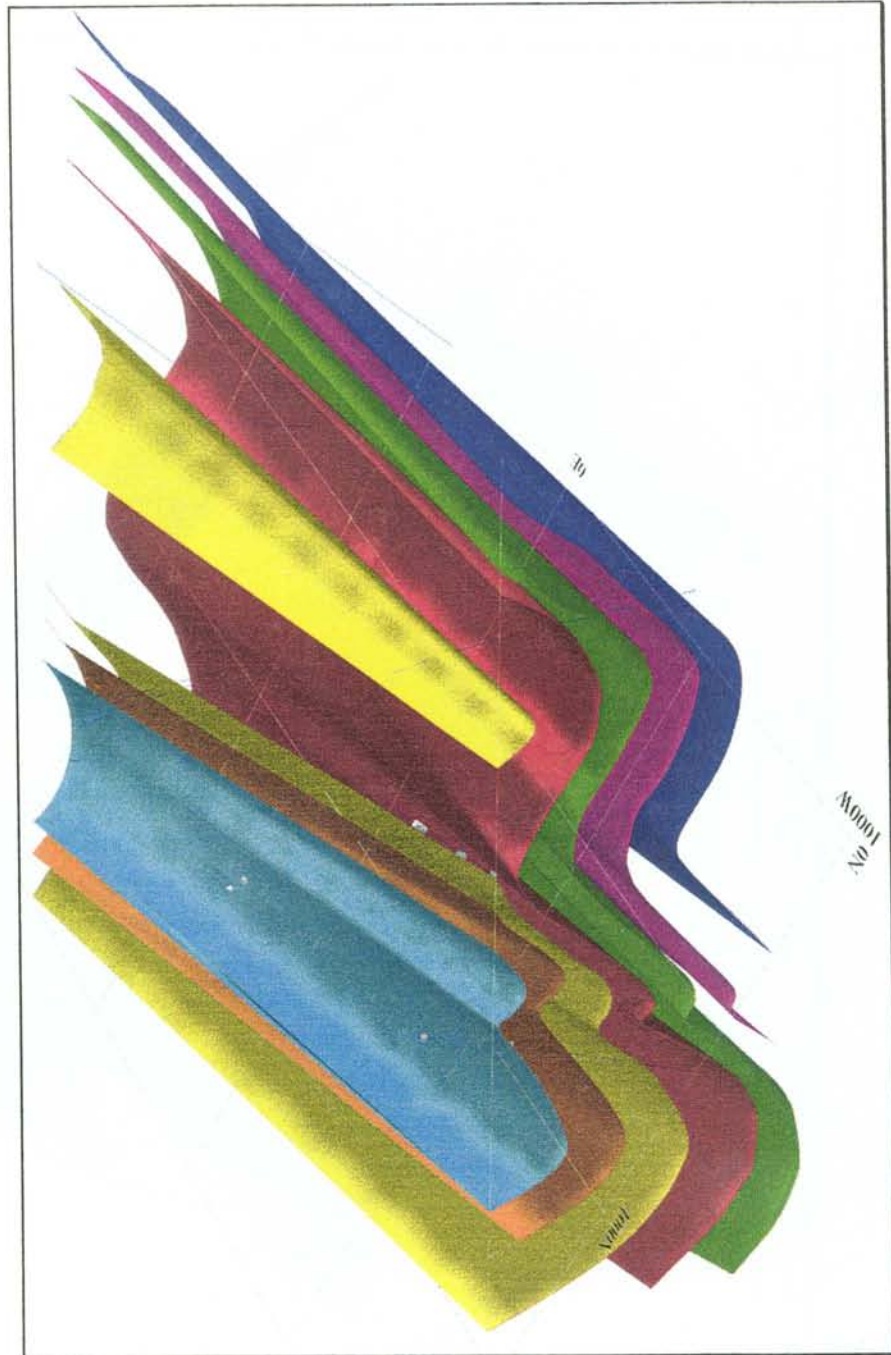


Figure 6-2 Three-dimensional model of foliation, fold structures and orthogneiss bodies

6.2 FRACTURE ZONES

The interpreted tectonic structures are shown in Figure 5-4, and their properties are summarised in Table 6-2. The structures are essentially the same as in the model before update (i.e. alternative 1), with some additional zones. The most important change is the different dips of Zones I and II as explained in Section 5. This is not shown on the map, but can be seen in Figure 5-7,

Figure 5-8 and in the three-dimensional zone model. The water conductive zones, I, II, XI and XII, all strike NNE to ENE which is parallel to the maximum horizontal stress measured in hole KGI 01 and also in the region.

6.2.1 Zone model

Figure 6-3 shows an overview of the zone model. The input to the model is electric, electro-magnetic, seismic refraction and other geophysical anomaly interpretation (Figure 3-4), data from percussion drilling and data from core drillings, including drill hole geophysics and hydraulic tests. This model is based on the interpretation presented in chapter 5 and features an update in dips of zones I and II and additional zones XI and XII.

Table 6-2 Characteristics of fracture zones

Zone No	Reliability (App 4)	Hole No	from	to	Strike	Dip	angle w hole	Width m	Fract/ m	k-value m/s	
I	certain	KGI 05	520	567	NNE	st E	60	41	12	<5E-12	
II A	certain	KGI 02	410	420	NNE	80 E	45	7	18	1.E-08	
	certain	KGI 05	210	232			45	16	6	2.E-06	
II B	certain	KGI 02	250	290	NNE	60 E	60	35		1.E-07	
	certain	KGI 05	120	160			60	35	6	5.E-06	
III A	certain	KGI 04	217	259	E-W	30 N	45	30	10	1.E-08	
	certain	KGI 06	51	80			90	29	13	1.E-07	
	certain	KGI 09	129	146			90	17	15	no data	
	certain	KGI 11	119	130			90	11	19	1.E-10	
III B	probable	KGI 06	222	240	E-W	st N	40	12	10	7.E-12	
	probable	KGI 11	345	352	E-W	st N	40	4	3	7.E-11	
IV	possible	KGI 04	606	655	E-W	st N	10	9	11	7.E-12	
V	possible	none			E-W	st N		50			
VI	probable	KGI 03	622	629	NNE	70 SE	60	6	17	5.E-09	
		KGI 04	670	690			30	10	11	<5e-12	
		KGI 07	362	397			5	3	18	2.E-11	
		KGI 12	52	61			60	8	13	no data	
VII	possible	KGI 03	329	342	NNW	75 E	40	8	9	7.E-11	
	possible	KGI 06	443	452			50	7	23	7.E-10	
VIII	possible	none			NW	st SW		10			
IX	possible	none			E-W	N		5			
X	possible	none			N-S	90		5			
XI A	probable	KGI 2	200	250	ENE	75 SE	30	25	9	5.E-07	
XI B	probable	KGI 2	90	110	ENE	75 SE	40	13	8	2.E-06	
XII	probable	HGI 07	30		ENE	75 SE			10	5.E-06	
		HGI 08	44								
		KGI 11	680	690			30	5	2.E-10		

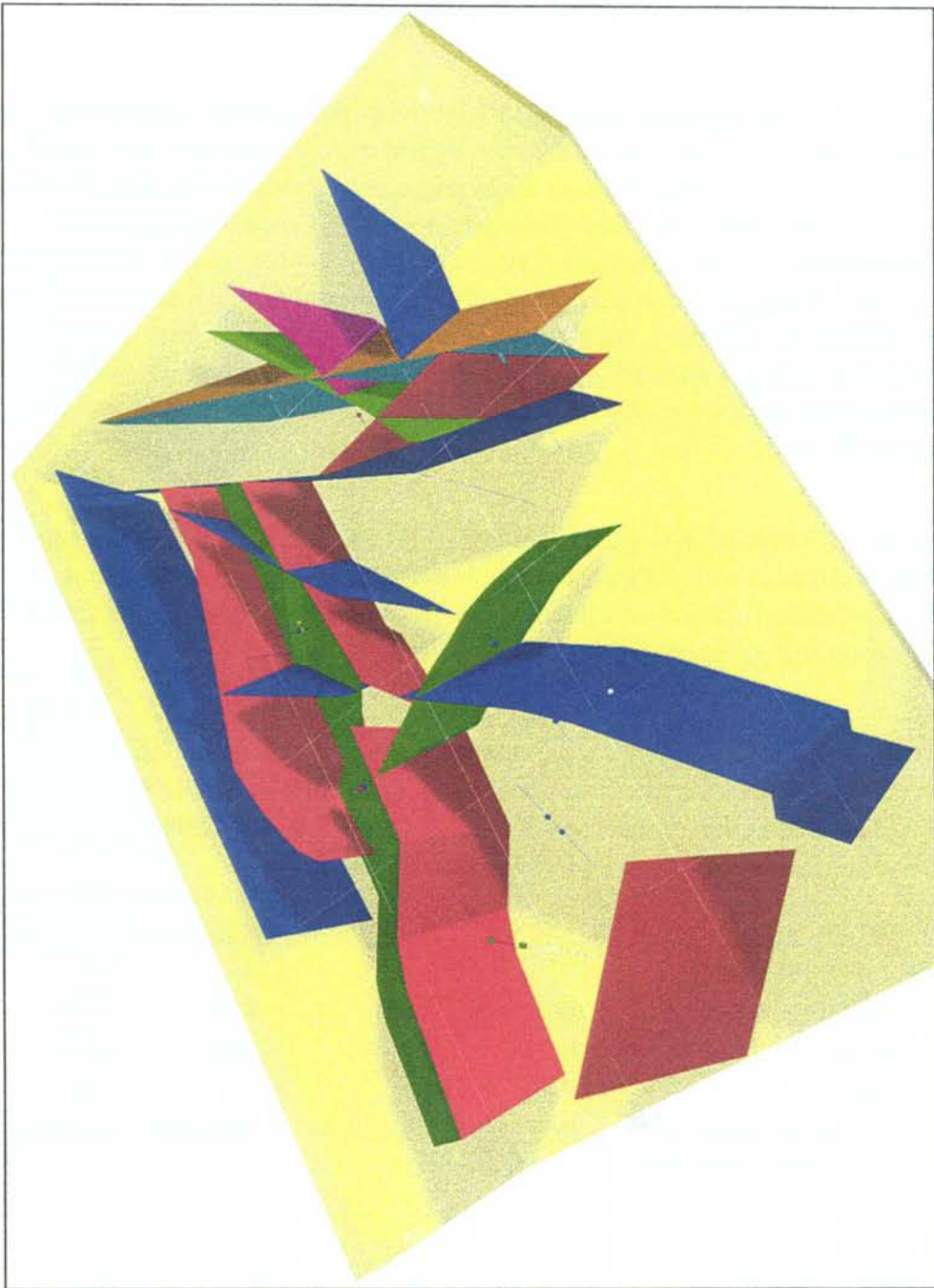


Figure 6-3 Three -dimensional model of fracture zones

6.3 HYDRAULIC PROPERTIES OF LITHOLOGICAL UNITS

The result of the approach outlined in Chapter 5 is presented in Figures 6-4 to 6-7. None of the cross plots in these figures suggest a correlation between $\log_{10}(K_{25m})$ and core length for any of the rock types. Regression analyses of $\log_{10}(K_{25m})$ for all core lengths greater than 0 m render flat regression lines, hence low degrees of determination ($r^2 \approx 0$). The same conclusion applies to Figure 6-8, which shows a cross plot of $\log_{10}(K_{25m})$ as a function of the number of rock contacts in each packer test interval. In summary, the approach used in this study suggests no correlation between $\log_{10}(K_{25m})$ and rock type nor the number of rock contacts. Whether this result applies to other scales of support than 25 m packer tests is beyond the scope of the present study.

The lack of correlation is quantified in statistical terms in Table 6-3. Regardless of whether all data or only data above the lower measurement limit are considered, the 95% confidence intervals for the different means show great overlaps, thus suggesting insignificant differences between the samples.

Table 6-3 Statistics of $\log_{10}(K_{25m})$ of the 25 packer tests at Gideå. Data are gathered according to the lithological logs of boreholes KG01-KGI08 and KGI11 at Gideå. By occurrence it is meant here that the considered rock type is present, either alone or as one of 2-4 possible rock types.

All data	Migmatite	Pegmatite	Granite	Dolerite
Number of intervals	200	109	61	37
Average $\log_{10}(K_{25m})$	-9.62	-9.68	-9.45	-9.69
Median $\log_{10}(K_{25m})$	-10.26	-10.35	-9.85	-10.38
STD $\log_{10}(K_{25m})$	1.69	1.68	1.41	1.66
95% confidence interval for the \log_{10} average, lower/upper	-9.86/-9.38	-10.01/-9.36	-9.81/-9.09	-10.24/-9.15
$K_{25m} > 10^{-11}$ m/s				
Number of intervals	132	69	53	26
Average $\log_{10}(K_{25m})$	-8.82	-8.82	-9.19	-8.20
Median $\log_{10}(K_{25m})$	-9.07	-9.07	-9.46	-8.80
STD $\log_{10}(K_{25m})$	1.57	1.55	1.34	2.82
95% confidence interval for the \log_{10} average, lower/upper	-9.10/-8.55	-9.19/-8.45	-9.56/-8.83	-9.30/-7.09

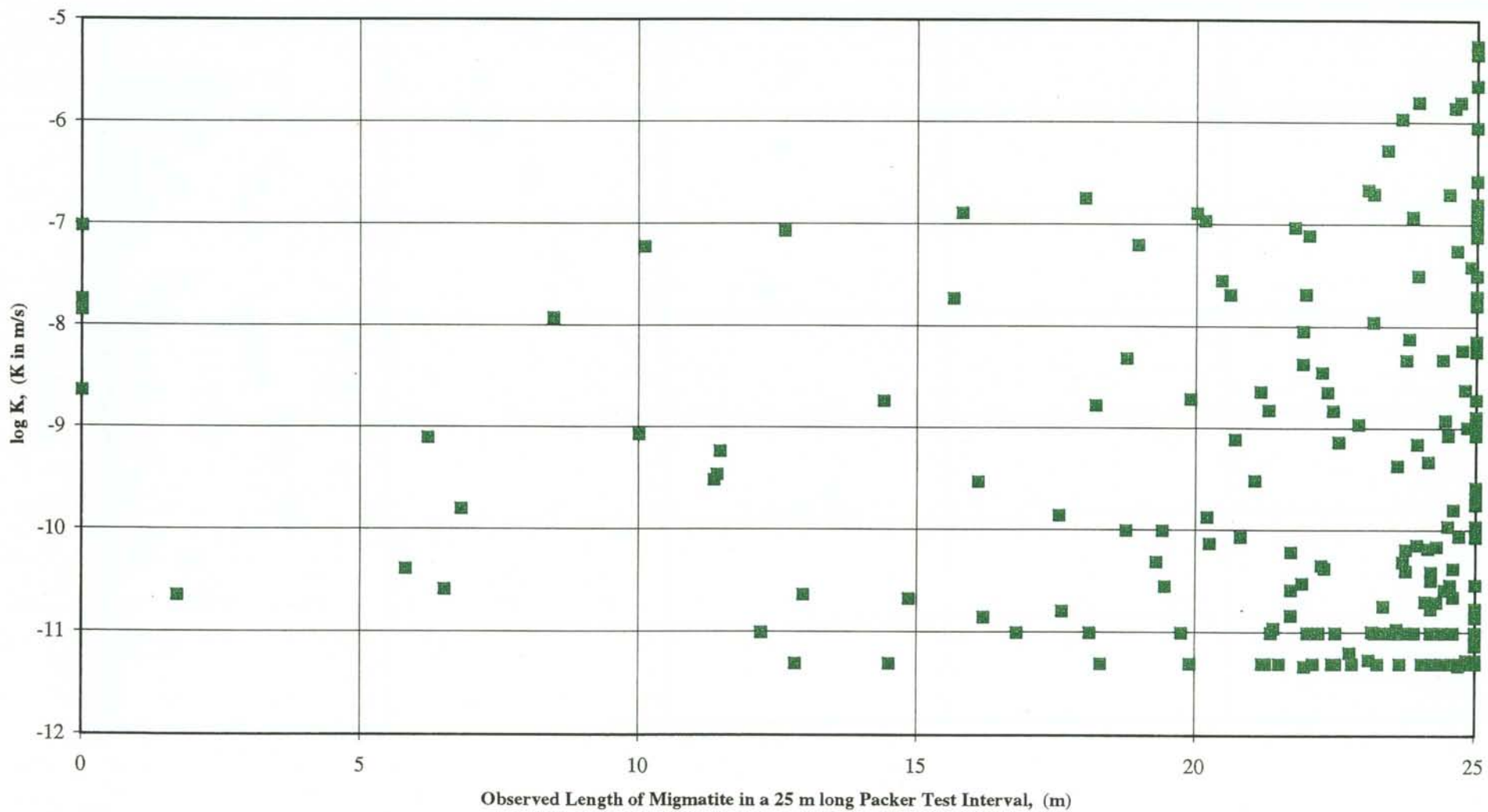
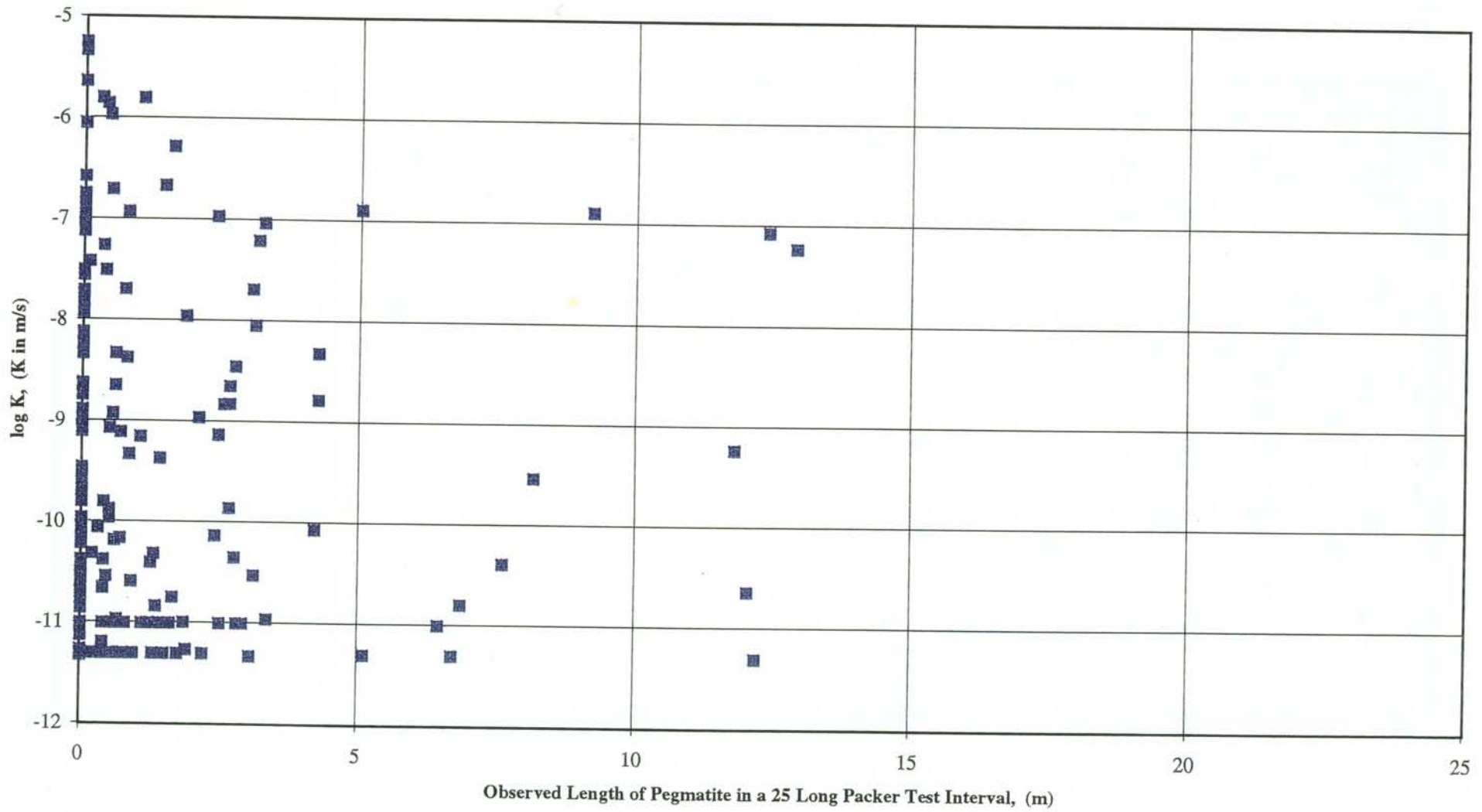


Figure 6-4 K of 25 m long packer test intervals which contain 0-25 m of Migmatite.



Figur 6-5 K of 25 m long packer test intervals which contain 0-13 m of Pegmatite.

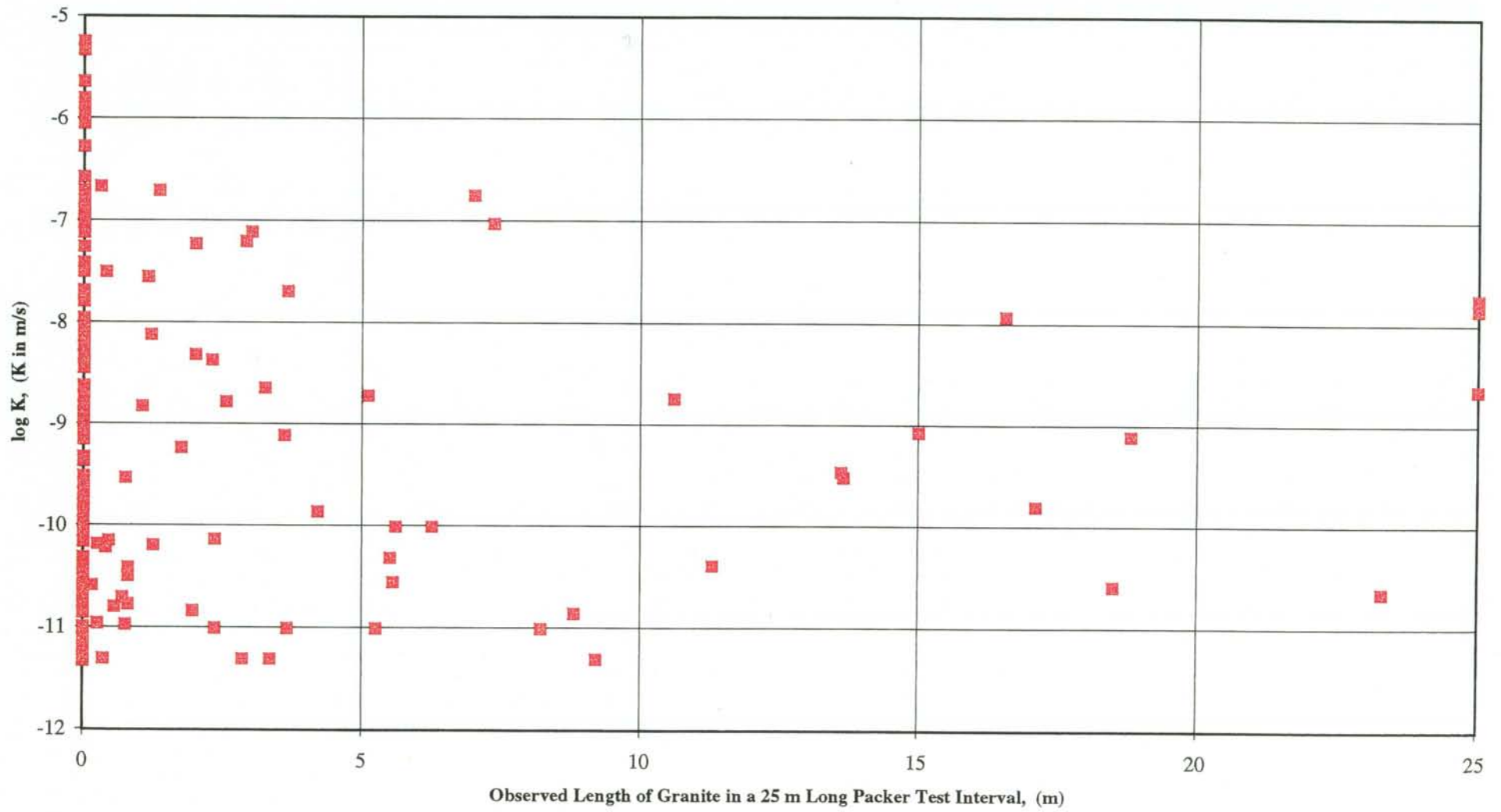


Figure 6-6 K of 25 m long packer test intervals which contain 0-25 m of Granite.

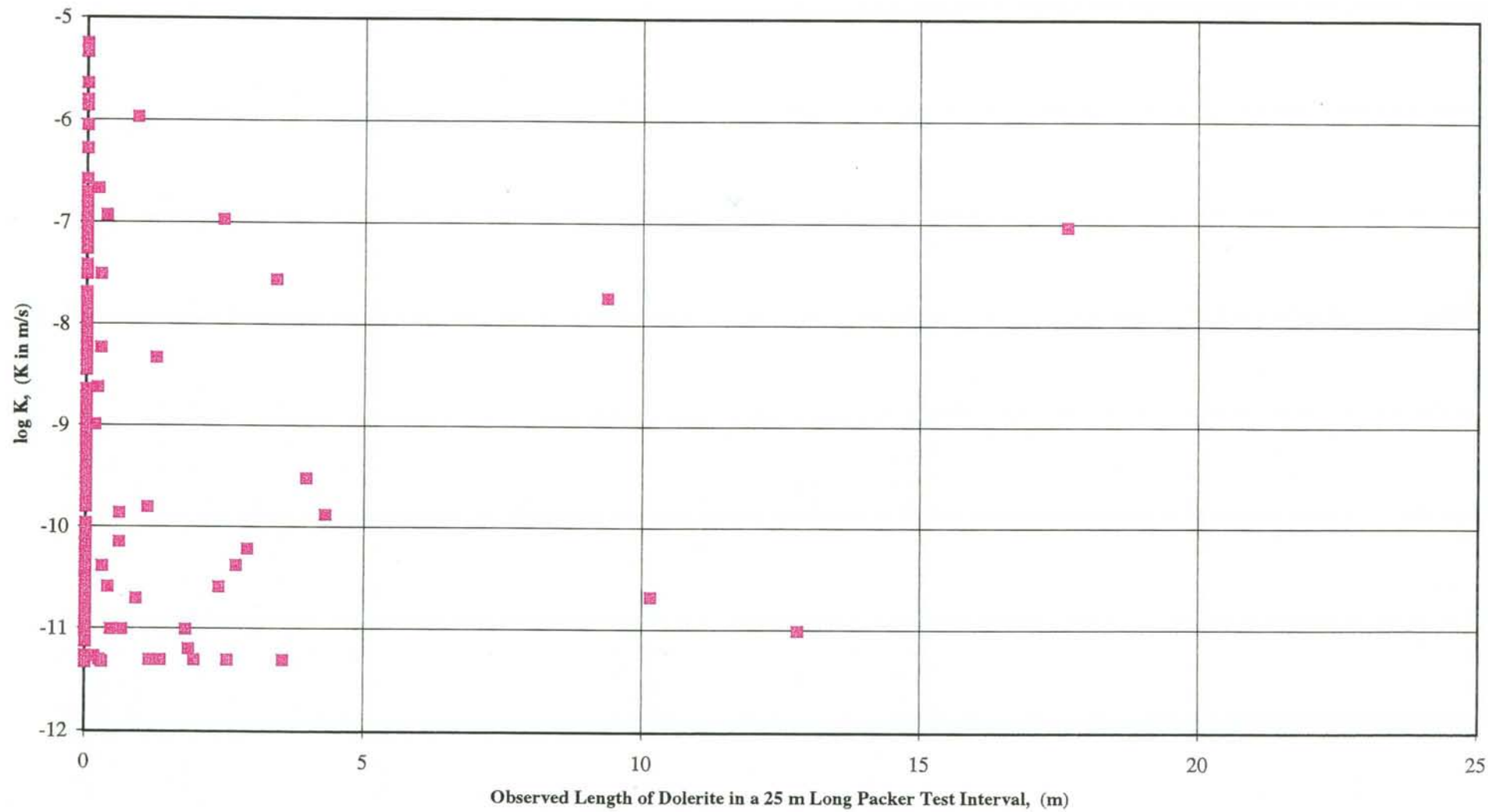


Figure 6-7 K of 25 m long packer test intervals which contain 0-17.5 m of Dolerite.

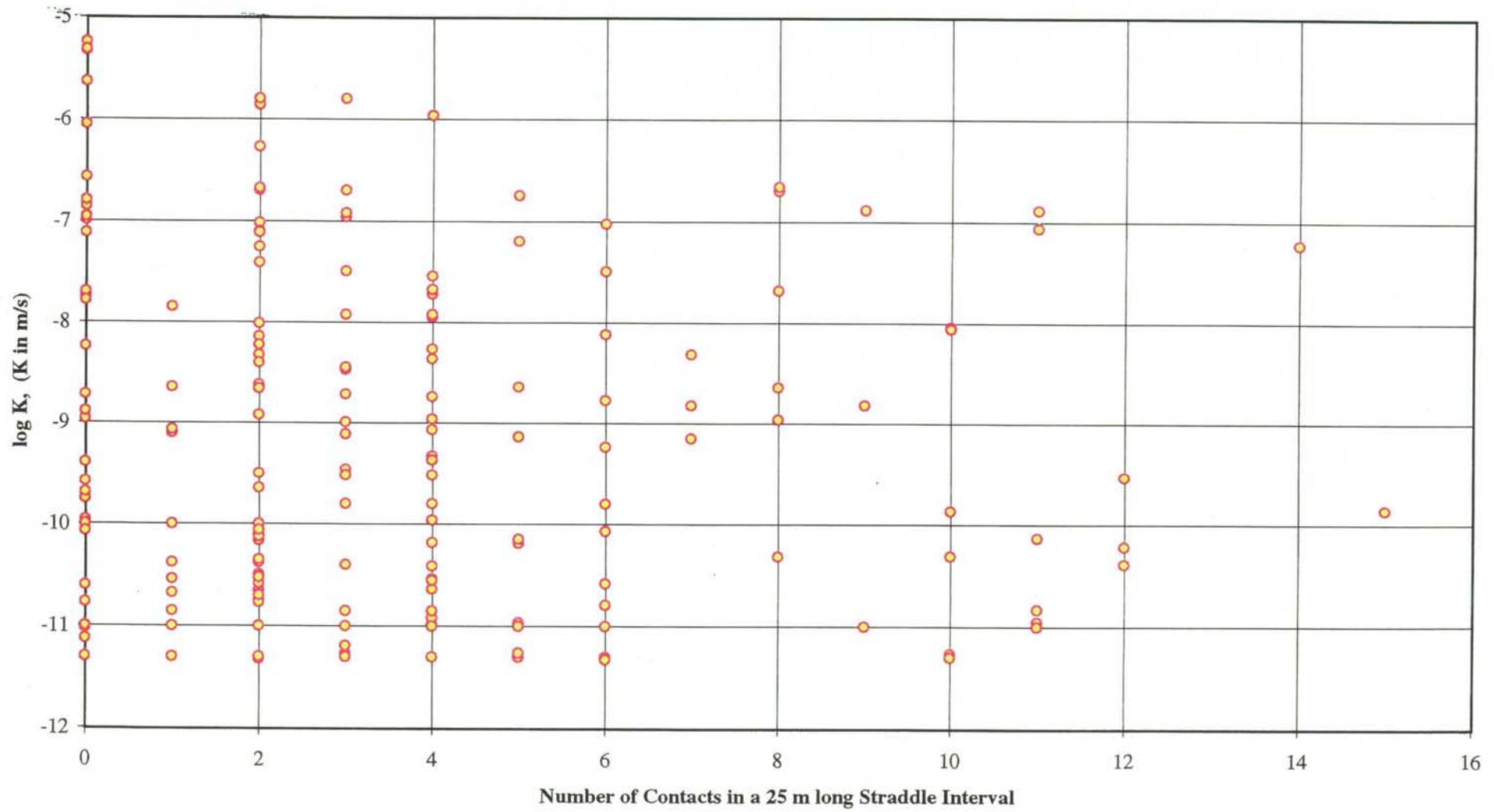


Figure 6-8 K plotted as a function of the number of rock contacts.

7 CONCLUSIONS

- The presented three-dimensional dolerite model includes subvertical dolerites of which indications are plural. The dolerites are essentially the same as presented in Ahlbom et. al (1991). Subhorizontal dolerite may exist but will have to be limited in extent as mapped dolerites in KGI01, the only vertical hole, have been reinterpreted not to exist. Further, possible intercepts in KGI08, 10, 12 and KGI13 do not fit any subhorizontal plane. However, it cannot be ruled out that subhorizontal bodies of variable width and limited extent exist in the investigation area based on Lundquists (1990) regional geological studies. Only dolerites interpreted as **certain** or **probable** have been included in the model.
- Another model presents the folded foliation of the paragneiss (migmatite) along which elongated bodies of orthogneiss are layered with their longitudinal axis along the fold axis. The model has a lower degree of reliability than has the dolerite model.
- Interpretation Alternative 2 regarding Zones I and II can be regarded as established with many drill hole observations supporting it. Using the Bäckblom nomenclature (Appendix 2), the two zones can be regarded as **certain** (Table 6-2).
- The high artesian yield in HGI 20 needs some further comments. It would fit more or less with a more gentle dip of zone I, but in that case the problems described in Section 5.2.1 remain. However, there are also other nearby geophysical anomalies (Figure 5-4) which could explain the water occurrence, among them Zones I, X, II, XI c, XI a and XI b. Actually, HGI 20 lies on or very close to a WNW striking anomaly. Furthermore, sub-horizontal joints have been mapped in the rocky hills NNE and ESE of the hole, with an altitude of some 25 metres higher up.
- Zone III has kept its status of **certain**. It is being regarded as a not water bearing shear structure, due to the consistent results in KGI 06, 09 and 11, and in HGI 11 and 22.
- Some doubt exists on the extension of Zone X. The geophysical anomaly map (Figure 3-4) feature no continuous anomaly there, but a series of short anomalies between the more extended NE anomalies, and West of HGI 20 there is no corresponding anomaly at all.
- Zones XI a, XI b and XII appear to be **probable**, in particular Zone XI a which features a seismic velocity anomaly (Figure 3-4) very close to the anomaly of Zone X. The mise a la masse test in KGI 07 support an upgrade to a status of **probable** for Zone VI.
- In the cases where zones have changed orientation or new zones have emerged, updated hydraulic properties have been assigned to each zone.
- The orthogneiss lie as elongated lenticular bodies along the foliation with their longitudinal axis along the fold axis.

- Most of the highly conductive zones strike NNE to ENE (parallel with the maximum horizontal stress), dipping vertical or steeply to the SE.
- The dolerites appear to form impermeable layers acting against transport in the orthogneiss bodies.
- The dolerite dykes do not form impermeable boundaries with respect to the fracture zones
- Based on the analysis of 25 m packer tests there is no correlation of statistical significance between $\log_{10}(K_{25m})$ and rock type
- There is no obvious correlation between $\log_{10}(K_{25m})$ and the number of rock contacts, i.e. it seems that rock contacts at some locations are conductive but impermeable at others.
- Lithological sequence does not change within repository depth whereas the hydraulic conductivity of 25 m packer tests show higher magnitudes between ground level and 200 m depth than at repository depth (-500 m).

8 REFERENCES

- Ahlbom K, Andersson, J E, Nordqvist R, Ljunggren C, Tirén S & Voss C, 1991. Gideå Study Site. Scope of activities and main results. SKB Tech Rep 91-51. SKB, Stockholm.
- Ahlbom K., Albino B. Nilsson G., Olsson O., Stenberg L., Timje H., 1983. Evaluation of the geological, geophysical and hydrogeological conditions at Gideå. KBS Technical report 83-53.
- Albino B, Nilsson G, Stenberg L. Geologiska och geofysiska mark- och djupundersökningar. SKBF/KBS AR 83-19. SKB, Stockholm.
- Albino B., Nilsson G., 1982. Sammanställning av tekniska data för de olika borrhålen samt sprick- och bergartsloggar, typområdet Gideå. AR 84-23.
- Andersson, J., Almén, K-E., Ericsson, L O., Fredriksson, A., Karlsson, F., Stanfors, R., Ström, A., 1997. Parametrar av betydelse att bestämma vid geovetenskaplig platsundersökning. SKB rapport R-97-03.
- Carlsson, L., Winberg A., Grundfelt, B., 1983. Model calculations of the groundwater flow at Finnsjön, Fjällveden, Gideå and Kamlunge. SKBF KBS Technical report 83-45.
- Ericsson L O, & Ronge B, 1986. Correlation between tectonic lineaments and permeability values of crystalline bedrock in the Gideå area.
- Ljunggren, C., 1996. Personal communication. Stress field in Sweden.
- Lundqvist T, Gee D, Karis L, Kumpulainen R, Kresten P, 1990. Beskrivning till berggrundskartan över Västernorrlands Län (in Swedish with an English Summary). SGU Ba 31. Geological Survey of Sweden, Uppsala.
- Kulhánek, O., Wahlström, R. 1985. Macro seismic observations in Sweden 1980-1983. SGU C 808.
- Magnusson K-Å., 1985. Elektriska mellanhålmätningar i Gideå, Svartboberget och fjällveden. SKB AR 85-11.

Müller, B., Zoback, M. L., Fucha, K., Mastin, L., Gregersen, S., Pavoni, N., Stephansson, O. & Ljunggren, C., 1992. Regional Patterns of Tectonic Stress in Europe. *J. Geoph. Res.* 97, B (pp 11783-11803).

Pihl J., Hammarström M., Ivansson S., Morén P., 1987. Crosshole investigations - results from seismic borehole tomography. Stripa project. TR 87-06.

Timje H., 1983. Hydrogeologiska undersökningar inom typområdet Gideå. SKBF/KBS AR 83-26.

Sahlström , K. E., 1930. A seismological map of northern Europe. SGU C 364.

SICADA (SKB Site characterisation database) 1996. Background data delivered in three batches 961009, 961018 and 961202 by E. Eriksson, SKB, Äspö Hard Rock Laboratory.

Appendix 1 Reliability criteria for dolerite dykes

Reliability criteria for dolerite dykes with respect to extension and orientation (Modified after Bäckblom 1989)		
Reliability	Location	Observations
Possible	Surface	Extensive magnetic anomaly
	Subsurface	Observation in one drill core
	Surface and subsurface	Weak magnetic anomalies at surface and in drill holes in an area where certain dykes are present
Probable	Surface	Extensive magnetic anomaly similar to anomalies caused by certain dykes in the area, or One small outcrop with strike/dip
	Subsurface	Observation in two drill cores, or Observation in one tunnel
	Surface and subsurface	Extensive magnetic anomaly and one drill core
Certain	Surface	Extensive magnetic anomaly and observations in one outcrop with known dip, or Two or more outcrops with strike/dip, or One extended outcrop with strike/dip
	Subsurface	Observation in two tunnels, or Observation in one tunnel and at least one core, or Observations in three oriented drillcores
	Surface and subsurface	One outcrop with strike/dip and at least one drill core, or Extensive magnetic anomaly and two oriented drill cores

Appendix 2 Reliability criteria for zones (Bäckblom. SKB 25-89-007)

GUIDE-LINES FOR USE OF NOMENCLATURE ON FRACTURES, FRACTURE ZONES AND OTHER TOPICS.

VERSION 1, December 20, 1989

1 BACKGROUND

This guide-line treats aspects for use of nomenclature for site-investigations and addresses how geological, geophysical, geo-hydrological results should be named. A special section is devoted to the uniqueness and completeness of investigations.

In reports to SKB on site characterization it shall be stated that "The nomenclature used in this report follow the 'Guidelines for use of nomenclature on fracture, fracture zones and other topics, Version 1, SKB, Stockholm, TPM 25-89-007'".

2 BASIC DEFINITIONS

Lineament, AGI (1987)

"A linear topographic feature of regional extent that is believed to reflect crustal structure.

Fracture, AGI (1987)

"A general term for any break in a rock whether or not it causes displacement, due to mechanical failure by stress. Fractures include cracks, joints and faults.

Zone, AGI (1987)

"A belt, band or strip of earth material, however disposed, characterized as distinct from surrounding parts by some particular property or content." It is inferred that a zone is a three-dimensional (sub-planar) peculiarity with limited width.

3 EXTENSION OF BASIC DEFINITIONS RELATED TO ZONES.

The concept zone can be expanded by explaining what type of peculiarity that defines the zone.

Studies of topography gives morphological zones (lineaments).

Geophysical anaomalies are named magnetic zones, electric zones or ----- zones depending on peculiarity.

A fracture zone is a fracture zone - only and only - if geological field evidence supports zones with the peculiarity that the intensity of natural fractures is at least two times higher than in surrounding rock. (Completely) disintegrated and/or chemically altered rock is included in the definition for fracture zone.

The definition for fracture zone can be expanded by additional peculiarities. A fracture zone can thus be "a hydraulically conductive fracture zone" or a "a non-conductive fracture zone".

Hydraulic responses from interference testing is named transmissive or hydraulic contacts. Additional work is required to separate if the contacts are established by "a transmissive fracture zone" or "transmissive single fractures"

4 BASIC DEFINITIONS FOR RELIABILITY

A zone is a three-dimensional feature. Its extension and direction is certain after investigations or measurements in several points.

To define a "level of reliability" three separate definitions are used.

Possible (Möjlig in Swedish) is the lowest level of confidence. By additional studies the level of reliability can be raised to Probable (Trolig in Swedish) or Certain (Säker in Swedish).

Even if reliability can be discussed with reference to any zone, the following guide-line has been directed to fracture zones.

5 GUIDE-LINES FOR LEVEL OF RELIABILITY OF FRACTURE ZONES

Three basic cases are considered.

- A Fracture zones expressed at surface, Table 1.
- B Fracture zones not expressed at surface, Table 2.
- C Fracture zones expressed at surface and in borehole(s) and/or underground caverns (tunnel(s) shaft(s), raise(s)), Table 3.

Table 1 is applied to the early phase of investigations and in regions where drilling/tunnelling is not carried through.

Table 2 is applied to zones not observed at surface, whereas Table 3 should be applied to zones that have both surface and sub-surface expressions.

Increased fracture intensity in Tables 1, 2 and 3 is defined as a section where the intensity of natural fractures is at least two times greater than in surrounding rock.

6 REFERENCES

Bates R L & Jackson J A, 1987: Glossary of Geology. Third edition. American Geological Institute. Alexandria.

Table 1. Zones observed at surface

RELIABILTY	OBSERVATIONS*
Possible	Geophysical anomaly with extensiveness or increased fracture intensity in one outcrop
Probable	Zone with increased fracture intensity in at least two outcrops reasonably close, or geophysical anomaly with increased fracture intensity in one outcrop.
Certain	Probable zone with unique peculiarity between fractured outcrops or exposed zone of increased fracture intensity.
	* Statements on dip shall be substantiated by field evidence (i e dip measurements on exposed zone or (geophysical) measurements, like VLF).

Table 2. Zones not observed at surface

RELIABILTY	OBSERVATIONS
Possible	Increased fracture intensity in a section of a core, interpolation between two-three boreholes with sections of increased fracture intensity.
Probable	Interpolated possible fracture zone with some additional unique peculiarity observed (geophysical, geohydrological, geological or geochemical). Sections with increased fracture intensity in one borehole and one tunnel and with some additional unique peculiarity observed.
Certain	Probable fracture zone with unique peculiarity in three or more holes or probable fracture zone in two holes with (seismic or radar) connection in between. Sections with increased fracture intensity in two tunnels and with some additional unique peculiarity observed.

Table 3. Zones observed at surface and in sub-surface

RELIABILITY	OBSERVATIONS
Possible	Lineament from surface investigations and geophysical anomaly (radar) in borehole.
Probable	Zone with increased fracture intensity at one outcrop interpolated with sections of increased fracture intensity in at least one borehole (tunnel) reasonably close or zone with geophysical anomaly or other unique peculiarity interpolated with section of increased fracture intensity in at least one borehole (tunnel) reasonably close.
Certain	Probable fracture zone at surface with observed direction of dip at surface and unique peculiarity in at least two boreholes (tunnels).

Appendix 3 Co-ordinates of zones and lithological units

Appendix 3 contains co-ordinates for all identified structures at Gideå, i.e. zones and dolerites. The extracted co-ordinates have the following format;

Structure ID	name of the zone or the lithological structure.
Local x, y	local coordinates according to the nomenclature in chapter 1.4.
Z	level of depth (m).
RT_X,Y	RT38 co-ordinates.

The structures in the geological model is constructed by a planar projection of the mapped surface trace through the identified borehole intersections.

The co-ordinates are then extracted by digitizing points at a regular interval on the surface trace of the structure (i.e first group of points with identical Z-value). The similar procedure is performed on the “bottom” trace (i.e. second group of points with identical Z-values). When these co-ordinates are used to reconstruct the geological model shown in the report, slight variations will occur due to the simplification introduced by sampling points at a regular interval along the structure.

Local Y	Local X	Z	RT_Y	RT_X
ZONE-1				
801.11	10.63	100.00	1663589	7044343
1153.79	875.71	100.00	1663896	7045225
1896.67	1996.54	100.00	1664580	7046383
1003.73	128.43	-600.00	1663786	7044471
1356.41	993.50	-600.00	1664093	7045353
2099.29	2114.34	-600.00	1664776	7046511
ZONE-2A				
1016.39	6.55	100.00	1663805	7044350
1999.40	1661.48	100.00	1664700	7046054
1189.33	120.89	-600.00	1663971	7044473
2172.34	1775.81	-600.00	1664866	7046177
ZONE-2B				
1016.39	6.55	100.00	1663805	7044350
1999.40	1661.48	100.00	1664700	7046054
1414.01	-29.36	-600.00	1664204	7044335
2397.01	1625.56	-600.00	1665099	7046039
ZONE-3A WESTERN SEGMENT				
-854.70	1563.21	100.00	1661855	7045806
-396.96	1510.55	100.00	1662315	7045778
-246.89	1457.89	100.00	1662467	7045733
8.24	1277.36	100.00	1662731	7045566
412.09	1254.87	100.00	1663136	7045565
-839.07	2359.63	-600.00	1661829	7046602
-381.33	2306.97	-600.00	1662288	7046574
-231.25	2254.32	-600.00	1662441	7046529
23.88	2073.78	-600.00	1662705	7046362
427.73	2051.29	-600.00	1663110	7046361
ZONE-3B WESTERN SEGMENT				
-854.70	1563.21	100.00	1661855	7045806
-396.96	1510.55	100.00	1662315	7045778
-246.89	1457.89	100.00	1662467	7045733
8.24	1277.36	100.00	1662731	7045566
412.09	1254.87	100.00	1663136	7045565
-847.46	1641.14	-600.00	1661858	7045885
-389.72	1588.48	-600.00	1662318	7045856
-239.65	1535.82	-600.00	1662470	7045811
15.48	1355.29	-600.00	1662735	7045644
419.33	1332.80	-600.00	1663139	7045643
ZONE-3A EASTERN SEGMENT				
501.30	1133.59	100.00	1663231	7045448
920.20	1171.08	100.00	1663648	7045508
987.73	1216.22	100.00	1663713	7045556
1379.48	1216.22	100.00	1664104	7045577
384.31	1893.87	-600.00	1663075	7046201
803.20	1931.36	-600.00	1663491	7046261
870.74	1976.50	-600.00	1663556	7046309
2007.93	1976.50	-600.00	1664692	7046369

ZONE-3B EASTERN SEGMENT				
501.30	1133.59	100.00	1663231	7045448
920.20	1171.08	100.00	1663648	7045508
987.73	1216.22	100.00	1663713	7045556
1379.48	1216.22	100.00	1664104	7045577
467.85	1342.02	-600.00	1663187	7045655
886.75	1379.51	-600.00	1663603	7045714
954.28	1424.65	-600.00	1663668	7045763
1641.43	1424.65	-600.00	1664355	7045799
ZONE-4				
110.54	1588.60	100.00	1662817	7045882
179.71	1651.01	100.00	1662883	7045948
352.65	1720.35	100.00	1663052	7046026
556.71	1758.49	100.00	1663254	7046075
1276.13	1526.19	100.00	1663985	7045881
1589.08	1532.46	100.00	1664297	7045904
1748.90	1585.69	-600.00	1664454	7045965
1255.83	1575.80	-600.00	1663962	7045929
536.42	1808.11	-600.00	1663231	7046124
332.35	1769.97	-600.00	1663029	7046075
159.42	1700.62	-600.00	1662860	7045997
90.24	1638.21	-600.00	1662794	7045931
			1662790	7044290
ZONE-5				
0.09	1944.00	100.00	1662688	7046231
1995.77	1961.34	100.00	1664680	7046353
-11.49	2059.36	-600.00	1662671	7046346
1984.19	2076.70	-600.00	1664663	7046468
ZONE-6 EASTERN SEGMENT				
506.11	1196.75	100.00	1663233	7045512
883.91	1792.38	100.00	1663579	7046126
820.87	1391.78	-600.00	1663537	7045723
1043.10	1733.75	-600.00	1663741	7046076
ZONE-6 WESTERN SEGMENT				
-663.16	-0.05	100.00	1662128	7044255
-517.85	137.17	100.00	1662266	7044400
-458.02	111.44	100.00	1662327	7044377
3.53	523.10	100.00	1662766	7044813
131.74	660.32	100.00	1662887	7044956
389.67	1013.23	100.00	1663126	7045322
534.71	935.24	-600.00	1663275	7045252
290.93	601.69	-600.00	1663049	7044906
162.72	464.47	-600.00	1662928	7044762
-298.84	52.81	-600.00	1662489	7044327
-358.67	78.54	-600.00	1662428	7044350
-503.97	-58.68	-600.00	1662290	7044205
ZONE-7				
499.20	326.29	100.00	1663271	7044642
499.76	413.12	100.00	1663267	7044729
489.93	538.08	100.00	1663251	7044853
469.42	656.03	100.00	1663224	7044970

431.08	756.51	100.00	1663181	7045068
399.81	853.55	100.00	1663145	7045163
361.44	950.55	100.00	1663101	7045258
315.99	1047.51	100.00	1663051	7045353
252.57	1182.80	100.00	1662980	7045484
227.88	1235.48	100.00	1662953	7045536
655.84	367.02	-600.00	1663426	7044691
656.39	453.85	-600.00	1663422	7044778
646.56	578.81	-600.00	1663405	7044902
626.05	696.76	-600.00	1663379	7045019
587.71	797.24	-600.00	1663335	7045117
556.44	894.28	-600.00	1663299	7045212
518.08	991.28	-600.00	1663255	7045307
472.63	1088.24	-600.00	1663205	7045401
409.21	1223.53	-600.00	1663135	7045533
384.51	1276.21	-600.00	1663107	7045585
ZONE- 8				
-415.52	578.93	100.00	1662345	7044846
-906.93	1098.59	100.00	1661827	7045340
-1052.80	960.65	-600.00	1661688	7045194
-561.39	440.99	-600.00	1662206	7044701
ZONE-9				
1273.55	435.67	100.00	1664039	7044792
1996.42	352.46	100.00	1664765	7044746
2007.19	446.05	-600.00	1664771	7044840
1422.45	513.36	-600.00	1664184	7044877
ZONE-10				
1180.06	295.51	100.00	1663953	7044647
1166.59	895.02	100.00	1663908	7045245
1185.92	575.32	-600.00	1663944	7044927
1189.27	91.13	-600.00	1663973	7044443
ZONE-11A				
1033.76	549.65	100.00	1663794	7044893
1223.21	626.91	100.00	1663979	7044980
1906.39	1041.95	100.00	1664639	7045430
1980.78	907.43	-600.00	1664721	7045300
1297.60	492.39	-600.00	1664060	7044850
1123.09	421.22	-600.00	1663890	7044769
ZONE-11B				
1336.95	694.47	100.00	1664089	7045053
1595.34	744.63	100.00	1664344	7045117
1961.19	873.04	100.00	1664703	7045264
1641.80	700.63	-600.00	1664393	7045076
1989.36	822.62	-600.00	1664734	7045216
ZONE-12				
1493.33	1530.54	100.00	1664201	7045897
816.28	1080.60	100.00	1663549	7045412
1486.28	1580.42	-600.00	1664192	7045946
791.13	1118.45	-600.00	1663522	7045448

	Local Y	Local X	Z	RT_Y	RT_X
Dolerite 1	818.609	1993.831	118.574	1663503.138	7046323.941
	837.876	1689.732	118.574	1663538.294	7046021.267
	857.143	1385.632	118.574	1663573.450	7045718.593
	876.409	1081.533	118.574	1663608.605	7045415.918
	895.676	777.433	118.574	1663643.761	7045113.244
	914.943	473.334	118.574	1663678.917	7044810.569
	934.210	169.234	118.574	1663714.072	7044507.895
	953.476	-134.866	118.574	1663749.228	7044205.220
	972.743	-438.965	118.574	1663784.384	7043902.546
	992.010	-743.065	118.574	1663819.539	7043599.872
	681.952	1985.173	-626.600	1663367.122	7046308.143
	701.219	1681.074	-626.600	1663402.278	7046005.469
	720.486	1376.974	-626.600	1663437.433	7045702.794
	739.753	1072.875	-626.600	1663472.589	7045400.120
	759.019	768.775	-626.600	1663507.745	7045097.445
	778.286	464.675	-626.600	1663542.900	7044794.771
	797.553	160.576	-626.600	1663578.056	7044492.097
	816.820	-143.524	-626.600	1663613.212	7044189.422
	836.086	-447.623	-626.600	1663648.367	7043886.748
	855.353	-751.723	-626.600	1663683.523	7043584.073
Dolerite 2	1329.718	-804.624	-619.795	1664160.007	7043556.071
	1300.640	-553.525	-619.402	1664117.827	7043805.303
	1271.562	-302.427	-619.009	1664075.648	7044054.536
	1242.484	-51.329	-618.616	1664033.468	7044303.768
	1213.407	199.769	-618.223	1663991.288	7044553.000
	1184.329	450.867	-617.831	1663949.109	7044802.232
	1155.251	701.965	-617.438	1663906.929	7045051.464
	1126.173	953.063	-617.045	1663864.750	7045300.696
	1097.095	1204.161	-616.652	1663822.570	7045549.928
	1068.017	1455.259	-616.259	1663780.391	7045799.160
	1163.970	-824.975	119.905	1663995.550	7043527.073
	1134.892	-573.877	120.298	1663953.371	7043776.305
	1105.814	-322.779	120.691	1663911.191	7044025.537
	1076.736	-71.681	121.083	1663869.012	7044274.770
	1047.658	179.417	121.476	1663826.832	7044524.002
	1018.580	430.515	121.869	1663784.653	7044773.234
	989.502	681.614	122.262	1663742.473	7045022.466
	960.424	932.712	122.655	1663700.294	7045271.698
	931.346	1183.810	123.047	1663658.114	7045520.930
	902.268	1434.908	123.440	1663615.935	7045770.162
Dolerite 3	1136.109	714.560	-645.604	1663887.155	7045063.040
	1120.067	812.027	-645.604	1663866.034	7045159.534
	1104.026	909.494	-645.604	1663844.914	7045256.028
	1087.984	1006.960	-645.604	1663823.793	7045352.521
	1071.943	1104.427	-645.604	1663802.672	7045449.015
	1055.901	1201.894	-645.604	1663781.552	7045545.508
	1039.860	1299.361	-645.604	1663760.431	7045642.002
	1023.818	1396.827	-645.604	1663739.311	7045738.495
	1007.777	1494.294	-645.604	1663718.190	7045834.989
	991.735	1591.761	-645.604	1663697.070	7045931.483

	1060.318	702.086	124.300	1663812.120	7045046.617
	1044.276	799.553	124.300	1663791.000	7045143.110
	1028.235	897.020	124.300	1663769.879	7045239.604
	1012.193	994.486	124.300	1663748.759	7045336.098
	996.152	1091.953	124.300	1663727.638	7045432.591
	980.110	1189.420	124.300	1663706.518	7045529.085
	964.069	1286.887	124.300	1663685.397	7045625.578
	948.027	1384.353	124.300	1663664.276	7045722.072
	931.986	1481.820	124.300	1663643.156	7045818.565
	915.944	1579.287	124.300	1663622.035	7045915.059
Dolerite 4a	1447.946	187.724	-626.570	1664226.137	7044553.246
	1437.244	322.112	-626.570	1664208.416	7044686.890
	1426.542	456.500	-626.570	1664190.696	7044820.534
	1415.840	590.888	-626.570	1664172.975	7044954.178
	1405.138	725.276	-626.570	1664155.254	7045087.822
	1394.436	859.664	-626.570	1664137.533	7045221.465
	1383.734	994.053	-626.570	1664119.813	7045355.109
	1373.032	1128.441	-626.570	1664102.092	7045488.753
	1362.330	1262.829	-626.570	1664084.371	7045622.397
	1351.628	1397.217	-626.570	1664066.651	7045756.041
	1336.385	178.840	117.480	1664115.193	7044538.536
	1325.683	313.228	117.480	1664097.473	7044672.179
	1314.981	447.616	117.480	1664079.752	7044805.823
	1304.279	582.004	117.480	1664062.031	7044939.467
	1293.576	716.392	117.480	1664044.311	7045073.111
	1282.874	850.780	117.480	1664026.590	7045206.755
	1272.172	985.168	117.480	1664008.869	7045340.398
	1261.470	1119.556	117.480	1663991.148	7045474.042
	1250.768	1253.944	117.480	1663973.428	7045607.686
	1240.066	1388.332	117.480	1663955.707	7045741.330
Dolerite 4b	1363.850	577.561	117.606	1664121.754	7044938.148
	1360.371	642.812	117.606	1664114.864	7045003.127
	1356.891	708.063	117.606	1664107.974	7045068.106
	1353.412	773.313	117.606	1664101.085	7045133.086
	1349.932	838.564	117.606	1664094.195	7045198.065
	1346.453	903.815	117.606	1664087.306	7045263.044
	1342.974	969.066	117.606	1664080.416	7045328.024
	1339.494	1034.317	117.606	1664073.527	7045393.003
	1336.015	1099.568	117.606	1664066.637	7045457.982
	1332.536	1164.818	117.606	1664059.748	7045522.962
	1259.134	571.977	-652.274	1664017.473	7044927.091
	1255.654	637.228	-652.274	1664010.584	7044992.070
	1252.175	702.479	-652.274	1664003.694	7045057.050
	1248.696	767.730	-652.274	1663996.805	7045122.029
	1245.216	832.980	-652.274	1663989.915	7045187.008
	1241.737	898.231	-652.274	1663983.025	7045251.988
	1238.258	963.482	-652.274	1663976.136	7045316.967
	1234.778	1028.733	-652.274	1663969.246	7045381.946
	1231.299	1093.984	-652.274	1663962.357	7045446.926
	1227.820	1159.235	-652.274	1663955.467	7045511.905

Dolerite 7	-24.932	-1.021	121.101	1662765.156	7044287.676
	-13.571	128.832	121.101	1662769.705	7044417.945
	-2.211	258.685	121.101	1662774.254	7044548.214
	9.150	388.538	121.101	1662778.803	7044678.484
	20.511	518.390	121.101	1662783.352	7044808.753
	31.871	648.243	121.101	1662787.901	7044939.023
	43.232	778.096	121.101	1662792.450	7045069.292
	54.592	907.949	121.101	1662796.999	7045199.562
	65.953	1037.802	121.101	1662801.548	7045329.831
	77.314	1167.655	121.101	1662806.097	7045460.101
	-133.450	8.473	-621.764	1662656.290	7044291.477
	-122.089	138.326	-621.764	1662660.839	7044421.747
	-110.728	268.179	-621.764	1662665.388	7044552.016
	-99.368	398.032	-621.764	1662669.937	7044682.286
	-88.007	527.885	-621.764	1662674.486	7044812.555
	-76.647	657.737	-621.764	1662679.035	7044942.825
	-65.286	787.590	-621.764	1662683.584	7045073.094
	-53.925	917.443	-621.764	1662688.133	7045203.364
	-42.565	1047.296	-621.764	1662692.683	7045333.633
	-31.204	1177.149	-621.764	1662697.232	7045463.902
Dolerite 9a	1977.872	1540.764	115.240	1664684.524	7045932.166
	1976.537	1465.855	115.240	1664687.112	7045857.290
	1975.203	1390.947	115.240	1664689.699	7045782.414
	1973.868	1316.038	115.240	1664692.287	7045707.539
	1972.534	1241.130	115.240	1664694.875	7045632.663
	1971.199	1166.221	115.240	1664697.462	7045557.787
	1969.865	1091.312	115.240	1664700.050	7045482.912
	1968.530	1016.404	115.240	1664702.638	7045408.036
	1967.196	941.495	115.240	1664705.225	7045333.160
	1965.861	866.587	115.240	1664707.813	7045258.284
	2093.741	1538.699	-616.850	1664800.342	7045936.168
	2092.406	1463.791	-616.850	1664802.930	7045861.293
	2091.072	1388.882	-616.850	1664805.518	7045786.417
	2089.737	1313.974	-616.850	1664808.105	7045711.541
	2088.403	1239.065	-616.850	1664810.693	7045636.666
	2087.068	1164.157	-616.850	1664813.281	7045561.790
	2085.734	1089.248	-616.850	1664815.868	7045486.914
	2084.399	1014.340	-616.850	1664818.456	7045412.038
	2083.065	939.431	-616.850	1664821.044	7045337.163
	2081.730	864.523	-616.850	1664823.631	7045262.287
Dolerite 9b	1765.190	913.199	-618.386	1664504.977	7045294.330
	1753.355	1000.934	-618.360	1664488.567	7045381.325
	1741.520	1088.669	-618.333	1664472.157	7045468.321
	1729.685	1176.403	-618.307	1664455.746	7045555.316
	1717.850	1264.138	-618.281	1664439.336	7045642.311
	1706.015	1351.873	-618.255	1664422.925	7045729.306
	1694.180	1439.608	-618.229	1664406.515	7045816.301
	1682.345	1527.342	-618.203	1664390.104	7045903.296
	1670.510	1615.077	-618.177	1664373.694	7045990.291
	1658.675	1702.812	-618.150	1664357.283	7046077.286
1664.405	899.384	119.123	1664405.054	7045275.260	

	1652.570	987.119	119.149	1664388.644	7045362.255
	1640.735	1074.853	119.175	1664372.233	7045449.250
	1628.900	1162.588	119.202	1664355.823	7045536.245
	1617.065	1250.323	119.228	1664339.412	7045623.240
	1605.230	1338.058	119.254	1664323.002	7045710.235
	1593.395	1425.792	119.280	1664306.591	7045797.230
	1581.560	1513.527	119.306	1664290.181	7045884.225
	1569.725	1601.262	119.332	1664273.771	7045971.221
	1557.890	1688.997	119.358	1664257.360	7046058.216
Dolerite 9c	1672.413	1051.903	-632.335	1664405.069	7045427.988
	1668.220	1113.469	-632.335	1664397.659	7045489.250
	1664.027	1175.034	-632.335	1664390.250	7045550.513
	1659.834	1236.600	-632.335	1664382.841	7045611.774
	1655.641	1298.166	-632.335	1664375.431	7045673.036
	1651.448	1359.732	-632.335	1664368.022	7045734.299
	1647.255	1421.298	-632.335	1664360.613	7045795.561
	1643.062	1482.864	-632.335	1664353.203	7045856.823
	1638.869	1544.429	-632.335	1664345.794	7045918.085
	1634.676	1605.995	-632.335	1664338.385	7045979.347
	1562.082	1044.389	118.884	1664295.282	7045414.710
	1557.889	1105.954	118.884	1664287.872	7045475.972
	1553.696	1167.520	118.884	1664280.463	7045537.234
	1549.503	1229.086	118.884	1664273.054	7045598.496
	1545.310	1290.652	118.884	1664265.644	7045659.758
	1541.117	1352.218	118.884	1664258.235	7045721.020
	1536.924	1413.784	118.884	1664250.826	7045782.282
	1532.731	1475.349	118.884	1664243.416	7045843.544
	1528.538	1536.915	118.884	1664236.007	7045904.806
	1524.345	1598.481	118.884	1664228.598	7045966.068